# ELECTROMAGNETIC RADIATION FROM LIGHTNING RETURN STROKES TO TALL STRUCTURES

THÈSE N$^{O}$ 3713 (2007)

PRÉSENTÉE LE 26 JANVIER 2007

À LA FACULTÉ DES SCIENCES ET TECHNIQUES DE L'INGÉNIEUR

Laboratoire de réseaux électrique

SECTION DE GÉNIE ÉLECTRIQUE ET ÉLECTRONIQUE

ÉCOLE POLYTECHNIQUE FÉDÉRALE DE LAUSANNE

POUR L'OBTENTION DU GRADE DE DOCTEUR ÈS SCIENCES

PAR

Davide PAVANELLO

Laurea in Ingegneria Elettronica, Politecnico di Torino, Italie
de nationalité italienne

acceptée sur proposition du jury:

Prof. J. R. Mosig, président du jury
Dr F. Rachidi-Haeri, directeur de thèse
Prof. M. Rubinstein, rapporteur
Prof. A. Skrivervik, rapporteur
Prof. R. Thottappillil, rapporteur

ÉCOLE POLYTECHNIQUE
FÉDÉRALE DE LAUSANNE

Lausanne, EPFL
2007

*To Sara*

# Résumé

L’étude de l’interaction entre le champ électromagnétique rayonné par la foudre et les systèmes électriques, ainsi que la coordination des stratégies de protection sont généralement basées sur des distributions statistiques du courant mesuré à la base du canal de foudre obtenues en utilisant des tours instrumentées ou par la technique de déclenchement artificiel de la foudre.

Des études récentes basées sur des modélisations numériques et des observations expérimentales ont montré que la présence de la structure foudroyée, ou celle utilisée pour la déclencher, ‘contamine’ la mesure du courant de foudre. Cette ‘contamination’, qui dépend de la géométrie de la structure elle-même, compromet la fiabilité des statistiques adoptées jusqu’alors pour les paramètres du courant de foudre.

L’objectif de cette thèse est d’apporter de nouveaux éléments (issus d’études à la fois théoriques et expérimentales) à la compréhension des conséquences électromagnétiques de l’impact d’arcs en retour sur des tours élevées.

Le Chapitre 2 présente brièvement la phénoménologie des coups de foudre nuage-sol et souligne l’importance des modèles d’arc en retour. Parmi les différentes classes de modèles d’arc en retour existantes dans la littérature, l’attention est focalisée dans cette thèse sur ce qu’on appelle les ‘modèles d’ingénieur’. Ces modèles permettent une description de la distribution du courant le long du canal en fonction du courant à la base du canal et de la vitesse de l’arc en retour, deux grandeurs pour lesquelles il est possible d’obtenir des données expérimentales. Après une description de cinq modèles d’ingénieur de l’arc en retour pour des coups de foudre tombant au sol, l’attention est portée sur l’extension des modèles d’ingénieurs en tenant compte de la présence d’un objet élevé foudroyé.

Les contributions originales de cette thèse, comprenant des travaux théoriques et expérimentales, sont présentées dans les Chapitres 3 à 6.

Le Chapitre 3 est consacré au calcul du champ électromagnétique produit par l'impact d'arcs en retour sur des tours élevées, en se basant sur l'extension des modèles d'ingénieur pour inclure la présence d'un objet élevé qui a été présentée dans le chapitre précédent.

Il est montré, pour la première fois, que selon ces modèles d'ingénieurs, la distribution du courant le long du canal présente une discontinuité au front d'onde de l'arc en retour qui, bien que physiquement inconcevable, nécessite d'être prise en compte par un terme additionnel dans les équations du champ électromagnétique, le terme communément appelé 'turn-on term'. Une formule analytique générale décrivant ce 'turn-on term' associé à cette discontinuité est développée pour les différent modèles d'ingénieurs et des résultats de simulation illustrant l'effet de cette discontinuité sur les champs électrique et magnétique rayonnés sont présentés.

Dans la deuxième partie du chapitre, dédiée à l'étude des effets de propagation du champ électromagnétique de foudre se propageant le long d'un sol de conductivité finie, l'hypothèse habituelle d'un sol idéal parfaitement conducteur est abandonnée afin d'analyser, pour la première fois, comment le champ électromagnétique rayonné par un coup de foudre tombant sur un objet élevé est affecté suite à la propagation le long d'un sol de conductivité finie.

Les résultats de simulation montrent que l'atténuation du pic initial du champ rayonné par un coup de foudre tombant sur une tour, suite à la propagation le long d'un sol de conductivité finie, dépend fortement du temps de montée du courant, de la hauteur de la tour et de la conductivité du sol ; en outre, cette atténuation est, en général, bien plus importante que l'atténuation subie par le champ produit par un coup de foudre tombant au sol, suite à la propagation le long du même parcours.

Le Chapitre 4 présente une comparaison entre les prédictions des cinq modèles d'ingénieur généralisés pour tenir compte de la présence d'une structure élevée, décrits dans le Chapitre 2. Les distributions spatio-temporelles du courant le long de l'axe tour-canal prévues par les modèles d'ingénieur, ainsi que les champs électriques et magnétiques associés, calculés à différentes distances, sont comparés et discutés.

Les résultats montrent que les champs électromagnétiques associés à un coup de foudre tombant sur une tour élevée sont généralement moins dépendants du modèle d'arc en retour adopté que ceux correspondants à un coup de foudre tombant au sol, spécialement en ce qui concerne le premier pic du champ, lequel est quasi insensible au choix du modèle dans le cas d'une tour foudroyée.

Une analyse théorique est présentée dans la dernière partie du chapitre avec l'objectif d'obtenir, pour les mêmes cinq modèles d'ingénieur généralisés, des expressions liant le courant de l'arc en retour et les champs électrique et magnétique rayonnés correspondants.

Les résultats montrent qu'un modèle seulement, parmi les cinq considérés, est caractérisé par des formules analytiques simples reliant les valeurs du pic du courant et du pic du champ rayonné à longue distance. Sachant que la valeur du premier pic du champ est pratiquement indépendante du modèle choisi, ces expressions deviennent des expressions générales applicables à n'importe quel modèle d'ingénieur dans le cas d'arcs en retour tombant sur des tours élevées.

Il a également été montré que le pic du champ électromagnétique rayonné par un coup de foudre tombant sur une structure élevée est relativement insensible aux valeurs du coefficient de réflexion au sommet de la tour et de la vitesse de l'arc en retour. Ce dernier résultat est particulièrement important, car contrairement au cas des coups de foudre tombant au sol, pour lesquels le pic du champ lointain est fortement dépendant de la vitesse de l'arc en retour, le pic du champ lointain associé aux coups de foudre tombant sur des structures élevées est peu sensible à la vitesse de l'arc en retour. Étant donné que dans la plupart des cas pratiques, la vitesse de l'arc en retour est inconnue, ce résultat intéressant suggère une procédure de calibration pour les systèmes de détection de la foudre à travers la mesure directe du courant de foudre sur une tour instrumentée.

Le Chapitre 5 présente les mesures simultanées du courant de l'arc en retour et des champs électrique et magnétique à trois distances associé à coups de foudre tombants sur la CN Tower (553 m) de Toronto, obtenues durant l'été 2005. Durant cette campagne de mesure, nous avons obtenu pour la première fois au monde, des mesures simultanées de courant de foudre et de champs électriques et magnétiques à trois distances du point d'impact. Les chemins de propagation pour le champ électromagnétique reliant la tour et les deux stations de mesure les plus proches (situées respectivement à 2 km et à 16.8 km de la CN Tower) étaient à travers l'environnement urbain de la ville de Toronto, alors que pour la troisième

station (située à 50.9 km de la tour) le chemin de propagation était presque exclusivement le long de l'eau douce du Lac Ontario.

Les résultats de mesure montrent que les formes d'onde des champs électrique et magnétique à 16.8 km et 50.9 km présentent, à environ 5 microsecondes après l'établissement de l'arc en retour, un premier passage par zéro qui fait parti d'un creux étroit (undershoot) et qui peut être attribué au processus transitoires le long de la tour.

Les effets de propagation (décroissance du pic du champ et augmentation de son temps de montée) ont pu être observés dans les courbes expérimentales. Il a été montré que les champs à 50.9 km sont moins affectés par cette atténuation par rapport à ceux mesurés à 16.8 km, vraisemblablement dû au fait que le chemin de propagation, pour la station de mesure à 50.9 km, était presque entièrement sur la surface du Lac Ontario.

Les formes d'onde mesurées sont comparées avec les prédictions théoriques obtenues utilisant cinq modèles d'ingénieur, généralisés pour inclure la présence de l'objet foudroyé, et un accord raisonnable a été trouvé pour les courbes de champ magnétique aux trois distances considérées.

Une bonne concordance a été également constatée entre les prévisions théoriques et les observations expérimentales du rapport entre les pics de champ magnétique et de courant, bien que l'expression théorique semble sous-estimer les valeurs observées expérimentalement d'environ 25%. Cela peut être dû, au moins partiellement, à l'effet d'amplification du champ introduit par la présence du bâtiment sur lequel les antennes de mesure étaient placées.

Enfin, les courants de foudre mesurés directement sur la tour ont été corrélés et comparés avec les estimations de leur valeur de crête fournis par le système de détection de foudre américain (NLDN). Il est montré que les valeurs obtenues par le NLDN surestiment les valeurs de courant effectivement mesurées en raison du fait que la présence d'une tour élevée foudroyée produit une amplification du champ rayonné à longue distance (par rapport aux coups de foudre tombants au sol) et cet effet n'est pas considéré dans les algorithmes utilisés pour inférer le pic du courant à partir des mesures de champ lointain.

Il est montré dans cette thèse qu'en corrigeant les estimations du NLDN par un facteur de correction qui tient compte de la présence de la structure foudroyée, il est possible d'obtenir une excellente estimation du courant de foudre. Ceci est une importante conclusion de cette étude montrant que l'estimation du courant pour les coups de foudre tombants sur des structures élevées peut être fortement améliorée en considérant le facteur introduit par la tour.

Le Chapitre 6 est dédié à la mesure du champ électromagnétique rayonné par la foudre. Dans la première partie de ce chapitre, la nécessité d'établir des recommandations pour la présentation des données expérimentales liées à la foudre est soulignée.

La deuxième partie du chapitre présente la conception, la construction et les tests préliminaires d'un système de mesure à bas coût, multicanaux, pour la mesure simultanée de trois composantes du champ électromagnétique rayonné par la foudre. Le système proposé utilise une seule liaison optique pour la transmission de trois signaux, numérisés et multiplexés, réduisant considérablement le prix global du système lui-même.

**Liste des mots-clés:**

Foudre, Champ Electromagnétique, Tours Elevées, Modèles d'Arc en Retour, Modèles d'Ingénieur, Discontinuité de Courant, Effets de Propagation, Mesures Simultanées, Système de Mesure Multicanaux.

# Abstract

The study of the interaction of lightning electromagnetic fields with electrical systems and the design of appropriate protection strategies are generally based on statistical distributions of the lightning current measured at the channel base using either instrumented towers or artificial initiation of lightning using rockets. Recent studies based both on numerical modeling and experimental observations have shown that the presence of the structure struck by (or used to initiate) lightning does affect the current measurement in a way depending upon the geometry of the structure itself, compromising therefore the reliability of the statistics adopted so far for lightning data. The aim of this thesis is to provide new elements (from both theoretical and experimental investigations) to improve the understanding of the electromagnetic consequences of the impact of lightning return strokes to tall structures.

Chapter 2 introduces to the phenomenology of cloud-to-ground lightning and the importance of lightning return-stroke modeling. Among the different classes of return-stroke models existing in the literature, the attention is focused in this thesis on the so-called engineering models, which allow describing the current distribution along the channel as a function of the current at the channel base and the return-stroke speed, two quantities for which data can be obtained experimentally. After presenting a review of five engineering return-stroke models describing lightning strikes to ground, the extension of the engineering models to take into account the presence of an elevated strike object is presented and discussed.

The original contributions of this thesis, consisting of both theoretical and experimental works, are presented in Chapters 3 through 6.

Chapter 3 is devoted to the computation of the electromagnetic field produced by lightning return strokes to elevated strike objects, using the extension of the engineering models to include an elevated strike object presented in the previous chapter.

It is shown, for the first time, that the current distribution associated with these extended models exhibits a discontinuity at the return-stroke wavefront which (although not physically conceivable) needs to be taken into account by an additional term in the equations for the electromagnetic field, the so-called 'turn-on' term. A general analytical formula describing the 'turn-on' term associated with this discontinuity for various engineering models is derived and simulation results illustrating the effect of the 'turn-on' term on the radiated electric and magnetic fields are also presented.

In the second part of the chapter, dedicated to the investigation of the propagation effects on lightning electromagnetic field traveling along a finitely-conducting ground, the commonly-used assumption of an idealized perfectly-conducting ground is relaxed in order to analyze, for the first time, how the electromagnetic field radiated by a tower-initiated strike is affected while propagating along a soil characterized by a finite conductivity.

The results showed that the attenuation of the initial peak of the field radiated by a tower-initiated strike, resulting from the propagation over finitely conducting ground, depends strongly on the risetime of the current, the tower height and the ground conductivity and is, in general, much more important than the attenuation experienced, while propagating along the same finite ground, by the field produced by ground-initiated strikes.

Chapter 4 presents a comparison among the predictions obtained using the five extended engineering return-stroke models for lightning strikes to tall structures described in Chapter 2. The spatial-temporal current profiles along the tower-channel axis predicted by the engineering models, as well as the respective predictions for the radiated electric and magnetic fields, calculated at different distances, are compared and discussed.

It is shown that the computed electromagnetic fields associated with a strike to a tall tower are generally less model-dependent than those corresponding to a strike to ground, especially as far as the first-peak value is concerned, which is nearly model-insensitive in case of tall-tower strikes.

A theoretical analysis is performed in the last part of the chapter with the aim to provide, for the same five engineering models extended to take into account the presence of the tower, expressions relating the return-stroke current and the associated distant radiated electric and magnetic fields.

It is demonstrated, in addition, that only one model among the five presented is characterized by simple analytical formulas relating current-peak and far-field peak values, which (being the electromagnetic field peak value nearly independent of the adopted model) become general expressions applicable for any engineering return-stroke model in case of tower-initiated lightning.

It was also shown that the peak amplitude of the electromagnetic field radiated by a lightning strike to a tall structure is relatively insensitive to both the values of the top reflection coefficient and the return-stroke speed. This latter result is important, in particular, because, unlike ground-initiated strikes, for which the far-field peak is strongly dependent on the return-stroke speed, far field peaks associated with strikes to tall structures are little sensitive to the return stroke speed. Since in most practical cases the value of the return-stroke speed is unknown, this interesting result suggests a possible calibration procedure for lightning detection systems by means of direct measurement of lightning currents on instrumented towers.

Chapter 5 reports on the simultaneous measurements of the return-stroke current and of the electric and magnetic fields at three distances associated with lightning strikes to the Toronto CN Tower (553 m) that have been carried out during the summer of 2005. This is the first time ever that simultaneous records of lightning current and associated electric and magnetic fields at three distances have been obtained. Two propagation paths for the electromagnetic field to the first and to the second field measurement stations (located, respectively, 2.0 km and 16.8 km away from the CN Tower) were along the soil and through the Toronto city, whereas for the third location (50.9 km away) the propagation path was nearly entirely across the fresh water of Lake Ontario.

It is shown that the waveforms of the electric and magnetic fields at 16.8 km and 50.9 km exhibit a first zero-crossing about 5 microseconds after the onset of the return-stroke, which is part of a narrow undershoot and which may be attributed to the transient processes along the tower.

Effects of propagation (decrease of field amplitude and increase of its risetime) could also be observed in experimental records. It is shown that the fields at 50.9 km are less affected by such attenuation, compared to those at 16.8 km, presumably because the path of propagation was mostly across Lake Ontario.

The measured waveforms are compared with the theoretical predictions obtained using five engineering return-stroke models, extended to include the presence of the strike object,

finding a reasonable agreement for the magnetic field waveforms at the three considered distances.

The overall agreement between the theoretically predicted and the experimentally observed field-peak-to-current-peak ratio is reasonable, although the theoretical expression appears to underestimate the experimentally measured ratio (by about 25 %). This may be due, at least in part, to the enhancement effect of the buildings on which the field measurement antennas were installed.

Finally, the directly-measured lightning currents at the tower were correlated and compared with the current-peak estimations provided by the US National Lightning Detection Network (NLDN). It is shown that the NLDN-inferred values overestimate the actual current peaks because the presence of the tall struck object produces an enhanced radiated field at far distances (with respect to strikes to flat ground), which is not included in the algorithm used to infer lightning current peaks from remote field measurements. It is shown in this thesis that correcting the NLDN estimates using the correction factor introduced by the tower results in an excellent estimation of lightning current peaks. This is an important conclusion of this study showing that the estimation of lightning peak currents for tall towers can be greatly improved by considering the tower correction factor.

Chapter 6 is devoted to the measurement of electromagnetic fields radiated by lightning. In its first part, the need for guidelines for reporting lightning data obtained experimentally is emphasized.

The second part of the chapter presents the design, the construction and preliminary tests of a low-cost, multi-channel lightning field measuring system for the simultaneous measurement of three components of the electromagnetic field radiated by lightning. The proposed system uses one single optical link for the transmission of the three signals, appropriately digitized and multiplexed, lowering considerably the overall cost of the system itself.

**List of keywords:**

Lightning, Electromagnetic Field, Tall Towers, Return-Stroke Modeling, Engineering Models, Current Discontinuity, Propagation Effects, Simultaneous Measurements, Multi-channel Measurement System.

# Acknowledgments

There are many people and institutions I wish to thank for the precious support they provided to my work during the last four years, which contributed significantly to my personal and professional development.

First of all, the person who expressed his trust in me through this opportunity to join his group, working on the fabulous topic of lightning and getting involved in an exciting project dealing with both theoretical and experimental aspects. In addition to having made easily accessible to me his deep knowledge in the field of lightning research, like only the best supervisors can do, he was always the sympathetic friend, example of integrity, who anyone hopes to meet in his life. I am grateful to Dr Farhad Rachidi for having shown me how all those qualities can coexist in a single person.

I would like to express my sincere thanks to Prof. Alain Germond, who accepted me among the staff of the Power Systems Laboratory of the EPFL, where each colleague is a good friend and working is much easier than elsewhere.

A special thank goes to Prof. Michel Ianoz for his guidance. I still remember with tenderness the very first time I got in Lausanne: while I was a bit disoriented, he warmly welcomed me to the Power Systems Laboratory of the EPFL and he drew a straight line toward my future by presenting me the activities of this laboratory.

I was particularly blessed during my stay here because, beside an excellent supervisor, I had the opportunity to work closely with another outstanding scientist and great expert in lightning research, Prof. Marcos Rubinstein of the University of Applied Sciences of Western Switzerland, in Yverdon, to whom I address my deep gratitude for his continuous and meticulous help throughout all the phases of my project, for having accepted to be among the Experts of the jury for the final examination of my thesis, his plain speaking and his friendship.

I am also grateful to Prof. Juan Ramon Mosig and to Prof. Anja Skrivervik Favre of the Laboratory of Electromagnetics and Acoustics (LEMA) of the EPFL for having accepted to be part of the jury for the final examination of my thesis in capacity, respectively, as President and Expert, and for the interest they expressed in my work through their valuable questions and suggestions.

My sincere gratitude goes equally to Prof. Rajeev Thottappillil of the Ångström Laboratory of the University of Uppsala, Sweden, for having accepted to be among the Experts of the jury for the final examination of my thesis and for his continuous help and valuable suggestions provided throughout my work as a partner of my project, especially during my short, intense visit to his laboratory.

Special thanks are addressed to Prof. Carlo Alberto Nucci of the Department of Electrical Engineering of the University of Bologna, Italy, for his continuous encouragement and suggestions, as well as for having accepted to be present at the final examination of my thesis.

During the first half or so of my work, I had the opportunity to share the office with Dr José-Luis Bermudez, whose excellent Ph.D. thesis constitutes the natural preface of my study. I am thankful to him because he helped me a lot every day, with his natural good humor and by leaving his footprints clearly visible and easy to be followed.

I would like to express my sincere gratitude to Dr Pierre Zweiacker, whose valuable experience and deep knowledge of the measuring equipment prevented me from misinterpretations of the experimental data.

Two lightning measurement campaigns were carried out in Toronto during the Summer of 2004 and 2005. My profound gratitude is addressed to Prof. Wasyl Janischewskyj, Professor Emeritus at the Department of Electrical and Computer Engineering of the University of Toronto, Canada and head of the CN Tower Lightning Studies Group (CNT-LSG), who accepted me in his team and let me take advantage of his tremendous experience in the topic of lightning.

My sincere gratitude goes equally to the other senior members of the CNT-LSG, namely, Prof. Ali Hussein of both the Ryerson University and the University of Toronto, Prof. Jen-Shih Chang of the McMaster University in Hamilton, Canada, Prof. Volodymyr Shostak of the Kyiv Polytechnic Institute, Ukraine and Dr William Chisholm of Kinectrics, Toronto for their continuous support and coordinated supervision of the measurement campaigns.

I am sincerely grateful to Dr Emanuel Petrache, now with Kinectrics, Toronto, good friend of mine and former colleague in Lausanne, whose brilliant solutions as a member of the CNT-LSG were a decisive factor in the achievement of the measurement campaigns.

I would like to express my gratitude to the other members of the CNT-LSG (permanent or not) with whom I had the opportunity to work and who played a fundamental role in the accomplishment of the measurement campaigns, namely, Mr Ivan Boev, Mr Alex Lafkovici, Mr Mariusz Milewski, Mr Faizan Jabbar, Mr Faisal Mohammad and Mr Saad Faisal.

I also address my gratitude to the people who accepted to let me install electromagnetic field measuring equipment on the roof of their building, namely, Dr Paul Joe, Mr Edmund Wu, Mr Ihab Abboud and Ms Amal Samanter of Environment Canada in Toronto and the staff of Place Polonaise in Grimsby, Canada.

A considerable part of the equipment brought to Canada for the measurement campaigns was borrowed from the Swiss Defense Procurement Agency (Armasuisse) in Spiez, Switzerland. I am therefore sincerely grateful to Dr Alain Jaquier, Dr Markus Nyffeler and Mr Beat Reusser of Armasuisse for their precious collaboration, availability and interest.

Special thanks are due to the people who invested great efforts in contributing to the development of a measuring system specially designed for lightning signals, namely, Mr Patrick Favre, Mr Daniel Bommottet and Mr Flavien Baumgartner of Wavemind SA, Ecublens, Switzerland, for their fundamental help in developing the electronics of the system, Mr Cédric Candolfi of the HEIG-VD, Yverdon, Switzerland for his precious help in developing a customized linear power supply for the system, Mr Georges Vaucher of the EPFL for his help in soldering the components on the PCBs, Mr Jean-Paul Brugger and Mr Roland Dupuis of the EPFL for their support in realizing custom-made solutions for antennas and enclosures.

I am sincerely grateful to all the members of the lightning research community I had the opportunity to discuss with throughout the last four years, in particular to Prof. Vladimir Rakov of the Department of Electrical and Computer Engineering of the University of Florida for his continuous support and for his valuable questions and comments.

My sincere gratitude is addressed to Dr Nelson Theethayi of the Ångström Laboratory of the University of Uppsala, Sweden for his precious suggestions and for his friendship.

I also express my sincere gratitude for valuable discussions to Dr Gerhard Diendorfer and Dr Wolfgang Schulz (ALDIS-OVE, Austria), Mr Hannes Pichler (Technical University, Vienna, Austria), Prof. Vernon Cooray and Mr Marley Becerra (Ångström Laboratory,

University of Uppsala, Sweden), Mr Eric Montandon (EMC Consulting, Worb, Switzerland), Dr Fridolin Heidler (University of Federal Armed Forces, Munich, Germany), Prof. Joan Montanyà, Dr David Romero and Ms Glòria Solà (Universitat Politècnica de Catalunya, Terrassa, Spain), Prof. Mario Paolone (University of Bologna, Italy), Prof. Carlo Mazzetti (University La Sapienza, Roma, Italy), Dr Yoav Yair and Dr Colin Price (Open University of Israel and Tel Aviv University, respectively), Dr Rouzbeh Moini (Amirkabir University of Technology, Teheran, Iran), Prof. Nikolay Korovkin (St-Petersburg State Technical University, St-Petersburg, Russia), Prof. Philip Krider (University of Tucson, Arizona, US), Mr Richard Kithil (National Lightning Safety Institute, Colorado, US), Dr Ken Cummins and Dr Jean-Yves Lojou (Vaisala, US), Dr Vlado Djurica (University of Ljubljana, Slovenia), Dr Daohong Wang (Gifu University, Japan), Dr Takatoshi Shindo and Mr A. Asakawa (CRIEPI, Japan), Dr Yoshihiro Baba (Doshisha University, Japan), Prof. Silverio Visacro (Federal University of Minas Gerais, Brazil) and Prof. Alexandre Piantini (University of São Paulo, Brazil).

This work was financially supported by the Swiss National Science Foundation (Grant No. 2000-068147). I am sincerely and profoundly grateful to this Institution for the provided support.

Another significant financial support was granted by '*Les Electriciens Romands'* (RDF P199) to support the development of the lightning measurement system. I would like to express my sincere gratitude to this Institution, in particular, to Mr Michel Aguet and Mr Charles Garneri for having trusted in the possibilities offered by this project.

Part of this work was developed within the framework of the European COST Action P18 (The Physics of Lightning Flash and its Effects), an intergovernmental European framework for international co-operation between nationally funded research activities. My sincere gratitude goes also to this Institution for the opportunities offered by its support.

As mentioned before, working at the Power System Laboratory of the EPFL was an enriching experience, especially thanks to the friendly atmosphere I found there. I would like to express my sincere gratitude to Mrs Andrée Moinat, our secretary, for her charming efficiency, and all to my colleagues not mentioned above, namely, Ms Ana Vukicevic,

Mrs Lena Vdovina-Beck, Mrs Elvira Kägi-Kolisnychenko, Dr Rachid Cherkaoui, Mr Abbas Mosaddeghi, Mr Sylvian Wenger, Mr Abdenabi Mimouni, Mrs Isabelle Nzazi and Mr Simon Cottier, as well as the former colleagues I had the privilege to meet: Ms Anne-Claude Maillefer and Dr Alexandre Oudalov. Thanks from the bottom of my heart to all of you.

I would like also to address special thanks to Dr Abraham Rubinstein and Dr Emmanuel Marthe, former colleagues and good friends, whose precious support and suggestions were always available throughout my work.

I also would like to thank all the students that I had the opportunity to supervise during my thesis for their valuable help and their efforts: Mr Alexey Negodyaev, Mr Diego Ravaglia, Mr Vincent Rey, Mr Stéphane Décoppet and Mr Alberto Pagnetti.

I shall be eternally grateful to my parents for the education I received and I am sincerely thankful to my mother, to my sister Claudia and to my brother Alex, because their support and encouragement were always by my side throughout the last four years making geographical distances considerably shorter.

All phenomena in physics require a starter mechanism to initiate. My wife Sara is mine. All the good things happened in my life since I met her come from her inspiration and I am immensely grateful for her continuous support and tender encouragement.

# Table of Contents

# Chapter 1

# Introduction

Lightning electromagnetic effects represents nowadays a major issue in electromagnetic compatibility. Besides the deleterious effects caused by direct strikes, in which case the electric current flowing in the lightning channel is totally injected into the impact point, the danger from lightning is also represented by its indirect effects, due to the induced disturbances produced when the electromagnetic field radiated by remote strikes couples with sensitive electronics or power lines.

The study of the interaction of lightning electromagnetic fields with electrical systems and the design of appropriate protection strategies are generally based on statistical distributions of the lightning current measured at the channel base using either instrumented towers or artificial initiation of lightning using rockets. Recent studies based both on numerical modeling and experimental observations have shown that the presence of the structure struck by or used to initiate lightning does affect the current measurement in a way depending upon the geometry of the structure itself, compromising therefore the reliability of the statistics adopted so far for lightning data.

On the other hand, the indirect estimation of lightning current parameters from measured electromagnetic fields has grown in importance in the past few years thanks to the wide diffusion of Lightning Location Systems (LLS). The enormous amount of data they can provide and the possibility of offering local statistics justifies further investigation of theoretical aspects related to their utilization, namely, the impact of propagation effects of lightning electromagnetic fields on the inferred lightning current.

The above observations constitute the motivation for the present work, whose aim is to provide further elements (from both theoretical and experimental investigations) to improve

the understanding of the electromagnetic consequences of the impact of lightning return strokes to tall structures.

## 1.1 Organization of the thesis

**Chapter 2** introduces to the phenomenology of cloud-to-ground lightning and the importance of lightning return-stroke modeling. Among the different classes of return-stroke models existing in the literature, the attention is focused in this thesis on the so-called engineering models, which allow describing the current distribution along the channel as a function of the current at the channel base and the return-stroke speed, two quantities for which data can be obtained experimentally.

After presenting a review of five engineering return-stroke models describing lightning strikes to ground, the extension of the engineering models to take into account the presence of an elevated strike object is presented and discussed.

**Chapter 3** is devoted to the computation of the electromagnetic field produced by lightning return strokes to elevated strike objects, using the extension of the engineering models to include an elevated strike object presented in the previous chapter.

It is shown that the current distribution associated with these extended models exhibits a discontinuity at the return stroke wavefront which needs to be taken into account by an additional term in the equations for the electromagnetic field, the so-called ‘turn-on’ term. A general analytical formula describing the ‘turn-on’ term associated with this discontinuity for various engineering models is derived and simulation results illustrating the effect of the ‘turn-on’ term on the radiated electric and magnetic fields are also presented.

In the second part of the chapter, dedicated to the investigation of the propagation effects on lightning electromagnetic field traveling along a finitely-conducting ground, the commonly used assumption of an idealized perfectly-conducting ground is relaxed in order to analyze how the electromagnetic field radiated by a tower-initiated strike is affected while propagating along a soil characterized by a finite conductivity.

**Chapter 4** presents a comparison among the predictions obtained using the five extended engineering return-stroke models for lightning strikes to tall structures described in Chapter 2. The spatial-temporal current profiles along the tower-channel axis predicted by the engineering models, as well as the respective predictions for the radiated electric and

magnetic fields, calculated at different distances, are compared and discussed. Further, a model-validation analysis is performed in order to discuss their ability to reproduce the significant features of the observed fields.
A theoretical analysis is performed in the last part of the chapter with the aim to provide, for the same five engineering models extended to take into account the presence of the tower, expressions relating the return-stroke current and the associated distant radiated electric and magnetic fields.

**Chapter 5** reports on the simultaneous GPS-time-stamped measurements of the return-stroke current and of the electric and magnetic fields at three distances associated with lightning strikes to the Toronto CN Tower (553 m) during the summer of 2005. Two propagation paths for the electromagnetic field to the first and to the second field measurement stations (located, respectively, 2.0 km and 16.8 km away from the CN Tower) are along the soil and through the Toronto city, whereas for the third location (50.9 km away) the propagation path is nearly entirely across the fresh water of Lake Ontario.

The measured waveforms are compared with the theoretical predictions obtained using the same five engineering return-stroke models described in the previous chapter.

The theoretical relationship for tall strike objects relating current and field peaks is also tested versus the obtained sets of simultaneously-measured return-stroke currents and fields associated with lightning strikes to the CN Tower.

Finally, the directly-measured lightning currents at the tower are used to test the accuracy of current peak estimates provided by lightning location systems. The gathered data are correlated and compared with the data obtained from the US National Lightning Detection Network (NLDN) showing that the NLDN-inferred values may underestimate the actual current peaks, because the presence of the tall struck object is not included in the algorithm used to infer lightning current peaks from remote field measurements.

**Chapter 6** is devoted to the measurement of electromagnetic fields radiated by lightning. In its first part (Section 6.2), the need for guidelines for reporting lightning data obtained experimentally is emphasized.

The second part of the chapter (Section 6.3) presents the design and the construction of a low-cost, multi-channel lightning field measuring system for the simultaneous measurement of three components of the electromagnetic field radiated by lightning. The proposed system uses one single optical link for the transmission of the three signals, appropriately digitized

and multiplexed, lowering considerably the overall cost of the system itself. The system allows, in addition, controlling remotely the gain of the field antennas.

# Chapter 2

# Modeling of the Lightning Return-Stroke Current: the Engineering Models

## 2.1 Introduction

The practical limitations due to the very large scale of the lightning channel and its unpredictable trajectory make the measurement of a cloud-to-ground-lightning current only possible, at least at this time, at the channel base. All lightning-current data available in the literature have been collected at selected locations, characterized by a higher probability to get struck than flat ground, where it is worth installing permanent equipment. Such privileged points are localized in the grounding path of the structures supporting the two main techniques existing to collect lightning-current data: either a tall tower or the rocket launcher for the artificial initiation of lightning (rocket-triggered lightning).

Even in the presence of a successful measurement of the lightning current at the channel base, the spatial-temporal distribution of the lightning current along the channel remains unknown and needs to be modeled somehow. 'Any lightning model is a mathematical construct designed to reproduce certain aspects of the physical processes involved in the lightning discharge' [*Rakov and Uman*, 2003].

As stated in [*Nucci, et al.*, 1990], return-stroke modeling is of interest essentially for three reasons: (1) as a part of a general investigation into the physics of lightning, (2) as a mechanism by which return-stroke currents at ground can be determined from remotely measured electric and magnetic fields, and hence by which either currents of individual strokes or statistical distributions of the stroke currents can be obtained; and (3) as a mechanism for calculating realistic fields to be used in "coupling" calculations such as to

determine the lightning-induced voltages appearing on electric utility or telecommunication lines when lightning occurs near those lines.

In this chapter, after a brief introduction on the physics of lightning, the modeling of the lighting return stroke is introduced by presenting a brief review of the different modeling philosophies to approach the reality of the natural phenomenon. Among the different approaches existing in the literature, one class of return-stroke models, namely, the engineering models, which will be thoroughly employed throughout this thesis, is presented in detail in this chapter, starting first by their early formulations, introduced to model ground-initiated return strokes (see [*Nucci, et al.*, 1990] for a review) and describing then their extension (in particular the one proposed in [*Rachidi, et al.*, 2002]) introduced recently to take into account the presence of an elevated strike object.

## 2.2 Phenomenology of cloud-to-ground lightning

The lightning discharge is a natural phenomenon whose very complex physics is not completely understood so far. This section introduces to some aspects of lightning physics, those, in particular, which are relevant to the work accomplished within this thesis.
It is worth recalling here some basis of lightning terminology, adapted from [*Rakov and Uman*, 2003].

Lightning, or the lightning discharge, in its entirety, whether it strikes ground or not, is usually termed a "lightning flash" or just a "*flash*" and has a time duration of about half a second. A lightning discharge that involves an object on ground or in the atmosphere is sometimes referred to as a "lightning strike". The term "*stroke*" applies only to components of cloud-to-ground discharges. Each stroke lasts normally less than one millisecond, the separation time between strokes being typically few tens of milliseconds.

### 2.2.1 Classification of cloud-to-ground lightning strikes

Four categories of cloud-to-ground lightning strikes were identified by Berger [*Berger, et al.*, 1975] depending on the direction of the motion of the initial leader (upward or downward) and the sign of the charge deposited along the channel by that same initial leader (positive or negative), as illustrated in Fig. 2.1. The first category, cloud-to-ground lightning moving negative charge to the ground, is the most common (90% of the world-wide cloud-to-ground lightning). Ground-to-cloud (upward) flashes are relatively rare and generally occur either

from mountain tops and tall man-made structures, or they can be triggered from rockets launched toward thunderstorms [*Uman*, 1987]. Indeed, the experimental results presented in Chapter 5 of this thesis, relative to lightning strikes to the 553-m tall CN Tower in Toronto, are very likely to be of the upward type.

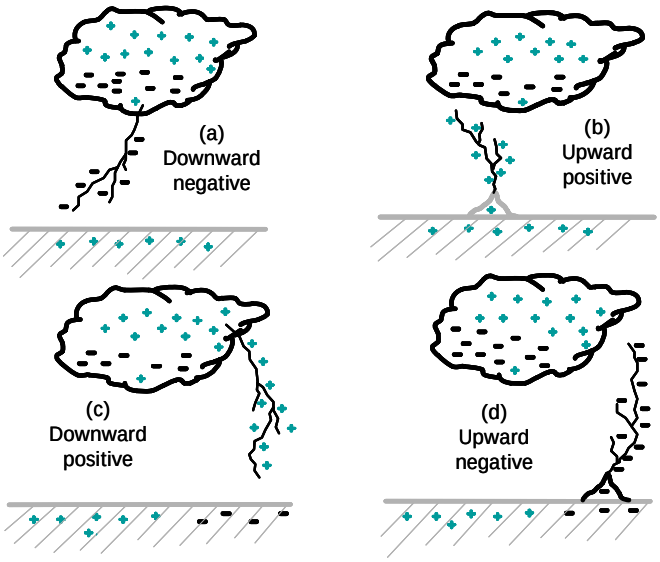


Fig. 2.1 – Drawing showing the four categories of cloud-to-ground lightning (adapted from [*Uman*, 1987]).

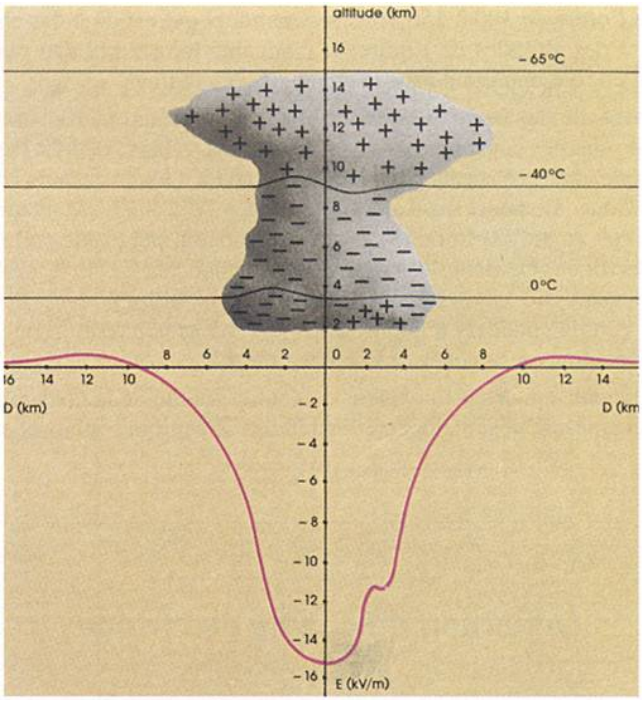


Fig. 2.2 – Drawing showing the charge distribution within a cumulonimbus in the imminence of a cloud-to-ground strike and the corresponding electrostatic field at ground (adapted from [*Gary*, 1995]).

### 2.2.2 Negative downward cloud-to-ground lightning

The explanation of the mechanisms of generation of the typical charge distribution within the thundercloud (cloud electrification, see Fig. 2.2) which precedes the development of a lightning discharge remains a challenge for the researchers and investigations in this sense are beyond the scope of this work.

A *preliminary discharge* within the electrified thundercloud (which is believed originating from the small distribution of positive charges at the bottom of the cloud) initiates the sequence of processes which concur in the development of a negative cloud-to-ground strike, described in Fig.2.3.

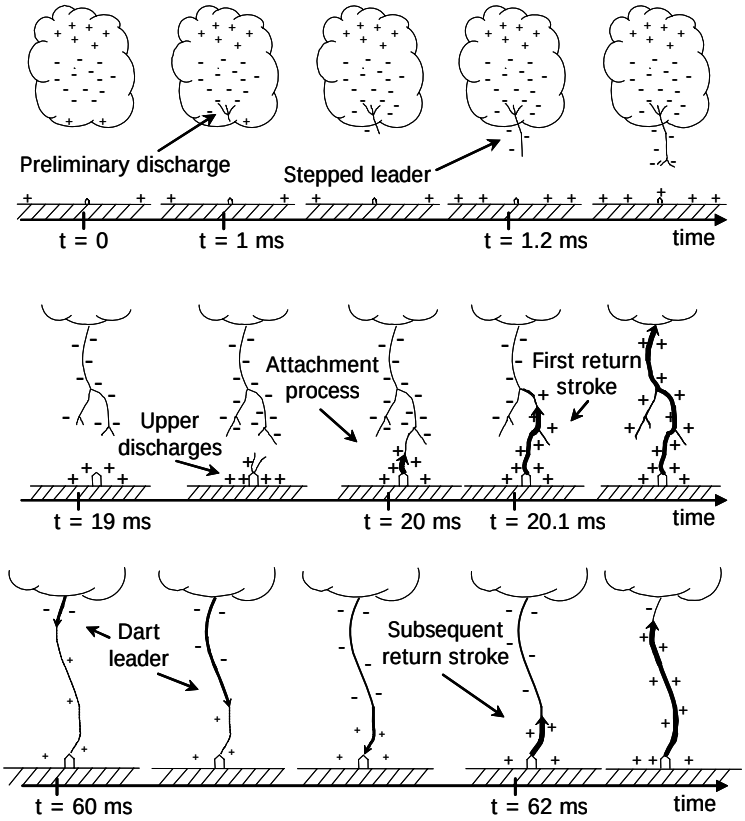


Fig. 2.3 – Drawing showing some of the various processes comprising a negative cloud-to-ground lightning flash (adapted from [*Uman*, 1987]).

A *stepped leader* (induced by the preliminary discharge) initiates the first return stroke in a flash by propagating from cloud to ground in a series of discrete steps. As the leader tip nears ground, the electric field at sharp objects on the ground or at irregularities of the ground itself

exceeds the breakdown value of air and one or more upward-moving discharges from the ground are initiated at those points, thus beginning the *attachment process* [*Uman*, 1987].

When one of the upward-moving discharges from the ground contacts the downward-moving stepped leader some tens of meters above ground, the leader tip is connected to ground potential. The leader channel is then discharged when a ground potential wave, the first return-stroke, propagates continuously up the previously ionized and charged leader path.

After the return-stroke current has ceased to flow, the flash, including the charge motion in the cloud, may end. The lightning is then called a single-stroke flash.

On the other hand, if additional charge is made available to the top of the channel, a continuous *dart leader* may propagate down the residual first-stroke channel. The dart leader then initiates the second (or any subsequent) return-stroke [*Uman*, 1987].

Dart leaders and subsequent strokes are usually not branched.

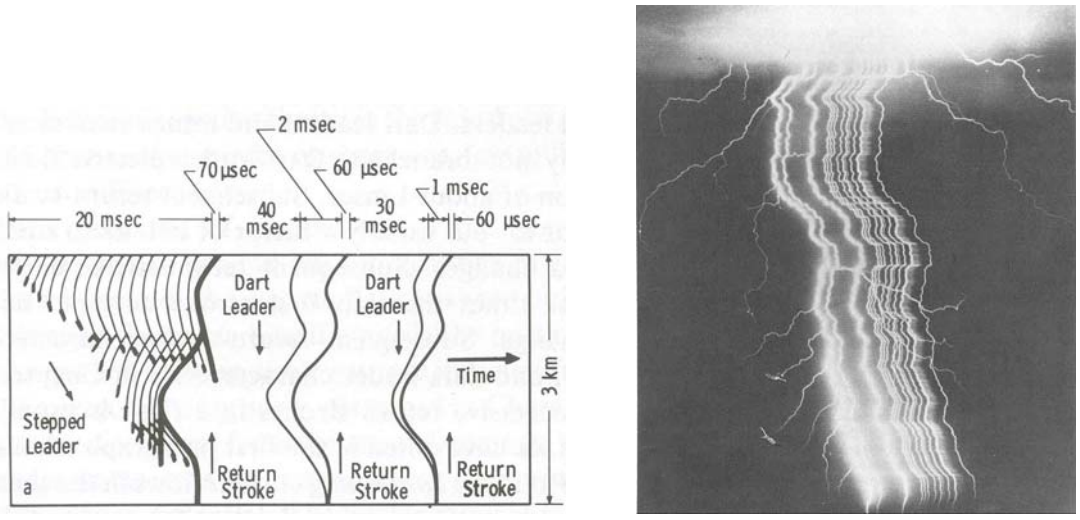


Fig. 2.4 – (a) Drawing of the luminous features of a lightning flash below a 3-km cloud base as would be recorded by a streak camera; (b) streak-camera photograph of a 12-stroke lightning flash (adapted from [*Uman*, 1987]).

### 2.2.3 Upward-initiated lightning from fixed structures

Uman [*Uman*, 1987] defines artificially initiated lightning as a discharge that occurs because of the presence of a man-made structure or event (e.g. a tall tower or rocket-triggered lightning).

Such lightning is characterized by an initial upward-moving leader, recognizable by the presence of upward branches.

Discharges initiated by upward-moving leaders do also occur naturally, for example, from mountain tops.

Upward-initiated lightning has no first return stroke of the type always observed in downward-initiated lightning. Rather its place is taken by an upward-moving leader and any continuous current that may follow when the leader reaches the cloud. This initial upward discharge, however, is often followed by a sequence of dart leaders and subsequent (upward-moving) return strokes which are very similar to the one observed in normal cloud-to-ground lightning [*Uman*, 1987].

## 2.3 Lightning Return-Stroke Models

Four classes of lightning return-stroke models have been defined, primarily distinguished by the type of governing equations [*Rakov and Uman*, 2003]:

1. The first defined class of models, *gas-dynamic* or "physical" models, is primarily concerned with the radial evolution of a short segment of the lightning channel and its associated shock wave. Principal model's outputs include temperature, pressure, and mass density as a function of the radial coordinate and time (e.g. [*Plooster*, 1970; , 1971a; 1971b]).

2. The *electromagnetic* models are usually based on a lossy, thin-wire antenna approximation of the lightning channel. These models involve a numerical solution of Maxwell's equations to find the current distribution along the channel from which remote electric and magnetic field can be computed (e.g. [*Baba and Ishii*, 2001; *Moini, et al.*, 2000; *Petrache, et al.*, 2005a; *Petrache, et al.*, 2005b]).

3. The third class of models is the *distributed-circuit* models, also called RLC transmission line models. They can be viewed as an approximation to the electromagnetic models and they represent the lightning discharge as a transient process on a transmission line characterized by resistance, inductance and capacitance, all per unit length. These models are used to determine the channel current versus time and height and can therefore also by used for the computation of remote electric and magnetic fields. (e.g. [*Little*, 1978; *Price and Pierce*, 1972]).

4. The last class of models comprises the *engineering* models, in which a spatial and temporal distribution of the channel current (or the channel line charge density) is specified based on such observed lightning return-stroke characteristics as the current at the channel

base, the speed of the upward-propagating front, and the channel luminosity profile (e.g. [*Gomes and Cooray*, 2000]; [*Nucci, et al.*, 1990]; [*Rakov and Uman*, 1998]). In these models, the physics of the lightning return stroke is deliberately downplayed[1], and the emphasis is placed on achieving agreement between the model-predicted electromagnetic fields and those observed experimentally at distances from tens of meters to hundreds of kilometers.

Throughout this thesis, the attention will be basically focused on this last class of models[2], essentially for two reasons: firstly, because the engineering models are characterized by a small number of adjustable parameters, usually only one or two besides the specified channel-base current. And, secondly, because their formulation allows the return-stroke current at any point along the lightning channel, $i(z',t)$, to be simply related to a specified channel-base current $i_o(t)$. Indeed, it is only the channel-base current that can be measured directly and for which experimental data are available.

An equivalent formulation of the engineering models in terms of line charge density $\rho_L(z',t)$ along the channel can be obtained using the continuity equation [*Thottappillil, et al.*, 1997].

Among the multiple return strokes that normally take place within a lightning flash, the first stroke is substantially different from the others (subsequent strokes) because, beside a return-stroke current characterized by higher peak value and larger risetime, it is the only one experiencing the presence of channel branches.

Since the engineering models generally do not consider lightning channel branches, they best describe subsequent strokes [*Rakov and Uman*, 2003]. Some works have been published on the effect of including eventual channel branches and tortuosity in the return-stroke model (e.g. [*Shostak, et al.*, 2003]). However, the investigation of the effect of the channel geometry is beyond the scope of this thesis and all the lightning return-stroke models presented in this study will be based on a straight vertical channel geometry, without any branches.

Throughout this thesis we will discuss five engineering return-stroke models among the most widely used ones present in the literature, namely, the Bruce and Golde (BG) model [*Bruce and Golde*, 1941], the traveling current source (TCS) model [*Heidler*, 1985], the transmission line (TL) model [*Uman and McLain*, 1969] and two different modifications of this latter: the modified transmission line model with linear current decay with height

[1] Note, however, that engineering models can indeed be associated with physical processes (e.g. [*Cooray and Theethayi,*2005]).

[2] In Chapter 4, use will also be made of the electromagnetic (or Antenna Theory) models.

(MTLL) [*Rakov and Dulzon*, 1987] and the modified transmission line model with exponential current decay with height (MTLE) [*Nucci, et al.*, 1988; *Rachidi and Nucci*, 1990]. The formulation of each one of them is described in detail in what follows.

## 2.4 Review of Engineering Models

### 2.4.1 The Bruce-Golde (BG) model

The original and perhaps the simplest return-stroke current model is described in [*Bruce and Golde*, 1941]. It considers that the current $i(z',t)$ equals the current at ground $i_o(t)$ beneath the wavefront of the upward-moving return stroke and, like in all the other return-stroke models, the current is zero above it.

Mathematically,

$$\begin{aligned} i(z',t) &= i_o(t) \qquad \forall \quad z' \le vt \\ i(z',t) &= 0 \qquad \forall \quad z' > vt \end{aligned} \tag{2.1}$$

where $v$ is the propagation speed of the return-stroke wavefront and z' is the vertical coordinate.

### 2.4.2 The Traveling Current Source (TCS) model

In the TCS model [*Heidler*, 1985], a current source travels upward at speed $v$ from ground to the cloud. The current injected by this source at height $z'$ is assumed to propagate down the channel at the speed of light $c$. Therefore, the current at height $z'$ would be equal to the current at ground at a later time $z'/c$. This is mathematically described by

$$\begin{aligned} i(z',t) &= i_o(t + z'/c) \qquad \forall \quad z' \le vt \\ i(z',t) &= 0 \qquad \forall \quad z' > vt \end{aligned} \tag{2.2}$$

In both the BG and the TCS models a discontinuity appears at the return-stroke wavefront, which represents an instantaneous removal of charge from the channel at each height $z' = vt$ by the return-stroke wavefront. It has to be noted that it is not physically possible for the current to have the BG or the TCS form (although it may be an approximation to the actual current) because, besides the discontinuity mentioned above, if the return-stroke current is to be uniform with altitude, every point on the return-stroke channel must instantaneously assume the current value at the return-stroke wavefront, and such information transfer cannot

take place at an infinite speed, like predicted for instance by the BG model (e.g. [*Nucci, et al.*, 1990]).

### 2.4.3 The Transmission Line (TL) model

This model assumes that the lightning channel can be represented by a lossless transmission line. Therefore, the current waveform at the ground travels upward, without suffering any distortion or attenuation, at a constant propagation speed *v*.
Mathematically, the TL model is described by

$$\begin{aligned} i(z',t) &= i_o(t - z'/v) \qquad \forall \quad z' \le vt \\ i(z',t) &= 0 \qquad\qquad\qquad\quad \forall \quad z' > vt \end{aligned} \tag{2.3}$$

The TL model only allows the transfer of charge from the bottom of the leader channel to the top and does not remove any net charge from the channel; this is one reason why the field calculated adopting this model does not agree with measurements, particularly at longer times and closer ranges [*Nucci, et al.*, 1990].

Since the TL model does not allow charge to be removed from the leader channel and hence does not produce fields that are realistic at long times, two modifications to the TL model have been proposed by [*Rakov and Dulzon*, 1987] and by [*Nucci, et al.*, 1988].
These two models are described hereunder.

### 2.4.4 The Modified Transmission Line model with linear current decay (MTLL)

In this first modification, proposed in [*Rakov and Dulzon*, 1987], the return-stroke current is supposed to decay linearly while propagating up along the channel and is expressed by

$$\begin{aligned} i(z',t) &= i_o(t - z'/v)\left(1 - z'/H_{tot}\right) \qquad \forall \quad z' \le vt \\ i(z',t) &= 0 \qquad\qquad\qquad\qquad\qquad\quad \forall \quad z' > vt \end{aligned} \tag{2.4}$$

where the factor $H_{tot}$ is the total channel height.

### 2.4.5 The Modified Transmission Line model with exponential current decay (MTLE)

In this second modification, proposed in [*Nucci, et al.*, 1988] (see also [*Rachidi and Nucci*, 1990]), the return-stroke current is supposed to decay exponentially while propagating up the channel and it is expressed by

$$\begin{aligned} i(z',t) &= i_o(t - z'/v)\, e^{-z'/\lambda} \qquad \forall \quad z' \le vt \\ i(z',t) &= 0 \qquad\qquad\qquad\qquad\quad \forall \quad z' > vt \end{aligned} \tag{2.5}$$

where the factor λ determines the decay rate of the current with height. This constant has been determined using experimental data to be about 2 km [*Nucci and Rachidi*, 1989]. The decay constant λ was introduced to take into account the effect of charges stored in the corona sheath of the leader which are subsequently neutralized during the return-stroke phase.

It is worth mentioning here a recent improvement proposed by [*Cooray, et al.*, 2004] to the modified-transmission-line (MTLL and MTLE) models, which, adopting a non-constant attenuation function with height, allows these models to reproduce more accurately some typical features characterizing the electric field measured at several distances from the impact point. This improvement will be discussed more in detail in Section 4.3.3 of this thesis.

### 2.4.6 Distribution and Propagation of Return-stroke Current along the Channel

This Section, largely inspired from [*Rakov and Uman*, 2003] describes clearly the three different approaches characterizing the TL model (and relative modifications to it), the BG model and the TCS model[3].

The three simplest models, BG, TCS and TL are illustrated in Fig. 2.1, in which they are distinguished upon their different values of the current-wave speed *v*. For all three models we assume the same current wavefront at the channel base (*z'* = 0) and the same front speed, represented in *z',t* coordinates by the slanting line labeled $v_f$. The current-wave speed is represented by the line labeled *v*, which coincides with the vertical axis for the BG model and with the $v_f$ line for the TL model. The two modified transmission line models (MTLL and MTLE) are not shown because they exhibit the same current-wave speed as the TL model, from which they only differ in the attenuation of the current waveform along the *z'* axis.

Shown for each model are the current versus time waveforms at the channel base (*z'* = 0) and at heights $z_1'$ and $z_2'$. Because of the finite front-propagation speed $v_f$, the current at height, say, $z_2'$ experiences a delay $z_2'/v_f$ with respect to the current at the channel base. The dark portion of the waveform indicates the current that actually flows through a given

[3] The notation adopted in [*Rakov and Uman,* 2003] (and, hence, in this section) is slightly different from the one adopted in this rest of this thesis: in particular, the current-wave speed is referred as v and the return-stroke speed is referred as $v_f$.

channel section, the blank portion being shown for illustrative purposes only. As can be seen in Fig. 2.1, the TCS, BG and TL models are characterized by different current profiles along the channel, the difference being, from a mathematical point of view, due to the use of different values of $v$ [*Rakov and Uman*, 2003].

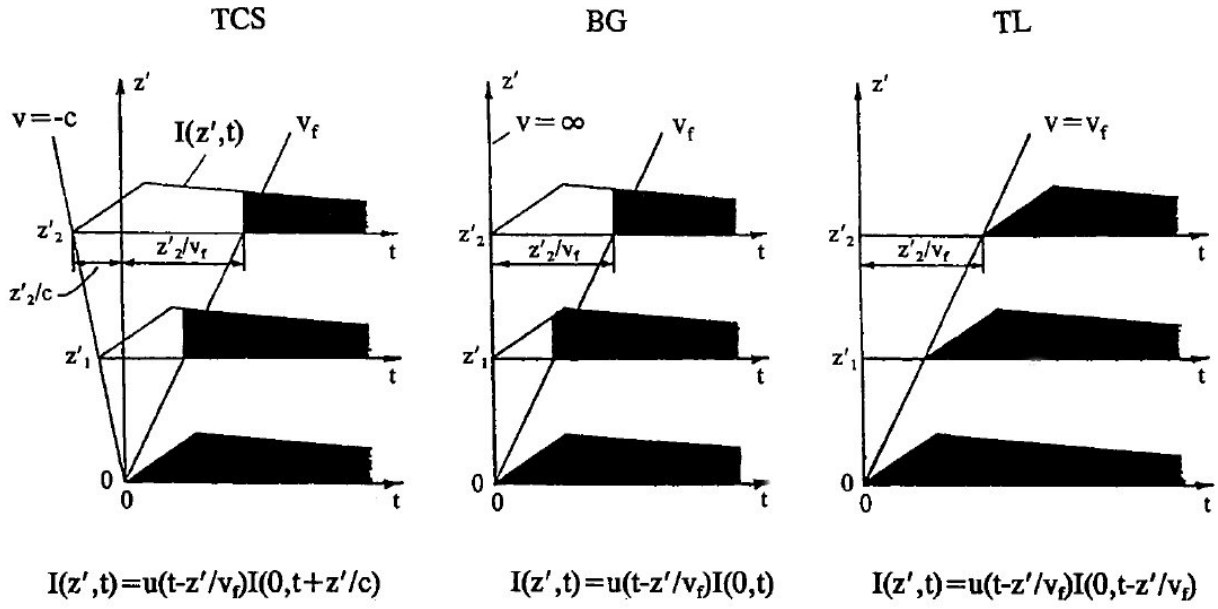


Fig. 2.1 - Current versus time waveforms at ground ($z' = 0$) and at two heights $z'_1$ and $z'_2$ above ground for the TCS, BG, and TL return-stroke models. Slanted lines labeled $v_f$ represent upward speed of the return-stroke front and lines labeled $v$ represent speed of the return-stroke current wave. The dark portion of the waveform indicates current that actually flows through a given channel section. Note that the current waveform at $z' = 0$ and $v_f$ is the same for all three models (adapted from [*Rakov*, 1997]).

The reader is invited to pay attention to the fact that the current distribution along the channel exhibits a discontinuity at the return-stroke wavefront for both the BG and the TCS models, as shown in Fig. 2.1 at the interception between the slanting line $v_f$ and the time axis. Such a discontinuity implies that the charge at each height is removed instantaneously from the channel by the return-stroke wavefront. The treatment of any eventual discontinuity at the return-stroke wavefront will be discussed later in this thesis (Section 3.4).

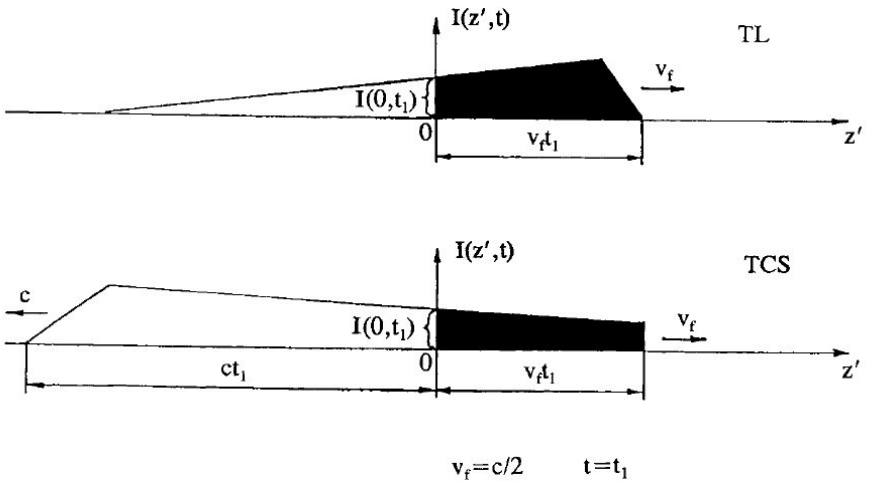


Fig. 2.2 - Current versus height *z'* above ground at an arbitrary fixed instant of time $t = t_1$ for the TL and TCS models. Note that the current at $z' = 0$ and $v_f$ are the same for both the models (adapted from [*Rakov*, 1997]).

### 2.4.7 Two categories of engineering models

The most-used engineering models can be grouped into two categories: the transmission-line-type models and the traveling-current-source-type models[4]. The first category contains the TL, MTLL and MTLE models, which can be viewed as incorporating a current source at the channel base injecting a specified current wave which propagates upward into the channel without any distortion.

In the traveling-current-source-type models category, to which belongs the TCS and the BG models[5], the return-stroke current may be viewed as being generated at the upward-moving-return-stroke front and then propagating downward.

In Fig. 2.2, the relation between the TL and the TCS model is illustrative of the main difference between the two categories of engineering models when formulated in terms of current, namely, the direction of propagation of the current wave: upward for the transmission-line-type models and downward for the traveling-current-source-type models. Note that in Fig. 2.2, the current at ground ($z' = 0$) and the upward-moving front speed $v_f$ are the same for both the TL and the TCS models. Again, as in Fig. 2.1, the dark portion of the waveform indicates the current that actually flows in the channel while the white portion is shown for illustrative purposes only.

[4] The same two categories are referred by [*Cooray,* 2003] as, respectively, current generation (CG) models and current propagation (CP) models.

[5] Since the BG model includes a current wave propagating at an infinitely large speed, the wave's direction of propagation is indeterminate and this model can be associated either with the first or the second category of engineering models [*Rakov and Uman,* 2003]

Note that even though the direction of propagation of the current wave in a model can be either up or down, the direction of the charge flow is the same: charge of the same sign is transported to ground in both types of engineering model. For the most common return stroke, which lowers negative charge to ground, the sense of the positive charge flow is upward so that the current $I$ is by convention positive.

It is worth adding that any engineering model of the transmission-line type (CP models) can be equivalently represented as a traveling-current-source type (CG) model and vice-versa. A mathematical demonstration of this can be found in [*Rachidi and Nucci*, 1990] for the MTLE model and in [*Cooray*, 2003] for all engineering models.

### 2.4.8 General representation of the return-stroke models

All the considered five engineering models can be represented in a general, compact formulation for the current distribution along the channel (see [*Rakov*, 1997] and [*Rakov*, 2002]):

$$i(z',t) = P(z')\, i_o\left(t - z'/v^*\right) u\left(t - z'/v\right) \tag{2.6}$$

where $u(\tau)$, known as the Heaviside function, defined equal to unity for $t \geq z'/v$ and zero otherwise, describes the absence of current flow in the channel above the return-stroke wavefront and allows taking into account any possible current discontinuity at return-stroke wavefront (inherently included in the BG and TCS models formulations). $P(z')$ is the height-dependent current attenuation factor and $v^*$ is the current-wave propagation speed. Table 2.1 defines these two parameters for the introduced five engineering models, in which $H_{tot}$ is the total channel height, $\lambda$ is the current decay constant and $c$ is the speed of light.

Table 2.1 - $P(z')$ and $v^*$ appearing in Eq. (2.6) for five simple engineering models (adapted from [*Rakov*, 1997]).

| Model | $P(z')$ | $v^*$ |
|---|---|---|
| BG | 1 | $\infty$ |
| TCS | 1 | $-c$ |
| TL | 1 | $v$ |
| MTLL | $1-z'/H_{tot}$ | $v$ |
| MTLE | $\exp(-z'/\lambda)$ | $v$ |

## 2.5 Analytical representation of the channel-base current

The analytical expressions usually adopted to represent the channel-base current $i_o(t)$ are based on the one proposed by [*Heidler*, 1985] and frequently referred to as the "Heidler function", defined as

$$i_o(t) = \frac{I_o}{\eta} \frac{(t/\tau_1)^n}{1+(t/\tau_1)^n} e^{-t/\tau_2} \tag{2.7}$$

where

- $I_o$ is the amplitude of the channel-base current
- $\tau_1$ is the front time constant
- $\tau_2$ is the decay time constant
- $n$ is an exponent having values between 2 to 10
- $\eta$ is the amplitude correction factor, obtained by

$$\eta = e^{-\frac{\tau_1}{\tau_2}\left(n\frac{\tau_2}{\tau_1}\right)^{1/n}} \tag{2.8}$$

The Heidler function has been introduced because it satisfies many desired constraints: it features a second-order time derivative equal to zero at $t$ = 0, consistent with measured return-stroke current wave shapes and, additionally, it allows precise and easy adjustment of the current amplitude, maximum current derivative and electrical charge transferred nearly independently by varying $I_o$, $\tau_1$ and $\tau_2$, respectively [*Rakov and Uman*, 2003].

Combinations of a first Heidler function with a second one (e.g. [*Rachidi, et al.*, 2001] ), or with a double-exponential function (e.g. [*Nucci, et al.*, 1990]), are commonly used in order to reproduce a specific return-stroke waveform obtained by measurements.

The formulation of the channel-base current proposed by [*Nucci, et al.*, 1990] for a subsequent return stroke has been lately adopted as a standard channel-base waveform in many other papers from different research groups (e.g. [*Moini, et al.*, 2000; *Pavanello, et al.*, 2004]). This current is expressed as the sum of a Heidler function and a double exponential function according to Equation (2.9)

$$i_o(h,t) = \frac{I_{o1}}{\eta} \frac{(t/\tau_1)^2}{1+(t/\tau_1)^2} e^{-t/\tau_2} + I_{o2}\left(e^{-t/\tau_3} - e^{-t/\tau_4}\right) \tag{2.9}$$

Adopting in Eq. (2.9) the following choice for the parameters: $I_{o1}$ = 9.9 kA, $\eta$ = 0.845, $\tau_1$ = 0.072 μs, $\tau_2$ = 5.0 μs, $I_{o2}$ = 7.5 kA, $\tau_3$ = 100.0 μs and $\tau_4$ = 6.0 μs, this current, whose waveform is shown in Fig. 2.3, exhibits a peak value of 11 kA and a maximum time derivative of 105 kA/μs.

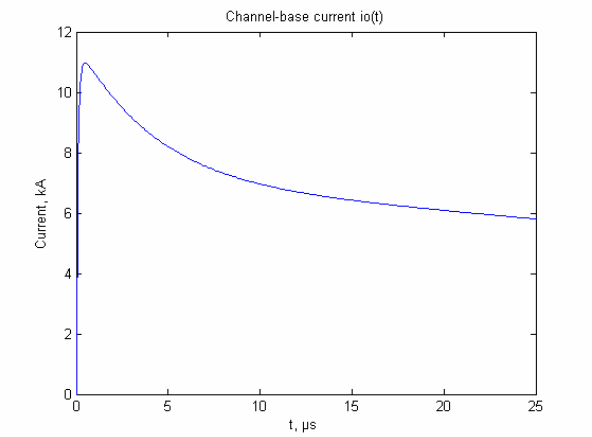


Fig. 2.3 – Channel-base current proposed by [*Nucci, et al.*, 1990]

The currents proposed in [*Rachidi, et al.*, 2001] and in [*Nucci, et al.*, 1990] will be presented in detail later in this thesis, respectively, in Sections 3.4 and 3.5, where they will be adopted for the computations of the field radiated by lightning.

## 2.6 Discussion on the adequacy of engineering return-stroke models

A thorough discussion on the adequacy of engineering return-stroke models has been presented in [*Bermudez, et al.*, 2003b] (see also [*Nucci*, 1995]). The general conclusion is that, for engineering calculations, most of the considered models are adequate since they reproduce fields which are reasonable approximations to available experimental data. The modified versions of the TL model (MTLE and MTLL) are probably the most reasonable compromise between mathematical simplicity and accuracy. However, the TL model is recommended for the estimation of the initial field peak from the current peak or, conversely, the current peak from the field peak, since it is the mathematically simplest model with a predicted field-peak/current-peak relation that is equally or more accurate than that of the more mathematically complex models.

Interestingly, Thottappillil et al. [*Thottappillil, et al.*, 2001] analytically showed that for the TL model the waveforms of the electric and magnetic fields at all points in space and the waveform of their causative current would be identical, if the return-stroke speed were equal to the speed of light.

## 2.7 Extension of the engineering models to take into account ground-based objects

The interaction of lightning with tall strike objects has recently attracted considerable attention among lightning researchers (see [*Rakov*, 2002] for a review), mainly because lightning current data are often collected by means of instrumented towers. For this reason, some of the return-stroke models, initially developed for the case of return strokes initiated at ground level [*Nucci, et al.*, 1990], have been extended to take into account the presence of a vertically-extended strike object [*Rachidi, et al.*, 2002].

The generalized extended return-stroke model considered in this work is based on the solution proposed by [*Rachidi, et al.*, 2002]. According to this model extension, based on a distributed-shunt-current-source representation of the lightning channel, it is assumed that a current pulse $i_o(t)$, associated with the return-stroke process, is injected at the lightning attachment point producing two current pulses, one into the strike object and one into the channel.

The upward-moving wave propagates along the channel at the return-stroke speed $v$ as specified by the return-stroke model and the downward-moving wave propagates at the speed of light $c$ along the strike object (Fig. 2.4). The strike object, considered electrically long, is assumed to be a lossless uniform transmission line characterized by its characteristic impedance $Z_t$ and having constant non-zero reflection coefficients at its top and its bottom, $\rho_t$ and $\rho_g$, respectively.

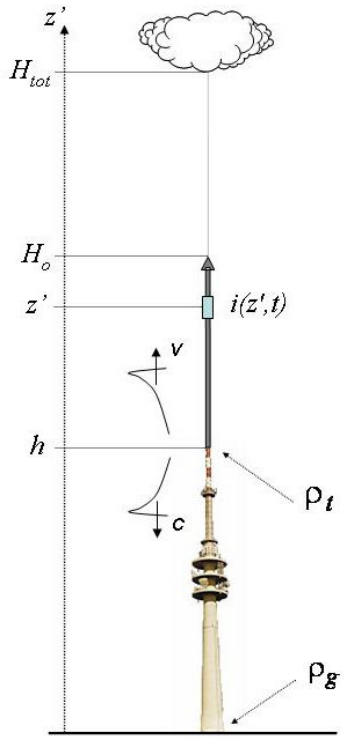


Fig. 2.4 – Propagation of the current pulses along the channel and along the tower

Assuming a distributed-shunt-current-source representation of the lightning channel, the current distributions along the channel and along the strike object are described, respectively, by the following equations:

$$i(z',t)=\left[P(z'-h)\,i_o\left(h,t-\frac{z'-h}{v^*}\right)-\rho_t\,i_o\left(h,t-\frac{z'-h}{c}\right)+\right.$$
$$\left.+(1-\rho_t)(1+\rho_t)\sum_{n=0}^{\infty}\rho_g^{n+1}\rho_t^n\,i_o\left(h,t-\frac{h+z'}{c}-\frac{2nh}{c}\right)\right]u\left(t-\frac{z'-h}{v}\right) \qquad \text{for } h<z'<H_0 \qquad (2.10)$$

$$i(z',t)=(1-\rho_t)\sum_{n=0}^{\infty}\left[\rho_t^n\,\rho_g^n\,i_o\left(h,t-\frac{h-z'}{c}-\frac{2nh}{c}\right)+\right.$$
$$\left.+\rho_t^n\,\rho_g^{n+1}\,i_o\left(h,t-\frac{h+z'}{c}-\frac{2nh}{c}\right)\right]u\left(t-\frac{h+z'}{c}-\frac{2nh}{c}\right) \qquad \text{for } 0\le z'\le h \qquad (2.11)$$

where $\rho_t$ and $\rho_g$ are the top and bottom current reflection coefficients for upward and downward propagating waves, respectively, assumed to be constant and frequency-independent for simplicity, given by:

$$\rho_t = \frac{Z_t - Z_{ch}}{Z_t + Z_{ch}} \tag{2.12}$$

$$\rho_g = \frac{Z_t - Z_g}{Z_t + Z_g} \tag{2.13}$$

Equations (2.10) and (2.11) are generalized for the same five engineering models[6] considered for the case of ground-initiated lightning according to the same height-dependent current attenuation function *P(z')* and the same current-wave propagation speed *v** shown in Table 2.1.

These equations are based on the concept of 'undisturbed current' $i_0\,(h,t)$, which represents the idealized current that would be measured at the tower top if the current reflection coefficients at both extremities of the tower were equal to zero.

For a given expression of $i_0\,(h,t)$, the current distribution along the tower, described by the Eq. (2.11), is essentially determined by the parameters of the lossless uniform transmission line adopted to represent the strike object, namely, its length and the reflection coefficients at its extremities.

Note that equations (2.10) and (2.11) can be equivalently expressed in terms of the short-circuit current $i_{sc}(t) = 2\,i_o(h,t)$ as described in the formulation proposed by [*Rakov and Uman*, 1998] in which a lumped series-voltage source appears at the junction point between the tower tip and the channel.

As in the expression (2.6), the presence of the Heaviside function $u(\tau)$ in (2.10) allows to represent the discontinuity which affects inevitably the current distribution at the return-stroke wavefront for a tower-initiated lightning[7].

The treatment of a discontinuous current at the wavefront in the computation of the electromagnetic field radiated by lightning will be thoroughly discussed in Section 3.4.

As an example of the transient processes that take place when a lightning current is injected at the tip of an elevated strike object, let us consider a simplified model of the 168-m tall Peissenberg Tower in Germany, considered as lossless, uniform transmission line with reflection coefficients set respectively to $\rho_t$ = -0.53 and $\rho_g$ = 0.7 [*Heidler, et al.*, 2001],

[6] It is important to note that the five return-stroke models presented before (like any other that could be adopted) describe only the spatial-temporal distribution of the current along the channel (see Eq. (2.10)), leaving the current distribution along the strike object model-independent (see Eq. (2.11)).

[7] Note that this discontinuity appears equally in the case of a ground-initiated lightning when the reflection at the channel base resulting from the grounding conditions is taken into account because, again, the reflection from ground is modeled to propagate upward at the speed of light.

adopting for the $i_0\,(h,t)$ the channel-base current proposed by [*Nucci, et al.*, 1990] described by Eq. (2.9). The figure 2.5 shows the temporal distribution of the current at the top (a) and at the bottom (b) of the tower, as predicted by Eq. (2.11) for $z' = 0$ and $z' = h$, respectively, significantly influenced by the multiple reflections of the current wave from the tower extremities.

This same example will be adopted for the computation of the radiated electromagnetic field in Section 3.5.

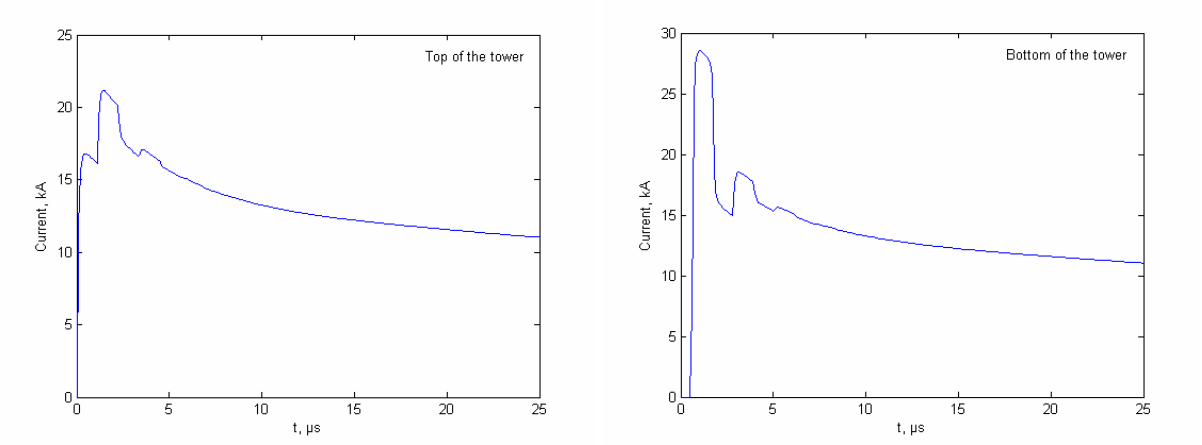


(a) (b)

Fig. 2.5 - Current calculated at the top (a) and at the bottom (b) of a 168-m tall tower.

## 2.8 Discussion on the idealized representation of the elevated strike object

In all extended engineering models, the elevated strike object is modeled as an ideal transmission line. To include the structural nonuniformities of the elevated strike object, several transmission line sections in cascade have also been considered (e.g. [*Rusan, et al.*, 1996; *Shostak, et al.*, 2002]). The transmission line representation of the elevated strike object has been shown to yield reasonable results in comparison with experimental data [*Bermudez, et al.*, 2003a]. However, one should bare in mind that experimental data associated with lightning to tall structures are 'affected' by other, less-easily controlled factors such as the variability of lightning channel impedance (and, consequently, of the reflection coefficient at the tower top) and possible reflections at the return stroke wavefront [*Shostak, et al.*, 2000].

Engineering models require that the reflection coefficients at the top and bottom of the strike object be known. In most of the studies, those coefficients are assumed to be constant and frequency-independent. The values of the reflection coefficients have been inferred by several authors from a limited experimental set of current waveforms found in the literature [*Beierl*, 1992; *Montandon and Beyeler*, 1994; *Willett, et al.*, 1988]. The knowledge of reflection coefficients is also required to extract the undisturbed current, exempt from the disturbances introduced by the transient processes along the tower, using the Eq. (2.11) presented in Section 2.6.

Janischewskyj et al. [*Janischewskyj, et al.*, 1996] derived reflection coefficients at the CN Tower in Toronto from actual measurements and stated that their values depend on the initial risetime of the measured current, although the limited number of points in their plots renders the drawing of conclusions quite difficult. A dependence on the risetime would suggest that at least one of the reflection coefficients is a function of the frequency.

Bermudez et al. [*Bermudez, et al.*, 2003b] derived frequency-domain counterparts of expressions (2.10) and (2.11) which include the frequency-dependence of reflection coefficients. They also derived an expression to calculate the reflection coefficient as a function of frequency at the bottom of the lightning strike object from two currents measured at different heights along the strike object.

They showed that if the current and its time derivative overlap with reflections at the top or bottom of the strike object, it is impossible to derive the reflection coefficient at the top of the strike object exactly from any number of simultaneous current measurements. They proposed an extrapolation method to estimate this reflection coefficient. The proposed methodology was applied to experimental data obtained on the mentioned Peissenberg Tower consisting of lightning currents measured at two heights. The obtained results suggest that the reflection coefficient at ground level can be considered as practically constant in the frequency range 100 kHz to 800 kHz [*Bermudez, et al.*, 2003b].

## 2.9 Conclusions

This chapter introduced to the phenomenology of cloud-to-ground lightning and the importance of lightning return-stroke modeling.

Among the different classes of return-stroke models that exist in the literature, the attention is focused in this thesis on the so-called engineering models, which allow describing

the current distribution along the channel as a function of the current at the channel base and the return-stroke speed, two quantities for which data can be obtained experimentally.

A review of five engineering return-stroke models describing lightning strikes to ground is presented and the main differences among them are thoroughly discussed.

The interaction of lightning with tall structures has recently attracted considerable attention among lightning researchers and the extension of the engineering models which takes into account the presence of an elevated strike object basing on a distributed source representation of the lightning channel [*Rachidi, et al.*, 2002] is presented in Section 2.7.

Section 2.8 presented then a discussion which sustains the adequacy of an idealized representation for the elevated strike object.

# References


Baba, Y., and M. Ishii (2001), Numerical electromagnetic field analysis of lightning current in tall structures, *IEEE Transactions on Power Delivery*, *16*, 324-328.

Beierl, O. (1992), Front Shape Parameters of Negative Subsequent Strokes Measured at the Peissenberg Tower, paper presented at 21st ICLP (International Conference on Lightning Protection), Berlin, Germany, 21-25.09.1992.

Berger, K., R. B. Anderson, and H. Kroninger (1975), Parameters of lightning flashes, *Electra. no.*, *41*, 23-37.

Bermudez, J. L., F. Rachidi, W. A. Chisholm, M. Rubinstein, W. Janischewskyj, A. M. Hussein, V. Shostak, and J. S. Chang (2003a), On the use of transmission line theory to represent a nonuniform vertically-extended object struck by lightning, paper presented at 2003 IEEE Symposium on Electromagnetic Compatibility (EMC), Boston, USA.

Bermudez, J. L., M. Rubinstein, F. Rachidi, F. Heidler, and M. Paolone (2003b), Determination of Reflection Coefficients at the Top and Bottom of Elevated Strike Objects Struck by Lightning, *Journal of Geophysical Research*, *108*, 4413, doi: 4410.1029/2002JD002973.

Bruce, C. E. R., and R. H. Golde (1941), The lightning discharge, *The journal of the institution of electrical engineers*, *88*, 487-520.

Cooray, V. (2003), *The Lightning Flash*, IEE, London, UK.

Cooray, V., V. A. Rakov, F. Rachidi, C. A. Nucci, and R. Montaño (2004), On the constraints imposed by the close electric field signature on the equivalent corona current in lightning return stroke models, paper presented at International Conference on Lightning Protection, ICLP 2004, Avignon, France.

Cooray, V., and N. Theethayi (2005), Effects of corona on pulse propagation along transmission lines with special attention to lightning return stroke models and return stroke velocity, paper presented at VIII International Symposium on Lightning Protection SIPDA, São Paulo, Brazil.

Gary, C. (1995), *La foudre: Des mythologies antiques à la recherche moderne*, MASSSON, Paris, France.

Gomes, C., and V. Cooray (2000), Concepts of lightning return stroke models, *IEEE Transactions on Electromagnetic Compatibility*, *42*, 82-96.

Heidler, F. (1985), Traveling current source model for LEMP calculation, paper presented at 6th Symposium and Technical Exhibition on Electromagnetic Compatibility, Zurich, Switzerland.

Heidler, F., J. Wiesinger, and W. Zischank (2001), Lightning Currents Measured at a Telecommunication Tower from 1992 to 1998, paper presented at 14th International Zurich Symposium on Electromagnetic Compatibility, Zurich, Switzerland, February 20 - 22, 2001.

Janischewskyj, W., V. Shostak, J. Barratt, A. M. Hussein, I. Rusan, and J. S. Chang (1996), Collection and use of lightning return stroke parameters taking into account characteristics of the struck object, paper presented at 23rd ICLP (International Conference on Lightning Protection), Florence, Italy.

Little, P. F. (1978), Transmission line representation of a lightning return stroke, *Journal of Physics D*, *11*, 1893-1910.

Moini, R., B. Kordi, G. Z. Rafi, and V. A. Rakov (2000), A new lightning return stroke model based on antenna theory, *Journal of Geophysical Research*, *105*, 29693-29702.

Montandon, E., and B. Beyeler (1994), The Lightning Measuring Equipment on the Swiss PTT Telecommunications Tower at St. Chrischona, Switzerland, paper presented at 22nd ICLP (International Conference on Lightning Protection), Budapest, Hungary, 1994.

Nucci, C. (1995), Lightning-induced voltages on overhead power lines. Part I: Return stroke current models with specified channel-base current for the evaluation of the return stroke electromagnetic fields, in *Electra*, edited, pp. 74-102.

Nucci, C. A., G. Diendorfer, M. Uman, F. Rachidi, M. Ianoz, and C. Mazzetti (1990), Lightning return stroke current models with specified channel-base current: a review and comparison, *Journal of Geophysical Research*, *95*, 20395-20408.

Nucci, C. A., C. Mazzetti, F. Rachidi, and M. Ianoz (1988), On lightning return stroke models for LEMP calculations, paper presented at 19th international conference on lightning protection, Graz, may 1988.

Nucci, C. A., and F. Rachidi (1989), Experimental Validation of a Modification to the Transmission Line Model for LEMP Calculations, paper presented at 8th International Symposium on Electromagnetic Compatibility, Zurich, Switzerland, March 7-9.

Pavanello, D., F. Rachidi, V. A. Rakov, C. A. Nucci, and J. L. Bermudez (2004), Return Stroke Current Profiles and Electromagnetic Fields Associated with Lightning Strikes to Tall Towers: Comparison of Engineering Models, paper presented at International Conference on Lightning Protection, ICLP 2004, Avignon, France, September 2004.

Petrache, E., F. Rachidi, D. Pavanello, W. Janischewskyj, A. M. Hussein, M. Rubinstein, V. Shostak, W. A. Chisholm, and J. S. Chang (2005a), Lightning Strikes to Elevated Structures: Influence of Grounding Conditions on Currents and Electromagnetic Fields, paper presented at IEEE International Symposium on Electromagnetic Compatibility, Chicago, August 2005.

Petrache, E., F. Rachidi, D. Pavanello, W. Janischewskyj, M. Rubinstein, W. A. Chisholm, A. M. Hussein, V. Shostak, and J. S. Chang (2005b), Influence of the finite ground conductivity on the transient response to lightning of a tower and its grounding, paper presented at 28th General Assembly of International Union of Radio Science (URSI), New Delhi, India., October 23-29, 2005.

Plooster, M. N. (1970), Shock waves from line sources. Numerical solutions and experimental measurements, *Physics of Fluids*, *13*, 2665-2675.

Plooster, M. N. (1971a), Numerical model of the return stroke of the lightning discharge, *Physics of Fluids*, *14*, 2124-2133.

Plooster, M. N. (1971b), Numerical simulation of spark discharges in air, *Physics of Fluids*, *14*, 2111-2123.

Price, G. H., and E. T. Pierce (1972), The modeling of channel current in the lightning return stroke, *Radio Science*, *12*, 381-388.

Rachidi, F., W. Janischewskyj, A. M. Hussein, C. A. Nucci, S. Guerrieri, B. Kordi, and J. S. Chang (2001), Current and electromagnetic field associated with lightning return strokes to tall towers, *IEEE Trans. on Electromagnetic Compatibility*, *43*.

Rachidi, F., and C. A. Nucci (1990), On the Master, Uman, Lin, Standler and the Modified Transmission Line lightning return stroke current models, *Journal of Geophysical Research*, *95*, 20389-20394.

Rachidi, F., V. A. Rakov, C. A. Nucci, and J. L. Bermudez (2002), The Effect of Vertically-Extended Strike Object on the Distribution of Current Along the Lightning Channel, *Journal of Geophysical Research*, *107*, 4699.

Rakov, V. A. (1997), Lightning electromagnetic fields: modeling and measurments, paper presented at 12th International Zurich symposium and Technical Exhibition on electromagnetic compatibility, Zurich.

Rakov, V. A. (2002), Lightning Return Stroke Modeling: Recent Developments, paper presented at International Conference on Grounding and Earthing - GROUND 2002, Rio de Janeiro, Brazil.

Rakov, V. A., and A. A. Dulzon (1987), Results of calculation of the electromagnetic fields of lightning discharges, *Tekhnicheskaya Elektrodinamika. no.*, *1*, 87-89.

Rakov, V. A., and M. A. Uman (1998), Review and evaluation of lightning return stroke models including some aspects of their application, *IEEE Transactions on Electromagnetic Compatibility*, *40*, 403-426.

Rakov, V. A., and M. A. Uman (2003), *Lightning: physics and effects*, Cambridge University Press.

Rusan, I., W. Janischewskyj, A. M. Hussein, and J.-S. Chang (1996), Comparison of measured and computed electromagnetic fields radiated from lightning strikes to the Toronto CN tower, paper presented at 23rd International Conference on Lightning Protection (ICLP), Florence.

Shostak, V., W. Janischewskyj, A. Hussein, J. S. Chang, F. Rachidi, and J. L. Bermudez (2002), Modeling of the electromagnetic field associated with lightning return strokes to a complex tall tower, paper presented at 26th ICLP (International Conference on Lightning Protection), Cracow, Poland, 2002.

Shostak, V., W. Janischewskyj, and A. M. Hussein (2000), Expanding the modified transmission line model to account for reflections within the continuously growing lightning return stroke channel, paper presented at IEEE Power Engineering Society Summer Meeting, Cat. IEEE, Piscataway, USA, 2000.

Shostak, V., W. Janischewskyj, A. M. Hussein, F. Rachidi, J. L. Bermudez, and B. Kordi (2003), Electromagnetic Field associated with Lightning Return Strokes to a Tall Structure: Influence of Channel Geometry, paper presented at 2003 IEEE Bologna PowerTech Conference, Bologna, Italy.

Thottappillil, R., V. A. Rakov, and M. A. Uman (1997), Distribution of charge along the lightning channel: relation to remote electric and magnetic fields and to return-stroke models, *Journal of Geophysical Research*, *102*, 6987-7006.

Thottappillil, R., J. Schoene, and M. A. Uman (2001), Return stroke transmission line model for stroke speed near and equal that of light, *Geophysical Research Letters*, *28*, 3593-3596.

Uman, M. A. (1987), *The lightning discharge*, 377 pp., Academic Press, London, UK.

Uman, M. A., and D. K. McLain (1969), Magnetic field of lightning return stroke, *Journal of Geophysical Research*, *74*, 6899-6910.

Willett, J. C., V. P. Idone, R. E. Orville, C. Leteinturier, A. Eybert-Berard, L. Barret, and E. P. krider (1988), An experimental Test of the "Transmission -Line Model" of Electromagnetic Radiation From Triggered Lightning Return Strokes, *Journal of geophysical research*, *93*, 3867-3878.

# Chapter 3

# Computation of the Electromagnetic Fields Produced by Lightning Return Strokes

## 3.1 Introduction

This chapter is devoted to the computation of electromagnetic fields produced by lightning return strokes to elevated strike objects, basing on the so-called engineering models presented in Chapter 2.

It is shown in that chapter that the current distribution associated with these extended models exhibits a discontinuity at the return stroke wavefront. This discontinuity arises from the fact that the current injected into the tower from its top is reflected back and forth at its ends, and portions of it are transmitted into the channel; these transmitted pulses, which are assumed to travel at the speed of light, catch up with the return stroke wavefront traveling at a lower speed, providing there a non-zero current contribution. Since the engineering models do not consider any current flow into the leader region, this means that the current profile, which is not zero at the return stroke wavefront, must abruptly vanish above it.

Note that this discontinuity appears equally in the case of a ground-initiated lightning when the reflection at the channel base resulting from the grounding conditions is taken into account [*Bermudez*, 2003; *Heidler and Hopf*, 1994].

Until a new model without the discontinuity at the return-stroke front is developed, this discontinuity needs to be carefully treated when calculating the radiated electromagnetic field. However, to the best of our knowledge, the effect of this discontinuity has been disregarded in most studies dealing with the calculation of electromagnetic fields radiated by lightning to tall towers (e.g. [*Diendorfer*, 1991; *Guerrieri, et al.*, 1996; *Guerrieri, et al.*, 1998; *Janischewskyj,*

*et al.*, 1998; *Motoyama, et al.*, 1996; *Rachidi, et al.*, 1992; *Rusan, et al.*, 1996]. Indeed, the discontinuity needs to be represented by an additional term [*Le Vine and Willett*, 1992; *Nucci, et al.*, 1990; *Rubinstein and Uman*, 1990; *Rubinstein and Uman*, 1991 ; *Thottappillil, et al.*, 1997; *Thottappillil and Rakov*, 2001a; *Thottappillil and Rakov*, 2001b; *Thottappillil, et al.*, 1998], the so-called 'turn-on' term, in the well-known electromagnetic field equations.

A general analytical formula describing the 'turn-on' term associated with this discontinuity for various engineering models is derived in this chapter. Simulation results illustrating the effect of the 'turn-on' term on the radiated electric and magnetic fields are also be presented.

The second part of the chapter (Section 3.5) deals with the propagation effects along a finitely-conducting ground. The commonly used assumption of an idealized perfectly-conducting ground is relaxed in order to analyze how the electromagnetic field is affected while propagating along a soil characterized by a finite conductivity. The analysis of propagation effects on the fields radiated from lightning are of interest for several reasons. First, the detection and the localization of the return strokes which strike the ground are of importance in many engineering applications. The efficiency and accuracy of the systems developed for this purpose are influenced by the propagation effects. Second, the propagation effects needs to be taken into account in the determination of the lightning return-stroke current from remote electromagnetic field measurements (e.g. using lightning location systems).

## 3.2 Field computation for a ground-initiated lightning

Starting from Maxwell equations, Uman et al. [*Uman, et al.*, 1975] derived time-domain solutions for the electric and magnetic field radiated by cloud-to-ground lightning strikes as functions of the spatial-temporal distribution of the current along the channel. The simplified geometry considered in that work is composed of a lightning channel modeled as a mono-dimensional vertical antenna above a perfectly conducting ground[1].

For an observation point located at a distance $r$ from the lightning channel and at a height $z$ above the perfect ground, the electromagnetic field contributions from an elemental dipole of current $i(z',t)$ of length $dz'$ located along the vertical axis at $z'$ (see Fig. 3.1) are [*Rubinstein and Uman*, 1989; *Uman, et al.*, 1975]:

[1] The effect of field propagation along a finitely conducting ground will be dealt with in Section 3.5.

$$dE_z(r,z,z',t) = \frac{dz'}{4\pi\varepsilon_o}\left[\frac{2(z-z')^2 - r^2}{R^5}\int_{R/c}^{t} i(z',\tau - R/c)d\tau + \right.$$
$$\left. + \frac{2(z-z')^2 - r^2}{cR^4} i(z',t-R/c) - \frac{r^2}{c^2R^3}\frac{\partial i(z',t-R/c)}{\partial t}\right] \tag{3.1}$$

$$dE_r(r,z,z',t) = \frac{dz'}{4\pi\varepsilon_o}\left[\frac{3r(z-z')}{R^5}\int_{R/c}^{t} i(z',\tau - R/c)\, d\tau + \right.$$
$$\left. + \frac{3r(z-z')}{cR^4} i(z',t-R/c) + \frac{r(z-z')}{c^2R^3}\frac{\partial i(z',t-R/c)}{\partial t}\right] \tag{3.2}$$

$$dH_\phi(r,z,z',t) = \frac{dz'}{4\pi}\left[\frac{r}{R^3} i(z',t-R/c) + \frac{r}{cR^2}\frac{\partial i(z',t-R/c)}{\partial t}\right] \tag{3.3}$$

in which:

- $r$, $z$ are the cylindrical coordinates of the observation point,
- $R$ is the distance between the dipole and the observation point, $R = \sqrt{r^2 + (z'-z)^2}$,
- $i(z',t)$ is the dipole current,
- $c$ is the speed of light
- $\varepsilon_o$ is the permittivity of free space.

In equations (3.1)[2] and (3.2), which describe, respectively, the vertical component and the horizontal component of the electric field calculated at the observation point, three terms are distinguishable. The first term, depending upon the time-domain integral of the current, is known as the electrostatic term; the second one, proportional to the current, is known as the induction term and the third one, varying with the time-derivative of the current, is known as the radiation term. The equation (3.3) describes the azimuthal component of the magnetic

[2] Throughout this thesis, it is adopted for the vertical electric field at ground the sign convention historically accepted in atmospheric-electrical literature, according which an electric field at ground is called positive if it has the same direction as the field due to positive charge above ground level, that is, if the field vector is directed toward the Earth [*Uman,* 1987].

field, which is characterized by the absence of the electrostatic term and by an induction term and a radiation term which have the same dependency on the current distribution as the corresponding terms of the electric field components.

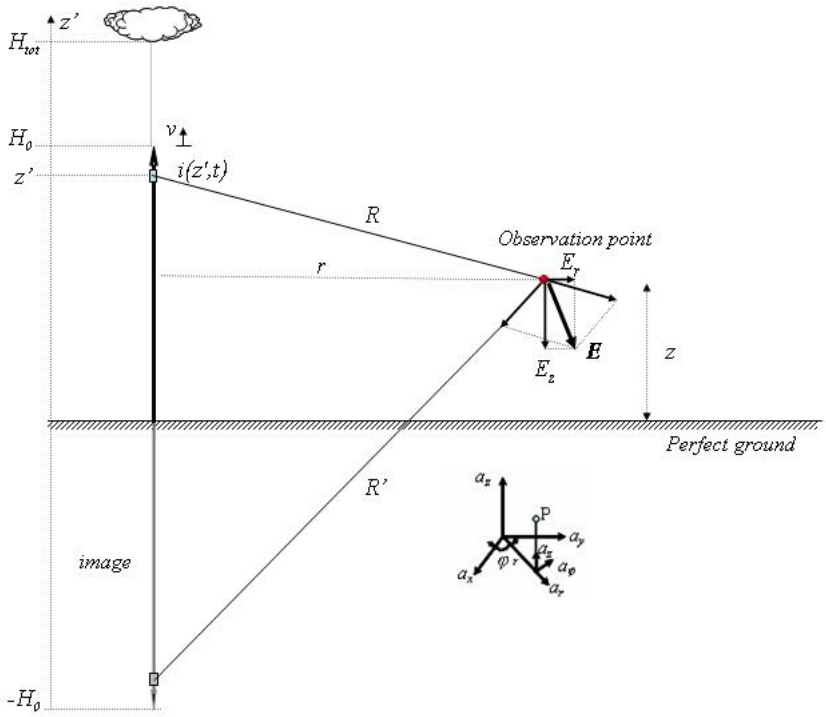


Fig. 3.1 – Adopted geometry for the computation of the field generated by a ground-initiated stroke

For each component of the electromagnetic field, the contribution from an elementary dipole must be added to the contribution produced by its image with respect to ground, because of the assumption of a perfectly-conducting ground. The vertical and radial (horizontal) components of the electric field, and the azimuthal component of the magnetic field calculated at the observation point are thus obtained by integration of (3.1), (3.2) and (3.3), respectively, over the vertical axis (positive and negative portions of it).

## 3.3 Field computation for a tower-initiated lightning

The extension of the simple mono-dimensional-vertical-antenna model adopted for lightning initiated at ground to a tower-initiated strike leaves the geometry unchanged as far as the computation of the electromagnetic field is concerned. This is shown in Fig. 3.2, where the tower, represented schematically by an icon for didactical purposes, is actually modeled by a lossless uniform transmission line. Only the input of the problem of the field computation is

different, namely, the spatial-temporal distribution of the current along the vertical conductor $i(z',t)$, described by the Eq. (2.6), which needs to be replaced by two different current distributions, one along the channel and one along the tower, described, respectively, by the Eqs. (2.10) and (2.11).

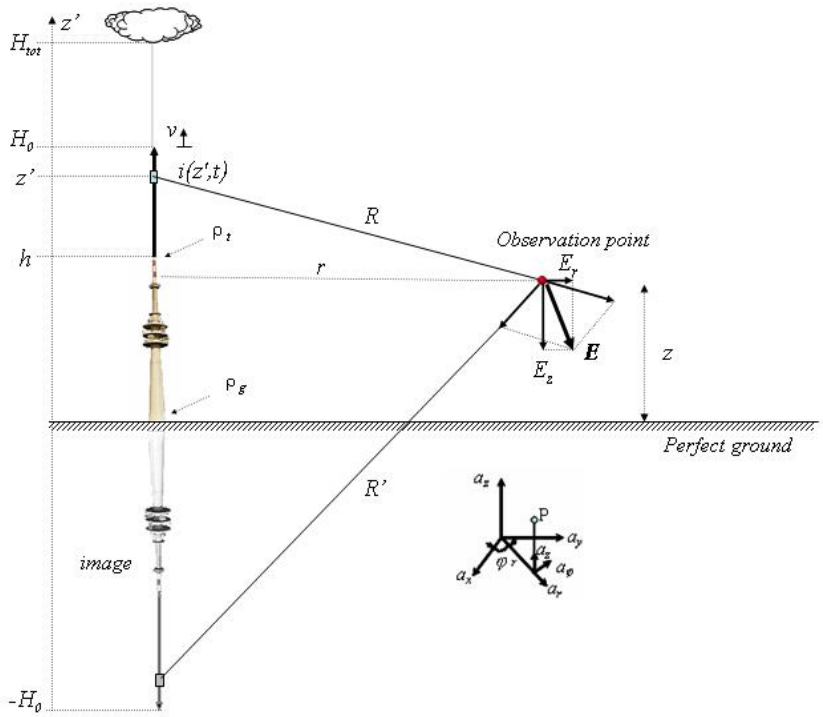


Fig. 3.2 – Adopted geometry for the computation of the field generated by a tower-initiated stroke

## 3.4 Treatment of the current discontinuity at the return-stroke wavefront

The extension of the engineering models which takes into account the presence of the tower (described in Section 2.2) produces a discontinuity in the current distribution at the return-stroke wavefront, which cannot be considered as physically plausible [*Pavanello, et al.*, 2004a]. As mentioned in the Introduction, this discontinuity arises from the fact that the current injected into the tower from its top is reflected back and forth at its ends, and portions of it are transmitted into the channel; these transmitted pulses, which are supposed to travel at the speed of light, catch up with the return-stroke wavefront traveling at a lower speed, providing there a non-zero current distribution. Since the engineering models do not consider

any current flow into the leader region, this means that the current profile, which is not zero at the return-stroke wavefront, must abruptly vanish above it.

This discontinuity needs to be carefully treated when calculating the radiated electromagnetic field through an additional term in the electromagnetic field equations, the so-called 'turn-on' term [*Pavanello, et al.*, 2004a].

The presence of a discontinuous wavefront will now be illustrated for an elevated strike object of height $h = 168$ m, a simplified model corresponding to the Peissenberg Tower in Germany, characterized by reflection coefficients $\rho_t$ = -0.53 and $\rho_g$ = 0.7 [*Heidler, et al.*, 2001][3].

Two different undisturbed channel-base currents are used in the analysis, each one being reproduced by means of a sum of two Heidler functions [*Heidler*, 1985] :

$$i_o(h,t) = \frac{I_{o1}}{\eta_1} \frac{(t/\tau_{11})^{N_1}}{1+(t/\tau_{11})^{N_1}} e^{(-t/\tau_{21})} + \frac{I_{o2}}{\eta_2} \frac{(t/\tau_{12})^{N_2}}{1+(t/\tau_{12})^{N_2}} e^{(-t/\tau_{22})} \tag{3.4}$$

The first waveform (a slow-front current) is characterized by a peak value of 30 kA and a maximum steepness of 12 kA/μs, whereas the second one (a fast-front current) has a peak value of 12 kA and a maximum steepness of 40 kA/μs [*Rachidi, et al.*, 2001]. The same value of the return-stroke speed, $v$ = 150 m/μs, is assumed for both cases. The two waveforms, whose parameters are given in Tab. 3.1, are shown in Fig. 3.3.

Tab. 3.1 – Parameters of the two Heidler functions used to reproduce the undisturbed channel-base current waveforms (adapted from [*Rachidi, et al.*, 2001]).

| | $I_{o1}$ (kA) | $\eta_1$ | $\tau_{11}$ (μs) | $\tau_{21}$ (μs) | $N_1$ | $I_{o2}$ (kA) | $\eta_2$ | $\tau_{12}$ (μs) | $\tau_{22}$ (μs) | $N_2$ |
|---|---|---|---|---|---|---|---|---|---|---|
| Slow-Front Stroke | 28 | 0.823 | 1.8 | 95 | 2 | - | - | - | - | - |
| Fast-Front Stroke | 10.7 | 0.639 | 0.25 | 2.5 | 2 | 6.5 | 0.876 | 2 | 230 | 2 |

[3] Note that there is an apparent contradiction between the choice of a value for $\rho_g$ different from the unity and the assumption of a perfectly conducting ground for the computation of the electromagnetic field. The validity of the definition of the ground reflection coefficient is actually intended to be limited exclusively to the transient processes along the tower and does not interfere with the problem of the field computation, where the soil conductivity is chosen independently from the value adopted for $\rho_g$.

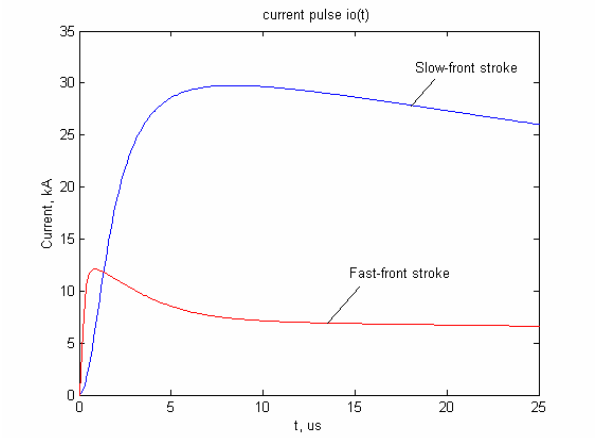


Fig. 3.3 – Undisturbed currents adopted for this study (adapted from [*Rachidi, et al.*, 2001])

The engineering model adopted for this analysis is the MTLE model, described in Section 2.3.5.

Figure 3.4 presents the distribution of the current along the lightning channel at different times for the two different undisturbed currents shown in Fig. 3.3. A discontinuity at the return-stroke wavefront can be clearly distinguished, especially for the 'slow-front' current waveform.

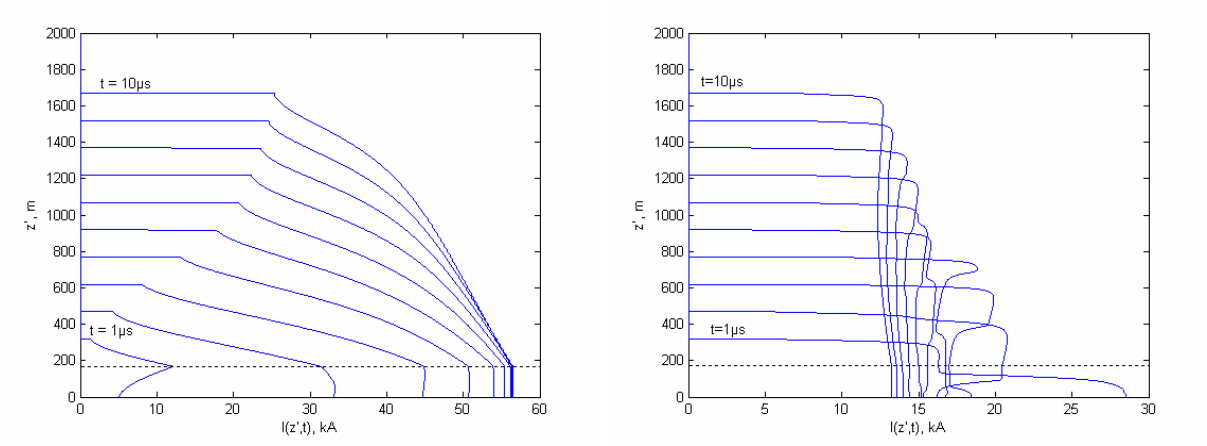


(a) (b)

Fig. 3.4 – Current as a function of z' at different times for slow-front (a) and fast-front (b) strokes. The dashed line corresponds to the height of the tower

### 3.4.1 Mathematical expression of the 'turn-on' term

In the presence of a current discontinuity, the radiation term, namely, the last term in each equation, which is proportional to the current time-derivative, introduces a singularity that needs to be treated separately [*Le Vine and Willett*, 1992; *Rubinstein and Uman*, 1990; *Rubinstein and Uman*, 1991; *Thottappillil, et al.*, 1997; *Thottappillil and Rakov*, 2001a; *Thottappillil, et al.*, 2001; *Thottappillil, et al.*, 1998].

The complete expression of the electromagnetic field is obtained by integrating (3.1) through (3.3) along *z'* from ground level to the wavefront and then by adding the corrective 'turn-on' term across the discontinuity in *H*, expressed as

$$\int_H f(z',z,r)\,\frac{\partial i(z',t-R/c)}{\partial t}\,dz' \tag{3.5}$$

where $f(z',z,r)$ can be $r^2/c^2R^3$, $r(z-z')/c^2R^3$ or $r/cR^2$, depending on which component of the field is being calculated.

It is important to notice here that the position of the wavefront $H_0$ and the position of its image $-H_0$, mentioned in Eq. (2.10) and indicated in Fig. 3.5, are the actual positions at the generic time instant *t*. Due to the propagation time delay, the observer is perceiving at the same instant *t* different positions of these wavefronts, in particular *H* instead of $H_0$, obtained from:

$$t=\frac{H-h}{v}+\frac{1}{c}\sqrt{r^2+(H-z)^2} \tag{3.6}$$

and $H'$ instead of $-H_0$, obtained from:

$$t=\frac{-H'-h}{v}+\frac{1}{c}\sqrt{r^2+(-H'+z)^2} \tag{3.7}$$

The reason for which an additional 'turn-on' term must be introduced in the field equations is that the presence of the Heaviside function in Eq. (2.10) cannot be disregarded when the time-derivative of the current is calculated. Its derivative, namely a delta function, multiplied by the amplitude of the current at the wavefront, needs to be added to the radiation term. In the

case when the current distribution presents no discontinuity at the return-stroke wavefront, this 'turn-on' term contribution vanishes.

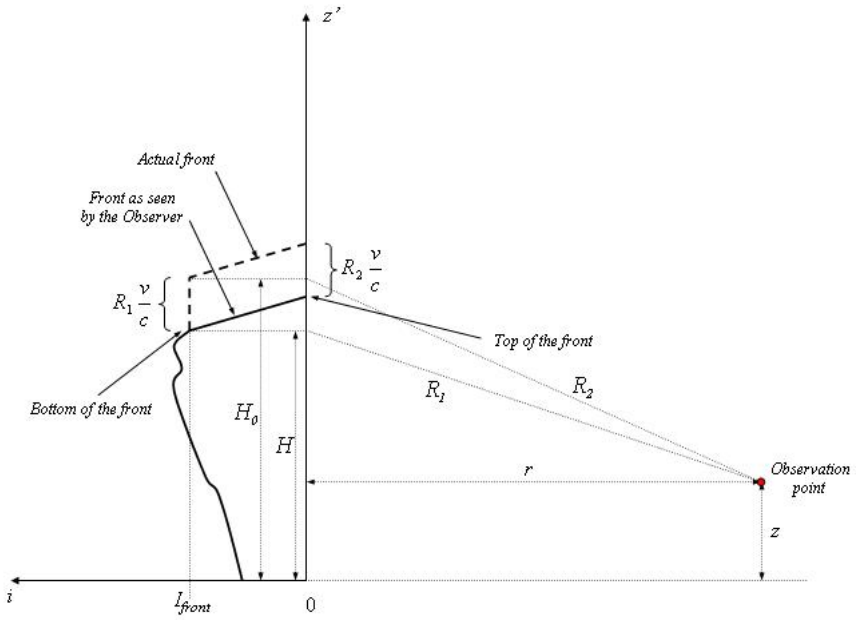


Fig. 3.5 – Treatment of the discontinuity at the return-stroke wavefront, as seen by the observer (Adapted from [*Rubinstein and Uman*, 1991]).

The discontinuity can be treated considering a non-discontinuous current wavefront of length $\Delta z$" which reaches the level $I_{front}$ linearly in a time $\Delta t$, and expressing the radiation integral across $H$ taking the limit when the front duration tends to zero [*Rubinstein and Uman*, 1991].

As a consequence of the different distances covered along the channel by the top and bottom of the front during the propagation time from the wavefront to the observation point, the front has a shorter apparent length $\Delta z$' [*Rubinstein and Uman*, 1990; *Rubinstein and Uman*, 1991] (see Fig. 3.5). $\Delta z$' and $\Delta z$" are related by:

$$\Delta z' = \Delta z'' - \left(R_2 - R_1\right)\frac{v}{c} \tag{3.8}$$

The integral in (8) across the discontinuity reads therefore:

$$\int_H f(z',z,r)\,\frac{\partial i(z',t-R/c)}{\partial t}\,dz' = f(H,z,r)\frac{I_{front}(H)}{\Delta t}\Delta z' = f(H,z,r)\cdot I_{front}(H)\cdot V \tag{3.9}$$

where $I_{front}$ is the amplitude of the discontinuity at the return-stroke wavefront and $V$ can be viewed as the apparent front speed as seen by the observer, which is related to the actual speed $v$ through the following expression:

$$\frac{\Delta z''}{\Delta t} = \frac{\Delta z'}{\Delta t}\left(1+\frac{(R_2-R_1)}{\Delta z'}\frac{v}{c}\right) \tag{3.10}$$

When one reduces the front length taking the limit as $\Delta z'$ goes to zero, both $R_2$ and $R_1$ converge towards $R=\sqrt{r^2+(H-z)^2}$, the distance between the discontinuity and the observation point. After expressing the distances in Cartesian coordinates, straightforward mathematical manipulations leads to the final expressions for the 'turn-on'-term fields, in which the apparent front speed appears as the reciprocal of the term between brackets:

$$H_{\Phi/turn-on} = \frac{I_{front}(H)\cdot r}{4\pi cR^2}\cdot\frac{1}{\left[\frac{1}{v}-\frac{(z-H)}{cR}\right]} + \frac{I_{front}(H')\cdot r}{4\pi cR'^2}\cdot\frac{1}{\left[\frac{1}{v}-\frac{(z-H')}{cR'}\right]} \tag{3.11}$$

$$E_{r/turn-on} = \frac{I_{front}(H)\cdot r\cdot(z-H)}{4\pi\varepsilon_0 c^2R^3}\cdot\frac{1}{\left[\frac{1}{v}-\frac{(z-H)}{cR}\right]} - \frac{I_{front}(H')\cdot r\cdot(z-H')}{4\pi\varepsilon_0 c^2R'^3}\cdot\frac{1}{\left[\frac{1}{v}-\frac{(z-H')}{cR'}\right]} \tag{3.12}$$

$$E_{z/turn-on} = -\frac{I_{front}(H)\cdot r^2}{4\pi\varepsilon_0 c^2R^3}\cdot\frac{1}{\left[\frac{1}{v}-\frac{(z-H)}{cR}\right]} - \frac{I_{front}(H')\cdot r^2}{4\pi\varepsilon_0 c^2R'^3}\cdot\frac{1}{\left[\frac{1}{v}-\frac{(z-H')}{cR'}\right]} \tag{3.13}$$

In equations (3.11)-(3.13), the two terms on the right-hand side represent the 'turn-on' term due to the discontinuity at the wavefront and at its image, respectively.

The general expression for the current at the wavefront is simply obtained from Eq. (2.10) in which the time variable $t$ appears implicitly through $H$ according to Eq. (3.6):

$$
\begin{aligned}
I_{front}(H) = P(H-h)\, i_0\left(h, \frac{H-h}{v} + \frac{1}{c}\sqrt{r^2+(H-z)^2} - \frac{H-h}{v^*}\right) \\
- \rho_t i_0\left(h, \frac{H-h}{v} + \frac{1}{c}\sqrt{r^2+(H-z)^2} - \frac{H-h}{c}\right) \\
+ (1-\rho_t)(1+\rho_t)\sum_{n=0}^{\infty} \rho_g^{n+1}\rho_t^n\, i_0\left(h, \frac{H-h}{v} + \frac{1}{c}\sqrt{r^2+(H-z)^2} - \frac{H+h}{c} - \frac{2nh}{c}\right)
\end{aligned}
\tag{3.15}
$$

It is worth observing that the first term on the right-hand side of Eq. (3.15) is non-zero only for the BG and the TCS models, and it corresponds to the inherent discontinuity predicted by these two models.

Fig. 3.6 shows the current at the return-stroke wavefront (amplitude of the current discontinuity) as a function of time. In the same figure is also shown the current as seen by an observer located at a distance $r = 2$ km.

If a very simple channel current distribution is considered, namely a constant step of magnitude $I_o$ propagating upward at constant speed $v$, then the radiation components of the electromagnetic field will only arise from the discontinuity and this leads back to the analysis provided by Rubinstein and Uman [*Rubinstein and Uman*, 1991].

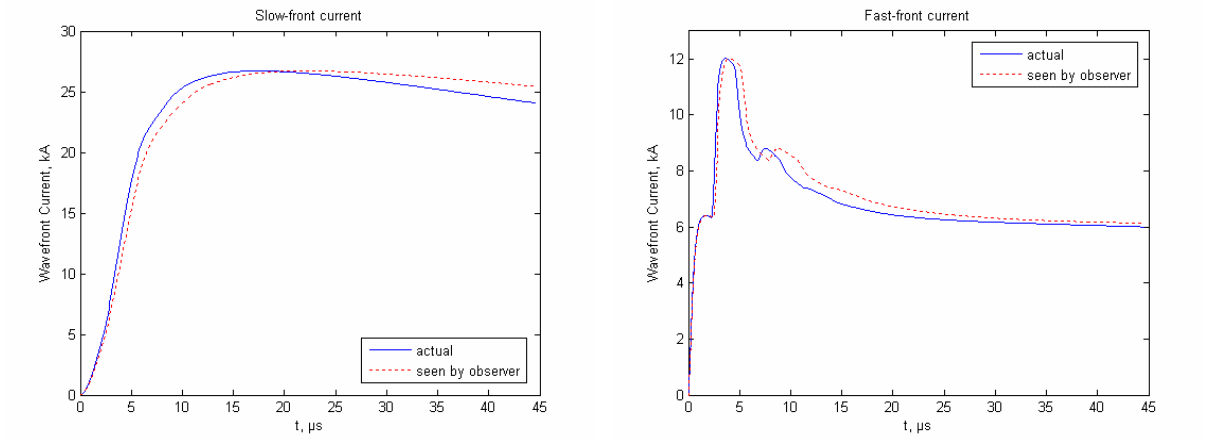


(a) (b)

Fig. 3.6 – Current at the return-stroke wavefront as a function of time for slow-front (a) and fast-front (b) strokes.

### 3.4.2 Influence of the the 'Turn-On' Term on the radiated Electromagnetic Field

Adopting the MTLE model [*Nucci, et al.*, 1988; *Rachidi and Nucci*, 1990] for the return-stroke channel, two examples of simulation for the case of a 168-m tall structure (corresponding to a simplified model of the Peissenberg Tower, Germany) are presented in Figs. 3.7 and 3.8. The structure is characterized by reflection coefficients of -0.53 at the top and 0.7 at the bottom, respectively [*Heidler, et al.*, 2001]. Other parameters used in the computations are the same as those described in Section 3.3.

Figs. 3.7 and 3.8 show the vertical electric and azimuthal magnetic fields produced by the two considered slow-front and fast-front return-stroke currents, observed at ground level 2 km away from the tower. In the same figure, the contribution of the 'turn-on' terms to the total fields is also emphasized. As can be seen, although the contribution to the very first peak of the field is only about 5 % for this example, it becomes more important for intermediate times. This aspect should be taken into account, especially for larger distances [*Pavanello, et al.*, 2004b], where the contribution of the 'turn-on' term can reduce the field decay, canceling the typical zero-crossing of the radiated field after about 40 μs after its onset [*Pavanello, et al.*, Accepted in 2006].

The contribution of the 'turn-on' term to the total field depends on many factors such as the height of the tower, the reflection coefficients at its extremities, the return-stroke speed and the position of the observation point (distance and elevation).

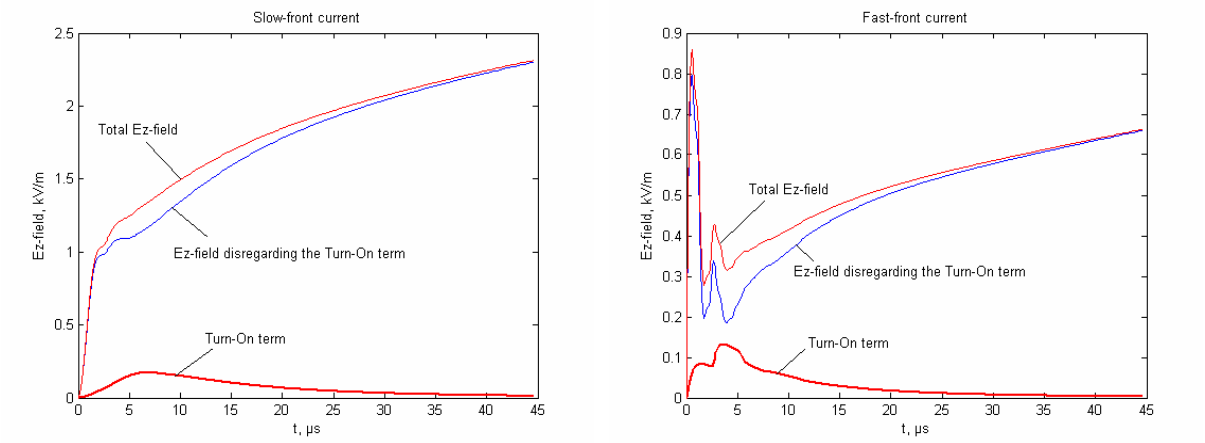


(a) (b)

Fig. 3.7 – Vertical electric field at 2 km from the structure for slow-front (a) and fast-front (b) strokes.

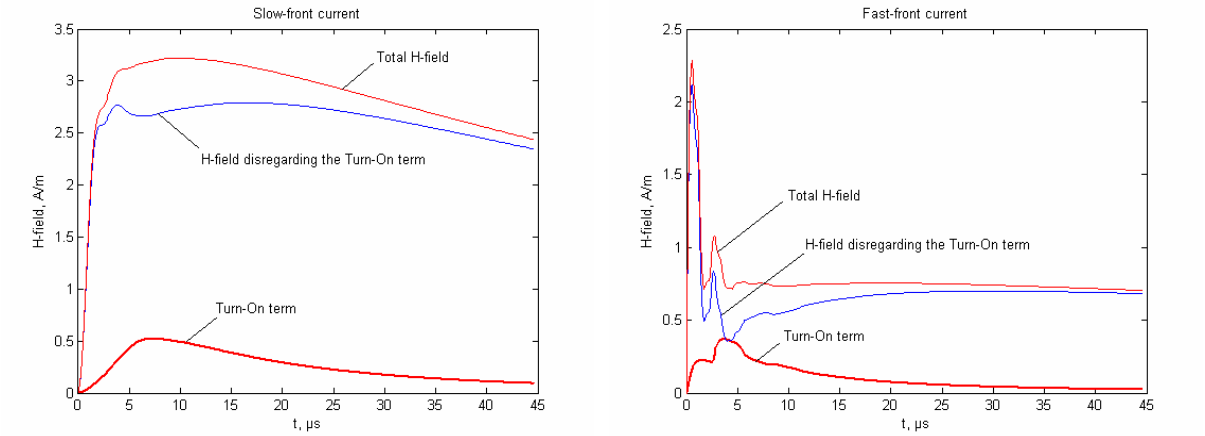


(a) (b)

Fig. 3.8 – Magnetic field at 2 km from the structure for slow-front (a) and fast-front (b) strokes.

### 3.4.3 Discussion on possible solutions to eliminate the current discontinuity

Possible modifications to engineering models could be suggested in order to eliminate this discontinuity, which cannot be considered as physically plausible. Introducing for example an exponential decay of the current in the leader region, modeled as a lossy line, could introduce a better behaved transition between the growing channel and the leader. Another possible solution to avoid the presence of such discontinuity is to assume a reflection coefficient at the return-stroke wavefront set to -1. In this case the value of the current at the return-stroke wavefront is forced to zero, avoiding therefore any discontinuity, but an important source of additional reflections is introduced to increase the complexity of the model.

Recently, Baba and Rakov [*Baba and Rakov*, 2006] presented a further generalization of the TL model to include a tall grounded object and an upward connecting leader. Their model incorporates a lumped voltage source at the junction point between the descending leader and an upward connecting leader launched from the top of the strike object. It is assumed for this model that the current propagation speed along the grounded object is equal to the speed of light $c$ and is equal to the return-stroke wavefront speed $v$ along the lightning channel. This assumption eliminates the existence of any current discontinuity at the return-stroke wavefront because all the reflected waves originated from the multiple reflections along the tower during the transient processes are injected into the channel with the same velocity as the return-stroke wavefront, without any possibility to intercept this latter.

No experimental evidence is available today to give more credit to the assumption of reflected waves propagating into the channel at the same speed of the return-stroke wavefront

(as considered in [*Baba and Rakov*, 2006]) rather than at the speed of light (as considered when writing Eq. (2.10)).

## 3.5 Propagation effects due to finite ground conductivity

Most of the theoretical studies dealing with electromagnetic field radiation from lightning strikes to tall towers assume the ground to be a perfectly-conducting plane. However, there is theoretical and experimental evidence that the finite ground conductivity affects the radiated electromagnetic fields (see e.g. [*Cooray*, 2003]). More precisely, the propagation of lightning electromagnetic fields along the earth surface results in the attenuation of the high frequency components of the field spectrum associated with the initial rise to peak of the electric and magnetic fields. This causes the amplitude of the field to decrease and its risetime to increase with increasing propagation distance and/or decreasing ground conductivity.

The analysis of propagation effects on the fields radiated from lightning are of interest for several reasons. First, the detection and the localization of the return strokes which strike the ground are of importance in many engineering applications. The efficiency and accuracy of the systems developed for this purpose are influenced by the propagation effects especially for distant observation points (about 50 km and beyond) [*Diendorfer, et al.*, 1998]. Knowledge of propagation effects would help to increase the accuracy of these systems.

Moreover, the study of propagation effects finds another important application in the determination of the lightning return-stroke current from remote electromagnetic field measurements (e.g. using lightning location systems), inference that is generally performed assuming a perfectly-conducting ground plane. Again, assessment of the validity of this assumption requires a good knowledge of propagation effects.

In this section it is investigated the effect of the finite ground conductivity on the amplitude and waveshape of the electromagnetic fields radiated by lightning return strokes to tall towers.

Most of the available studies on the propagation effects on lightning generated electromagnetic fields are confined to the case of lightning flashes striking flat ground [*Cooray*, 2003]. On the other hand, studies conducted recently show that the high frequency content in the electromagnetic fields of lightning flashes striking tall structures may differ from the ones striking flat ground [*Cooray, et al.*, 2006; *Pavanello, et al.*, 2005; *Schulz and Diendorfer*, 2004]. Consequently, the way in which the intial peak and the risetime of the

electromagnetic radiation field are modified by the propagation effects may differ in lightning striking tall structures in comparison to lightning striking flat ground.

### 3.5.1 Theory of the propagation adopted in this study

The propagation effects are evaluated using the theory elaborated by Cooray [*Cooray*, 2003], based on the early works of Norton [*Norton*, 1937], which will be summarized hereunder. The equations presented are valid for radiation (far) fields, for distances not exceeding distances of about 300 km, above which the curvature of the earth and the ionospheric effects have to be taken into account [*Wait*, 1986].

The geometry of the problem under consideration is shown in Fig. 3.9. For distant observation points, assuming a perfectly conducting ground and neglecting the static and induction components of the electric field, and considering $R \cong r$ and $r >> H$, the general expression for the electric and magnetic fields for an observation point located at ground level reduces to [*Uman*, 1985]

$$E_z^{far}(r,t) = -\frac{1}{2\pi\varepsilon_o c^2 r}\int_0^H \frac{\partial i(z', t - r/c)}{\partial t}\, dz' \tag{3.16}$$

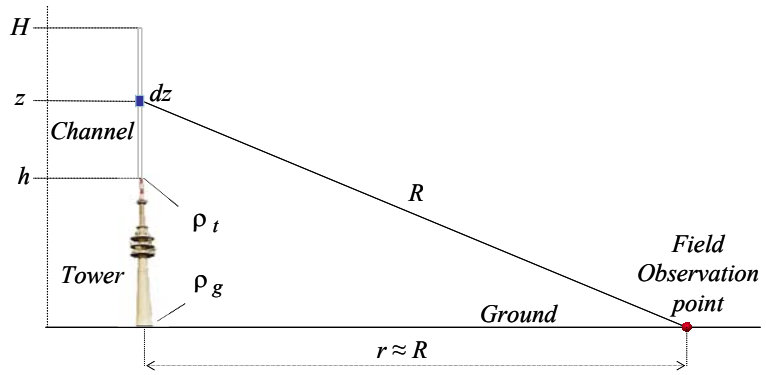


Fig. 3.9 – Geometry relevant to the calculation of the effects of the propagation over a ground of finite conductivity.

As shown by Cooray [*Cooray*, 1987], the expression for the radiated vertical electric field over a finitely conducting ground is given by

$$E_{z,\sigma}^{far}(r,t) = \int_0^t E_z^{far}(r, t-\tau)\, S(r,\tau)\, d\tau \tag{3.17}$$

In which *S(r,t)* is an attenuation function, given, for the case of a homogeneous ground, by [*Wait*, 1956; *Wait*, 1957] :

$$S(r,t) = \frac{d}{dt}\left[1 - \exp\left(-\frac{t^2}{4\zeta^2}\right) + 2\beta(\varepsilon_r + 1)\frac{J(x)}{t}\right] \tag{3.18}$$

where $J(x) = x^2(1-x^2)\exp(-x^2)$, $x = t/2\zeta$, $\beta = 1/(\mu_o \sigma c^2)$ and $\zeta^2 = r/(2\mu_o \sigma c^3)$.

It can be shown [*Cooray*, 1987] that the third term appearing in the brackets of Eq. (3.18), which takes into account the effect of the displacement current in the ground, becomes negligible for propagation distances beyond 1 km, as far as the risetime and the peak attenuation are concerned. This term has been neglected in the computations presented in this study.

Specific expressions for *S(r,t)* are available for inhomogeneous ground models (vertically- and horizontally-stratified) [*Cooray*, 2003].

### 3.5.2 Undisturbed current and tall tower configurations

In the present study of the propagation effects [*Pavanello, et al.*, 2005], the computations are performed assuming the MTLE model for the current distribution along the channel and considering for the undisturbed current $i_o(t)$ the expression proposed in [*Nucci, et al.*, 1990], whose expression is given in Eq. (2.9) and whose waveform is shown in Fig. 2.3.

In addition to the case of ground-initiated lighting, two simplified models of elevated strike objects are also considered in this study: (1) a 168-m tall model corresponding to the Peissenberg tower in Germany, with reflection coefficients set respectively to $\rho_t$ = -0.53 and $\rho_g$ = 0.7 [*Heidler, et al.*, 2001], and, (2) a 553-m tall model corresponding to the CN Tower in Canada, with reflection coefficients set respectively to $\rho_t$ = -0.48 and $\rho_g$ = 0.5 [*Rusan, et al.*, 1996].

### 3.5.3 Lightning return stroke initiated at ground level

Consider first the case of a return stroke initiated at ground level. Figure 3.10 represents the vertical electric field computed at 100 km from the lightning channel, considering two different values for the return-stroke speed (100 m/μs and 150 m/μs). The computations are performed considering a homogeneous ground with three different values for the ground conductivity, namely, infinity (perfect ground), 0.01 S/m and 0.001 S/m.

It is worth noting that, for this analysis of field radiated from ground-initiated lightning, the reflection coefficient at ground $\rho_g$ has been chosen equal to zero in accordance with the choice adopted in [*Nucci, et al.*, 1990].

It can be seen that, as expected, the propagation along an imperfectly conducting ground causes the amplitude of the field to decrease and its risetime to increase with decreasing ground conductivity.

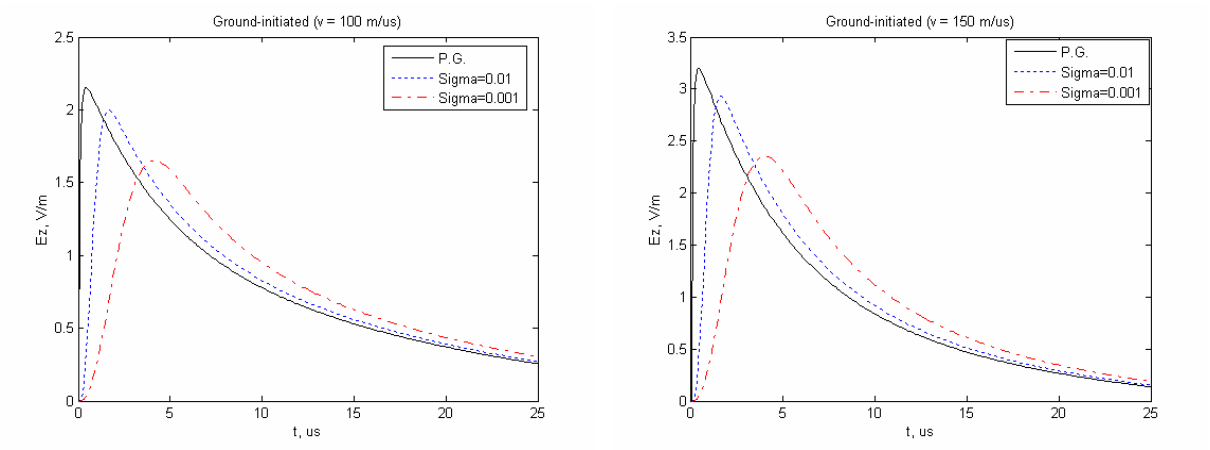


(a) (b)

Fig. 3.10 – Electric field at 100 km generated by a cloud-to-ground lightning return stroke. (a) Return-stroke speed $v$=100 m/μs, (b) $v$=150 m/μs.

### 3.5.4 Lightning return stroke to a tall tower

Figures 3.11 and 3.12 present the vertical electric field calculated at 100 km from the tower, for both tower configurations (Peissenberg tower and CN Tower). Again, the computations are performed starting from the undisturbed current $i_0(t)$ of Fig. 2.3 and considering different values for the return-stroke speed (100 m/μs and 150 m/μs) and for three ground conductivities (infinity, indicated as P.G. for perfect ground, 0.01 S/m and 0.001 S/m). Table 3.2 summarizes the main parameters of the electric field waveform for both a lightning strike to ground and to the tower, as a function of the ground conductivity, for the case of a return-stroke speed equal to 150 m/μs.

It can be seen that the effect of the finite ground conductivity on the field peak value depends strongly on the elevated strike object parameters. For a finite ground conductivity of 0.001 S/m, the peak value of the field generated by a ground-initiated stroke is reduced by a factor of 1.3, compared to the perfect ground case. This same ratio is about 2.5 for the

Peissenberg-tower model and 1.5 for the CN-Tower model. The differences are, however, less significant for the maximum steepness and time-to-peak risetime.

It is also interesting to note that the enhancement effect of the tower (with respect to a ground-initiated return stroke) on the peak field, which is considerable for a perfectly conducting ground, tends to become less significant for a lossy ground. Indeed, the ratio of the 168-m tall tower field peak to the ground-initiated one, about 4.7 for a perfectly-conducting ground, drops to 2.5 for a ground conductivity of 0.001 S/m.

Finally, Figs. 3.11 and 3.12 show that some of the fine structure of the electromagnetic fields associated with transient processes along the struck tower vanishes due to propagation effects.

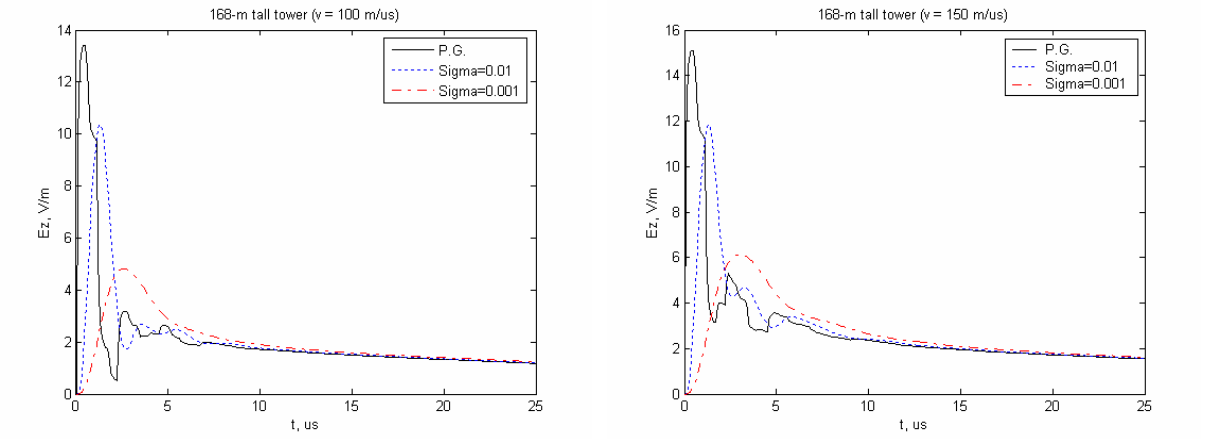


(a) (b)

Fig. 3.11 – Electric field at 100 km generated by a lightning return stroke to a 168-m tall tower. (a) Return-stroke speed $v$=100 m/μs, (b) $v$=150 m/μs.

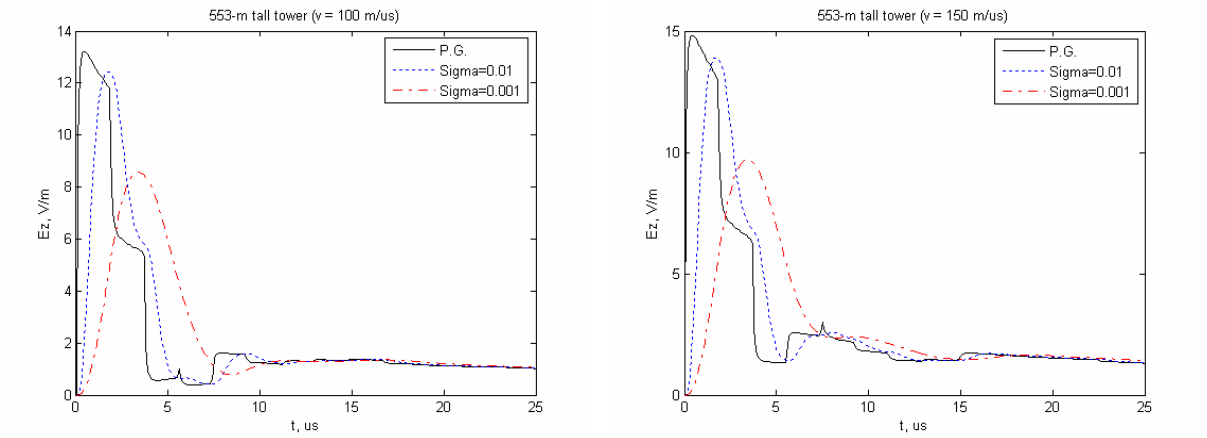


(a) (b)

Fig. 3.12 – Electric field at 100 km generated by a lightning return stroke to a 553-m tall tower. (a) Return-stroke speed $v$=100 m/μs, (b) $v$=150 m/μs.

Table 3.2 - Parameters of electric field at 100 km as a function of ground electrical conductivity for $v$ = 150 m/μs.

| | Ground-initiated return stroke | | | Return stroke to a 168-m tower | | | Return stroke to a 553-m tower | | |
|---|---|---|---|---|---|---|---|---|---|
| Ground conductivity (S/m) | Infinity | 0.01 | 0.001 | Infinity | 0.01 | 0.001 | Infinity | 0.01 | 0.001 |
| Peak (V/m) | 3.2 | 2.9 | 2.4 | 15.1 | 11.9 | 6.1 | 14.8 | 13.9 | 9.7 |
| Max. steepness (kV/μs) | 23.0 | 3.5 | 1.0 | 112.0 | 16.0 | 3.8 | 110.0 | 13.0 | 4.7 |
| Time to peak (μs) | 0.4 | 1.6 | 4.0 | 0.4 | 1.3 | 3.0 | 0.4 | 1.7 | 3.4 |

### 3.5.5 Systematic analysis of the parameters influencing the field propagation effects

In what follows, a more complete analysis, based on [*Cooray, et al.*, 2006], presents under a systematic approach the influence of various parameters of the model (namely, the current risetime, the tower height, the ground conductivity and the distance from the strike point) on the propagation effects affecting the radiated electromagnetic field, computed basing on the same theoretical fundaments described in Section 3.5.1.

Five different undisturbed currents are considered: the one adopted in Section 3.5.4 and described by Eq. (2.9) (characterized by a peak value of 11 kA and a risetime of 0.2 μs) and four more, having the same peak value (11 kA) but with progressively increased risetime values (0.4, 0.6, 0.8 and 1 μs), obtained by varying the values of the parameters in (2.9). The five currents are shown in fig. 3.13.

The length of the elevated strike object is varied from 0 to 300 m by steps of 50 m and the reflection coefficients at its extremities are assumed to be constant and equal respectively to $\rho_t$ = -0.5 and $\rho_g$ = 1.

The engineering model adopted to describe the current distribution along the channel for this systematic analysis is the TL model.

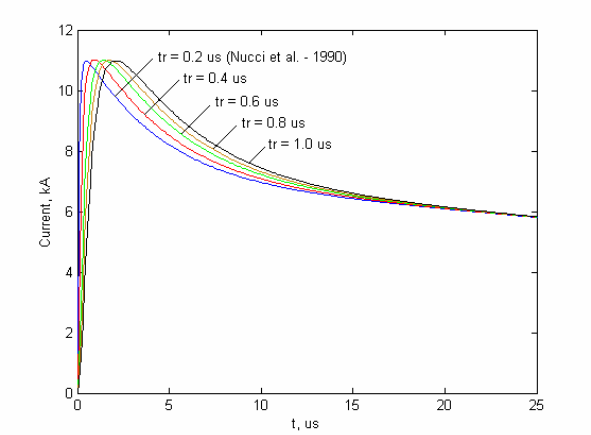


Fig. 3.13 - Undisturbed current waveforms adopted in this study (adapted from [*Cooray, et al.*, 2006]).

Let us first describe the effect of the current risetime on the electric field radiated over a perfectly conducting ground. The electric field at 100 km is calculated for three different configurations of strike object (strike to ground, strike to a 50-m tall tower and to a 300-m tall tower) considering the two cases characterized by the extreme values assumed for the current-risetime variation: 0.2 μs and 1.0 μs. These two cases are shown, respectively, in Subfigs. 3.14(a) and 3.14(b).

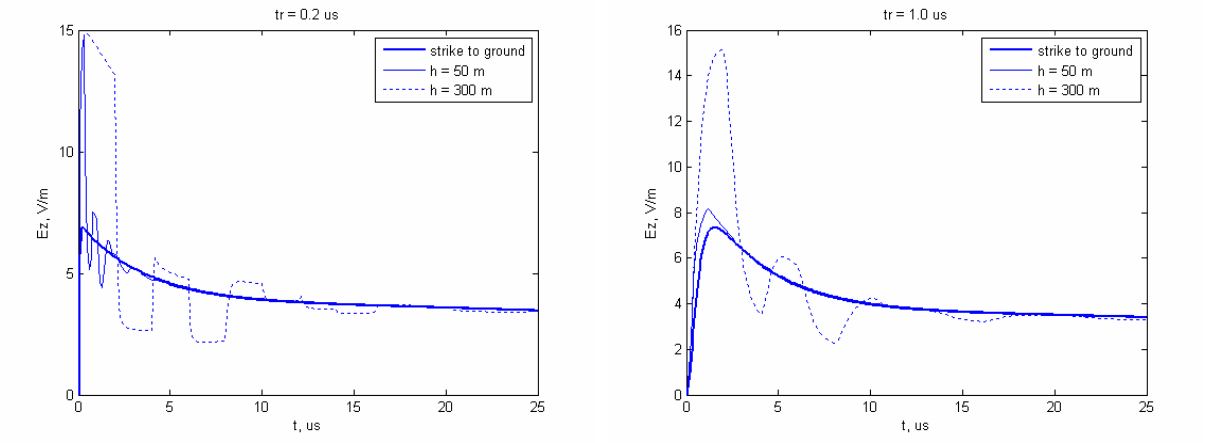


(a) (b)

Fig. 3.14 – Electric field at 100 km for three different tower heights assuming (a) $t_r$= 0.2 μs and (b) $t_r$=1.0 μs.

It can be observed in particular that for a 50-m tall tower a lightning current having a risetime equal to 1.0 μs will produce a field peak sensibly lower than what obtained with a faster current. This because the transient processes along the tower do not have enough time to develop completely since the propagation time of the current wave along the tower is much

smaller than the current risetime. For the same reason, such a difference between the field peaks obtained with the two currents is no more visible when considering a 300-m tall tower.

In order to analyze how the remoteness of the observer from the impact point affects the propagation over a finitely conducting ground, the electric field produced by a 0.2-μs-risetime current striking a 50-m tall tower is calculated for several distances.

The calculations, performed for three values of ground conductivity, namely, 0.01 S/m, 0.001 S/m and 0.0001 S/m, are shown, respectively, in Fig. 3.15 ((a), (b) and (c)).

Note that all the waveforms are normalized to 100 km assuming inverse distance dependence. This means that, in the absence of propagation effects, all the waveforms would have the same shape and amplitude.

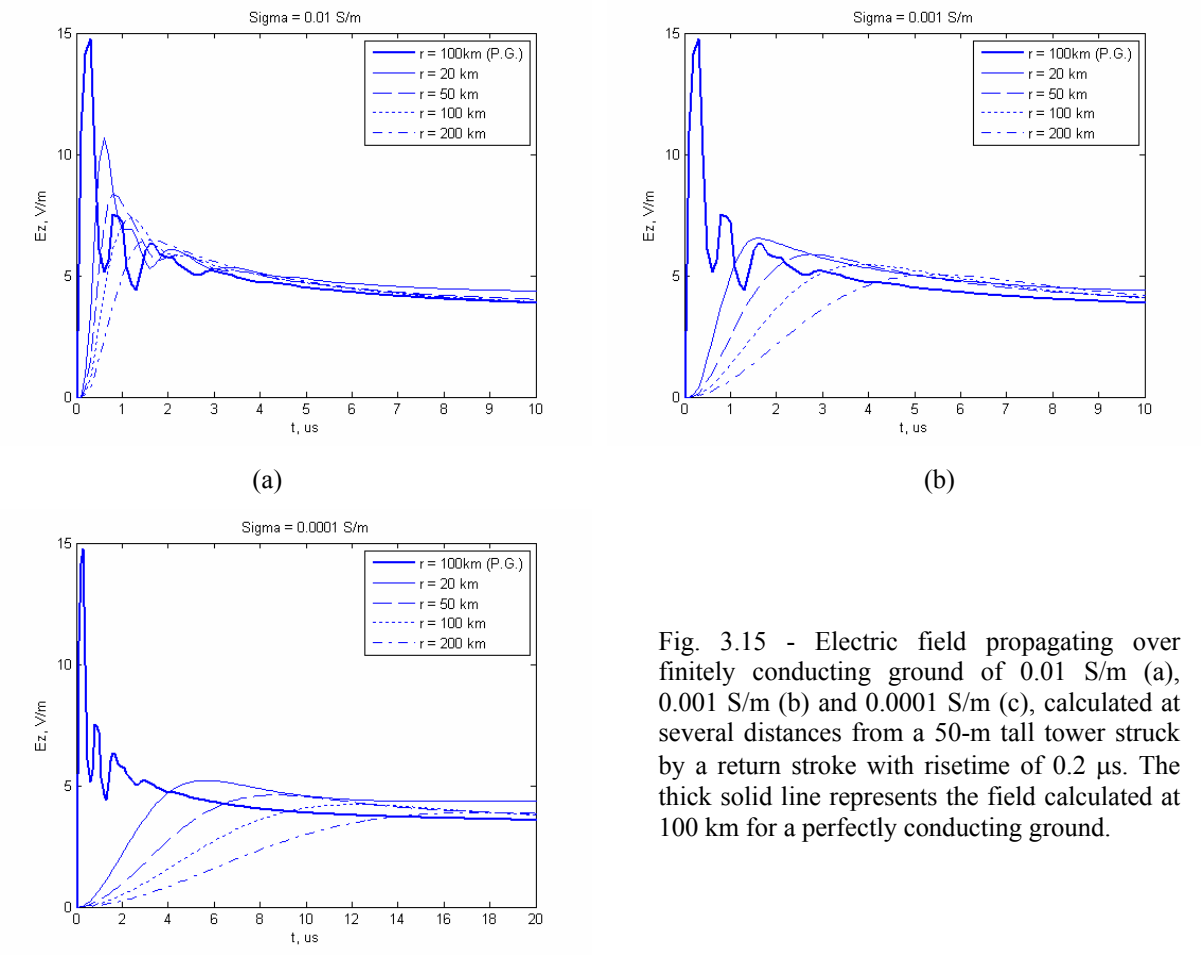


(a) (b)

(c)

Fig. 3.15 - Electric field propagating over finitely conducting ground of 0.01 S/m (a), 0.001 S/m (b) and 0.0001 S/m (c), calculated at several distances from a 50-m tall tower struck by a return stroke with risetime of 0.2 μs. The thick solid line represents the field calculated at 100 km for a perfectly conducting ground.

It can be seen how the field peak value decreases as far as the electromagnetic wave propagates along the finitely conducting ground, and how the fine structure of the field

waveform, produced by the transient processes along the tower, tends to smooth out with increasing distances.

Comparing for the three subfigures 3.15 ((a), (b) and (c)) the fields calculated at the same distance allows one to observe that decreasing the value of the ground conductivity affects the properties of the electric field in a similar way as increasing the propagation distance.

Fig. 3.16 shows the electric fields resulting from a 0.2-μs-risetime current striking a 50-m tall tower and a 300-m tall one, calculated at 100 km over a finitely conducting ground of 0.01 S/m (a), 0.001 S/m (b) and 0.0001 S/m (c). Interestingly, the peak value of the electric field radiated by the 50-m tall tower reduces to its half when compared to the same field calculated for perfect ground. The field produced in the same conditions by a 300-m tall tower (whose perfect-ground radiated field is characterized by the same peak value as the 50-m tall tower but also by a much larger peak width) does not experience such a high attenuation.

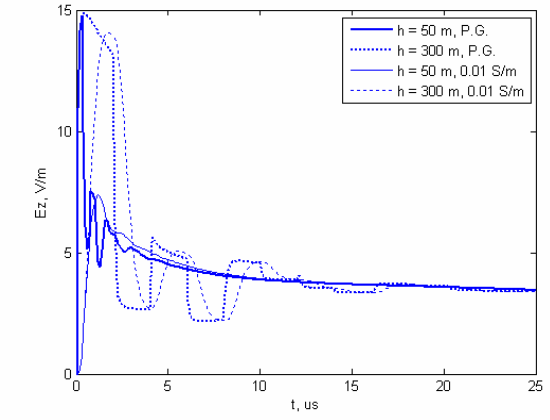


(a)

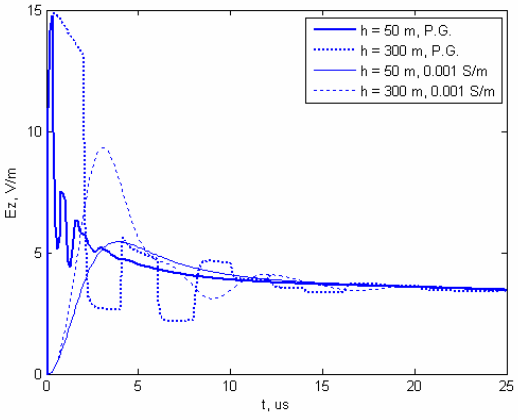


(b)

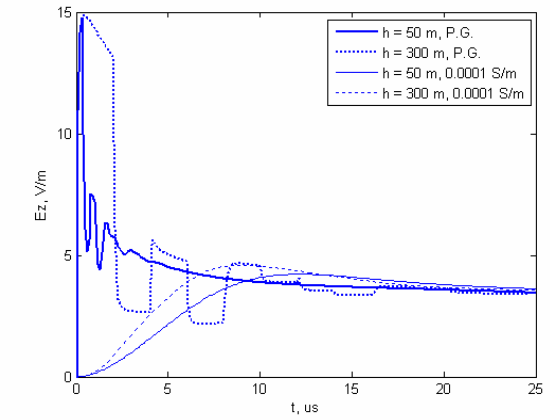


(c)

Fig. 3.16 - Electric field propagating over finitely conducting ground of 0.01 S/m (a), 0.001 S/m (b) and 0.0001 S/m (c) for a return stroke with risetime of 0.2 μs, striking a 50-m tall tower and a 300-m tall tower. The thicker lines represent the field calculated at 100 km for a perfectly conducting ground.

The same analysis presented in Fig. 3.16 for a 0.2-μs-risetime current is performed in Fig. 3.17 for a much slower current, having a risetime equal to 1.0 μs. The smoothing effect

produced on the field calculated for perfect ground by the larger current risetime makes the attenuation coefficient less dependent on the tower height with respect to the case presented in Fig. 3.16.

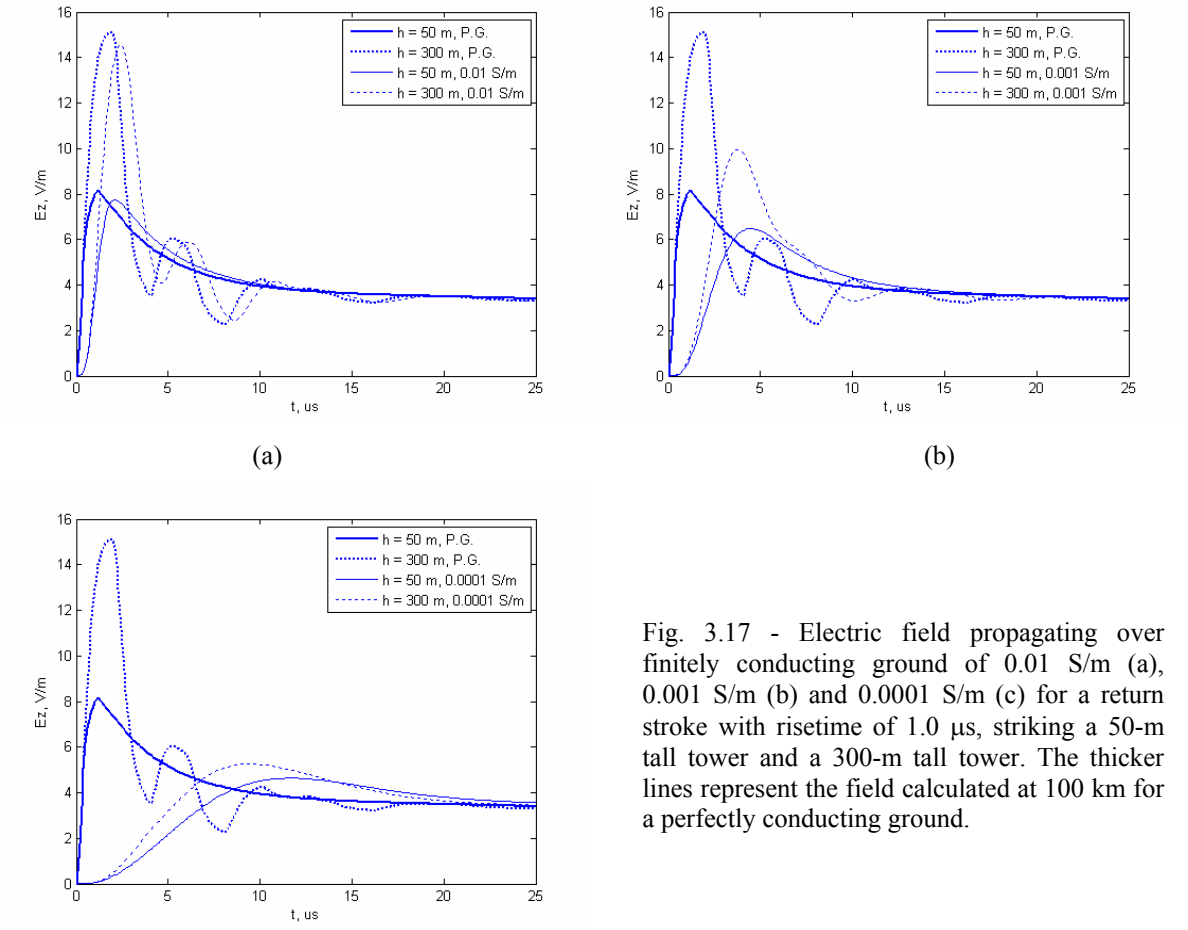


Fig. 3.17 - Electric field propagating over finitely conducting ground of 0.01 S/m (a), 0.001 S/m (b) and 0.0001 S/m (c) for a return stroke with risetime of 1.0 μs, striking a 50-m tall tower and a 300-m tall tower. The thicker lines represent the field calculated at 100 km for a perfectly conducting ground.

In order to summarize how the field peak varies for different current risetimes, tower heights and ground conductivities, let us define the attenuation coefficient $A$ as the ratio between the peak of the electric field calculated at a given distance over a finitely conducting ground to the peak of the same electric field calculated at the same distance over a perfectly conducting ground. Figure 3.18 ((a) to (c)) shows how the attenuation coefficient varies as a function of the tower height and the current risetime for three values of the ground conductivity.

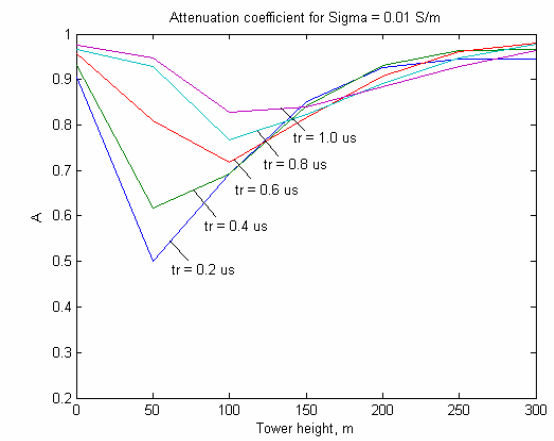


(a)

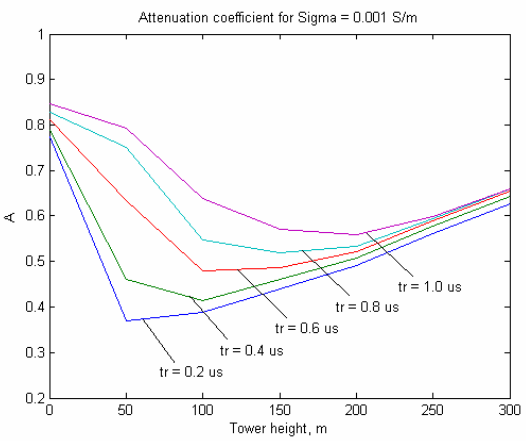


(b)

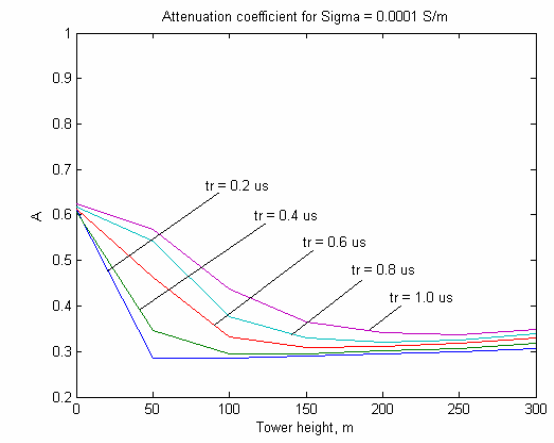


(c)

Fig. 3.18 - Attenuation coefficient A of the vertical electric field propagating over finitely conducting ground of 0.01 S/m (a), 0.001 S/m (b) and 0.0001 S/m (c) as a function of the tower height for return strokes having risetimes varying from 0.2 μs to 1.0 μs.

First, it can be observed in general that the attenuation coefficient presents a more or less pronounced V-shaped variation as a function of the tower height, indicating that the higher attenuations (minima of A) appear for tower heights in between the flat-ground configuration and the 300-m case. It is also interesting to observe how, for a given ground conductivity, increasing the current risetime produces a shift of the minimum of A toward higher values of the tower height.

The variation of the attenuation coefficient *A* as a function of the tower height can be interpreted as follows. For very short tower heights, transient processes along the tower (which contribute to the high frequency components of the radiation field spectrum) are nearly inexistent. Therefore, it is reasonable that *A* decreases initially with increasing tower heights. On the other hand, the transient processes (multiple reflections) for very tall structures tend also to affect less the initial rising portion of the field because the first

reflection from the ground affects the field waveform well after it has reached his peak. This explains the increase of the attenuation coefficient for taller towers. In between, when the current risetime is similar to the propagation time along the tower (0.2 μs corresponds to a 60-m tall tower, 0.4 μs to a 120-m tall one, and so on), the initial rising portion of the field is most affected by the multiple reflections, resulting in the most significant attenuation.

## 3.6 Conclusions

This chapter is devoted to the computation of the electromagnetic field produced by lightning return strokes to elevated strike objects, basing on the extension of the engineering models to include an elevated strike object presented in Chapter 2.

It was shown that the current distribution associated with these extended models exhibits a discontinuity at the return stroke wavefront which needs to be taken into account by an additional term in the equations for the electromagnetic field, the so-called 'turn-on' term. Note that this discontinuity appears equally in the case of a ground-initiated lightning when the reflection at the channel base resulting from the grounding conditions is taken into account.

A general analytical formula describing the 'turn-on' term associated with this discontinuity for various engineering models was derived and simulation results illustrating the effect of the 'turn-on' term on the radiated electric and magnetic fields (calculated adopting the MTLE model) were also presented.

The effect of this discontinuity, which, although not physically conceivable, is predicted by the model, has been disregarded in most studies dealing with the calculation of electromagnetic fields radiated by lightning to tall towers and, until a new model providing a non-discontinuous current at the return-stroke front is developed, this discontinuity needs to be carefully treated when calculating the radiated electromagnetic field.

Possible modifications to engineering models have been suggested in order to eliminate this discontinuity. Further work is needed in this respect.

In the second part of the chapter (Section 3.5), dedicated to the investigation of the propagation effects on lightning electromagnetic field traveling along a finitely-conducting ground, the commonly used assumption of an idealized perfectly-conducting ground is relaxed in order to analyze how the electromagnetic field is affected while propagating along a soil characterized by a finite conductivity.

It was shown that the propagation along an imperfectly conducting ground causes the amplitude of the field to decrease and its risetime to increase with decreasing ground conductivity.

The results show that the attenuation of the initial peak of the radiation field resulting from the propagation over finitely conducting ground depend strongly on the risetime of the current, the tower height and the ground conductivity.

In general, it was shown that the attenuation of the radiation field of lightning flashes striking towers is larger than that striking flat ground. In particular, this attenuation is generally more pronounced for higher current risetimes and reaches its maximum for risetime values which are close to the travel time of the current waves along the tower.

# References

Baba, Y., and V. A. Rakov (2006), Transmission Line Model of Lightning Return Strokes Generalized to Include a Tall Grounded Strike Object and an Upward Connecting Leader, paper presented at EMC Zurich Singapore.

Bermudez, J. L. (2003), Lightning currents and electromagnetic fields associated with return strokes to elevated strike objects, 178 pp, Ph.D. Thesis, EPFL, Lausanne, Switzerland.

Cooray, V. (1987), Effects of propagation on the return stroke radiation fields, *Radio Science*, *22*, 757-768.

Cooray, V. (2003), *The Lightning Flash*, IEE, London, UK.

Cooray, V., G. Diendorfer, C. A. Nucci, D. Pavanello, F. Rachidi, M. Becerra, M. Rubinstein, and W. Schulz (2006), On the effect of finite ground conductivity on electromagnetic field radiated from lightning to tall towers, paper presented at International conference on Lightning Protection, ICLP 2006, Kanazawa, Japan.

Diendorfer, G. (1991), Effect of an elevated strike object on the lightning electromagnetic fields, paper presented at 9th International Symposium on Electromagnetic Compatibility, Zurich, Switzerland, March 1991.

Diendorfer, G., W. Schulz, and V. A. Rakov (1998), Lightning characteristics based on data from the Austrian lightning locating system, *IEEE Transactions on Electromagnetic Compatibility*, *40*, 452-464.

Guerrieri, S., F. Heidler, C. A. Nucci, F. Rachidi, and M. Rubinstein (1996), Extension of two return stroke models to consider the influence of elevated strike objects on the lightning return stroke current and the radiated electromagnetic field: comparison with experimental results, paper presented at EMC '96 (International Symposium on Electromagnetic Compatibility), Rome, Italy.

Guerrieri, S., C. A. Nucci, F. Rachidi, and M. Rubinstein (1998), On the influence of elevated strike objects on directly measured and indirectly estimated lightning currents, *IEEE Transactions on Power Delivery*, *13*, 1543-1555.

Heidler, F. (1985), Traveling current source model for LEMP calculation, *Electromagnetic Compatibility*, *626*.

Heidler, F., and C. Hopf (1994), Lightning current and Lightning electromagnetic impulse considering current reflection at the earth's surface, paper presented at 22nd international Conference on Lightning Protection, Budapest.

Heidler, F., J. Wiesinger, and W. Zischank (2001), Lightning Currents Measured at a Telecommunication Tower from 1992 to 1998, paper presented at 14th International Zurich Symposium on Electromagnetic Compatibility, Zurich, Switzerland, February 20 - 22, 2001.

Janischewskyj, W., V. Shostak, and A. M. Hussein (1998), Comparison of lightning electromagnetic field characteristics of first and subsequent return strokes to a tall tower 1. Magnetic field, paper presented at 24th ICLP (international conference on lightning Protection), Birmingham, U.K., sept. 1998.

Le Vine, D. M., and J. C. Willett (1992), Comment on the transmission line model for computing radiation from lightning, *Journal of Geophysical Research*, *97*, 2601-2610.

Motoyama, H., W. Janischewskyj, A. M. Hussein, R. Rusan, W. A. Chisholm, and J. S. Chang (1996), Electromagnetic field radiation model for lightning strokes to tall structures, *IEEE Transactions on Power Delivery*, *11*, 1624-1632.

Norton, K. A. (1937), Propagation of radio waves over the surface of the earth and in the upper atmosphere, *Proceedings of the Institute of Radio engineering*, *25*.

Nucci, C. A., G. Diendorfer, M. Uman, F. Rachidi, M. Ianoz, and C. Mazzetti (1990), Lightning return stroke current models with specified channel-base current: a review and comparison, *Journal of Geophysical Research*, *95*, 20395-20408.

Nucci, C. A., C. Mazzetti, F. Rachidi, and M. Ianoz (1988), On lightning return stroke models for LEMP calculations, paper presented at 19th international conference on lightning protection, Graz, may 1988.

Pavanello, D., V. Cooray, F. Rachidi, M. Rubinstein, A. Negodyaev, M. Paolone, and C. A. Nucci (2005), Propagation effects on the electromagnetic field radiated by lightning to tall towers, paper presented at VIII International Symposium on Lightning Protection, SIPDA, São Paulo, Brazil, 21-25 November 2005.

Pavanello, D., F. Rachidi, J. L. Bermudez, M. Rubinstein, and C. A. Nucci (2004a), Electromagnetic Field Radiated by Lightning to Tall Towers: Treatment of the Discontinuity at the Return Stroke Wavefront, *Journal of Geophysical Research*, *109*.

Pavanello, D., F. Rachidi, V. A. Rakov, C. A. Nucci, and J. L. Bermudez (Accepted in 2006), Return Stroke Current Profiles and Electromagnetic Fields Associated with Lightning Strikes to Tall Towers: Comparison of Engineering Models, *Journal of Electrostatics*.

Pavanello, D., F. Rachidi, M. Rubinstein, J. L. Bermudez, and C. A. Nucci (2004b), On the calculation of electromagnetic fields radiated by lightning to tall structures, paper presented at International Conference on Lightning Protection, ICLP 2004, Avignon, France, September 2004.

Rachidi, F., M. Ianoz, C. A. Nucci, and C. Mazzetti (1992), Modified transmission line model for LEMP calculations. Effect of the return stroke velocity decreasing and elevated strike objects on close fields, paper presented at 9th International Conference on Atmospheric Electricity, St. Petersburg, Russia, June 15-19, 1992.

Rachidi, F., W. Janischewskyj, A. M. Hussein, C. A. Nucci, S. Guerrieri, B. Kordi, and J. S. Chang (2001), Current and electromagnetic field associated with lightning return strokes to tall towers, *IEEE Trans. on Electromagnetic Compatibility*, *43*.

Rachidi, F., and C. A. Nucci (1990), On the Master, Uman, Lin, Standler and the Modified Transmission Line lightning return stroke current models, *Journal of Geophysical Research*, *95*, 20389-20394.

Rubinstein, M., and M. A. Uman (1989), Methods for calculating the electromagnetic fields from a known source distribution: application to lightning, *IEEE Transactions on Electromagnetic Compatibility*, *31*, 183-189.

Rubinstein, M., and M. A. Uman (1990), On the radiation field turn-on term associated with traveling current discontinuities in lightning, *Journal of Geophysical Research*, *95*, 3711-3713.

Rubinstein, M., and M. A. Uman (1991), Transient electric and magnetic fields associated with establishing a finite electrostatic dipole, revisited, *IEEE Transactions on Electromagnetic Compatibility*, *33*, 312-320.

Rusan, I., W. Janischewskyj, A. M. Hussein, and J.-S. Chang (1996), Comparison of measured and computed electromagnetic fields radiated from lightning strikes to the Toronto CN tower, paper presented at 23rd International Conference on Lightning Protection (ICLP), Florence.

Schulz, W., and G. Diendorfer (2004), Lightning field peaks radiated by lightning to tall towers, paper presented at International Conference on Grounding and Earthing, Ground 2004, Belo Horizonte, Brazil, November 2004.

Thottappillil, R., V. Rakov, and M. Uman (1997), Distribution of charge along the lightning channel: relation to remote electric and magnetic fields and to return-stroke models, *Journal of Geophysical Research*, *102*, 6987-7006.

Thottappillil, R., and V. A. Rakov (2001a), On different approaches to calculating lightning electric fields, *Journal of Geophysical Research*, *106*, 14191-14205.

Thottappillil, R., and V. A. Rakov (2001b), On the computation of electric fields from a lightning discharge in time domain, paper presented at 2001 IEEE EMC International Symposium, Boston, USA.

Thottappillil, R., J. Schoene, and M. A. Uman (2001), Return stroke transmission line model for stroke speed near and equal that of light, *Geophysical Research Letters*, *28*, 3593-3596.

Thottappillil, R., M. A. Uman, and V. A. Rakov (1998), Treatment of retardation effects in calculating the radiated electromagnetic fields from the lightning discharge, *Journal of Geophysical Research*, *103*, 9003-9013.

Uman, M. A. (1985), Lightning return stroke electric and magnetic fields, *Journal of Geophysical Research*, *90*, 6121-6130.

Uman, M. A. (1987), *The lightning discharge*, 377 pp., Academic Press, London, UK.

Uman, M. A., D. K. McLain, and E. P. Krider (1975), The electromagnetic radiation from a finite antenna, *American Journal of Physics*, *43*, 33-38.

Wait, J. R. (1956), Transient fields of a vertical dipole over homogeneous curved ground, *Can. J. Phys.*, *36*, 9-17.

Wait, J. R. (1957), Propagation of a pulse across a coast line, *Proceedings of IRE*, *45*, 1550-1551.

Wait, J. R. (1986), Propagation effects for electromagnetic pulse transmission, *Proceedings of the IEEE*, *74*, 1173-1181.

# Chapter 4

# Return Stroke Current Profiles and Electromagnetic Fields Associated with Lightning Strikes to Tall Towers: Comparison of Engineering Models

## 4.1 Introduction

The determination of the peak return-stroke current from remotely measured electric or magnetic fields considerably facilitates the collection of data on the lightning return-stroke current without having to instrument tall towers or trigger the lightning artificially, especially nowadays because of the widespread use of lightning location systems. Indeed, such systems are already used to provide also estimates of lightning current parameters (e.g. [*Cummins, et al.*, 1998; *Herodotou, et al.*, 1993]).

The theoretical estimation of return-stroke currents from remote electromagnetic fields depends on several aspects, among which the choice adopted for the return-stroke model is crucial.

Significant works have been published about the computation of the electromagnetic field obtained using the engineering models applied to the case of lightning strikes to flat ground; an interesting review (whose main conclusions are recalled in Section 4.2) can be found in [*Nucci, et al.*, 1990].

This chapter is intended to provide theoretical elements to extend to the case of tower-initiated lightning the validity of the techniques of return-stroke current estimation existing for the case of strikes to ground.

Section 4.3 is dedicated to the comparison among the predictions obtained using the five extended engineering return-stroke models for lightning strikes to tall structures described in

Chapter 2 (namely, the Bruce-Golde (BG) model [*Bruce and Golde*, 1941], the transmission line (TL) model [*Uman and McLain*, 1969], the traveling current source (TCS) model [*Heidler*, 1985], and the two modified transmission line models (MTLL [*Rakov and Dulzon*, 1987] and MTLE [*Nucci, et al.*, 1988])). The spatial-temporal current profiles along the tower-channel axis predicted by the five models, as well as the respective predictions for the radiated electric and magnetic fields, calculated at different distances, are compared and discussed. Further, a model-validation analysis is performed in order to discuss their ability to reproduce the significant features of the observed fields.

A theoretical analysis is performed in the last part of the chapter (Section 4.4) with the aim to provide, for the same five engineering models extended to take into account the presence of the tower, expressions relating the return-stroke current and the associated distant radiated electric and magnetic fields [*Pavanello, et al.*, Submitted in 2006].

## 4.2 Comparison among engineering models of lightning strikes to flat ground

The predictions provided by different engineering models have been compared in the past for the case of lightning strikes to ground in a thorough analysis performed by Nucci et al. [*Nucci, et al.*, 1990]. The models considered in that work were: TL, MTLE (referred there as MTL), BG, TCS and MULS[1]. The paper investigates the different formulations of the models, which can be classified in two categories according to their treatment of the return-stroke wavefront: as an inherent discontinuity in the BG and the TCS models, and, as a fast-front current in the remaining models, characterized by the same finite risetime as the current at the channel base [*Nucci, et al.*, 1990].

The attention will be focused in this Section on the electromagnetic field predicted by those models, with the exception of the MULS model, replaced in the simulations presented in Figs. 4.1 to 4.3 by the MTLL model which was not considered in the analysis of Nucci et al. [*Nucci, et al.*, 1990]. A thorough analysis of the models and their ability to reproduce typically-observed features can be found in [*Nucci, et al.*, 1990].

Assuming the same channel-base current (described by Eq. (2.9) and shown in Fig. 2.3 of this thesis) and the same value of 130 m/μs for the return-stroke speed adopted by [*Nucci, et al.*,

[1] The MULS model will not be discussed in this thesis.
It has been shown in [*Rachidi and Nucci*, 1990] that MULS can be considered as equivalent to the MTLE model.

1990], the fields predicted by the five engineering models introduced in Chapter 2 at the three distances of 50 m, 5 km and 100 km are shown in Figs. 4.1 to 4.3.

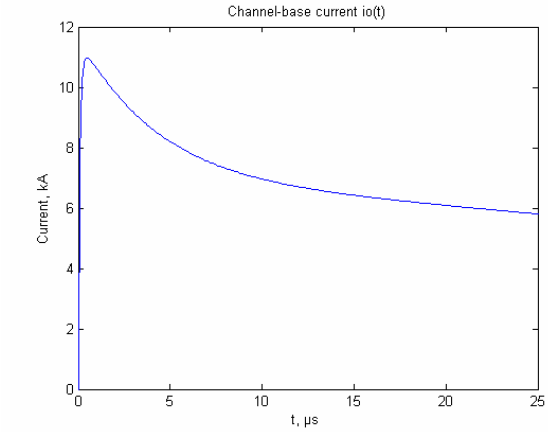


Recall of Fig. 2.3 - Channel-base current proposed by [*Nucci, et al.*, 1990].

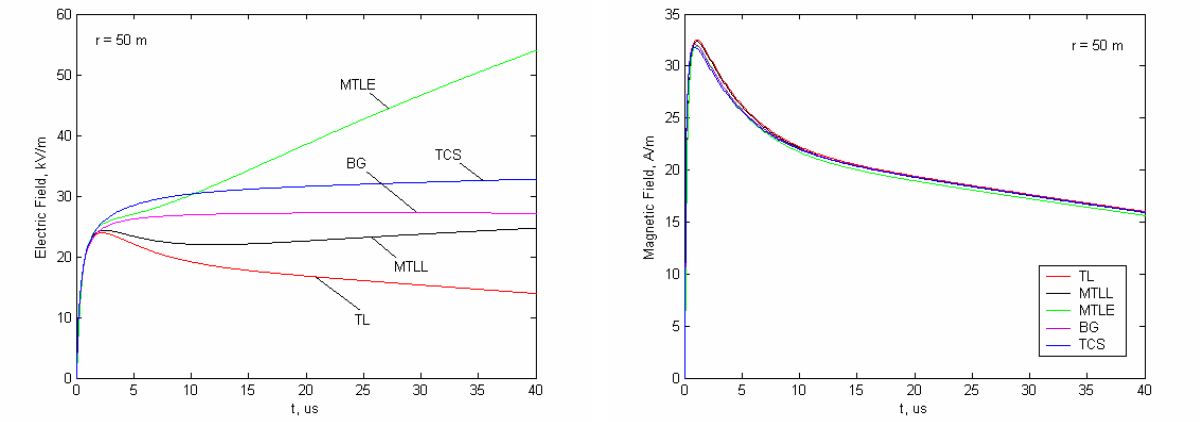


(a) (b)

Fig. 4.1 – Electric field (a) and magnetic field (b) radiated by a lightning strike to ground, calculated for five engineering models at a distance of 50 m.

The discrepancy among the values of the electric field (see Subfig. 4.1(a)) predicted by the different models after ten microseconds or so is due to the different distributions of charge removed from the leader channel near ground [*Nucci, et al.*, 1990]. It is remarkable, in particular, the difference between the two extreme cases of the TL model (which do not include any charge removal from the channel) and the MTLE model (which considers a continued charge removal from the lower portion of the channel).

Subfig. 4.1(b) shows that the predicted magnetic field is nearly model-independent. At this distance, the magnetic field is dominated by its induction term, and its waveshape is similar to the current at the base of the channel shown in Fig. 2.3.

Considering larger distances, 5 and 100 km, Figs. 4.2 and 4.3 show that the BG and TCS models exhibit a larger first peak with respect to the other three models, in reason of their inherent wavefront discontinuity [*Nucci, et al.*, 1990], their field predictions remaining close to each other also for later times. The three transmission-line-type models (TL, MTLL and MTLE), while predicting the same first peak (about 10 % lower than the one predicted by the 'discontinuous' models), tend to differ substantially among each other for later times.

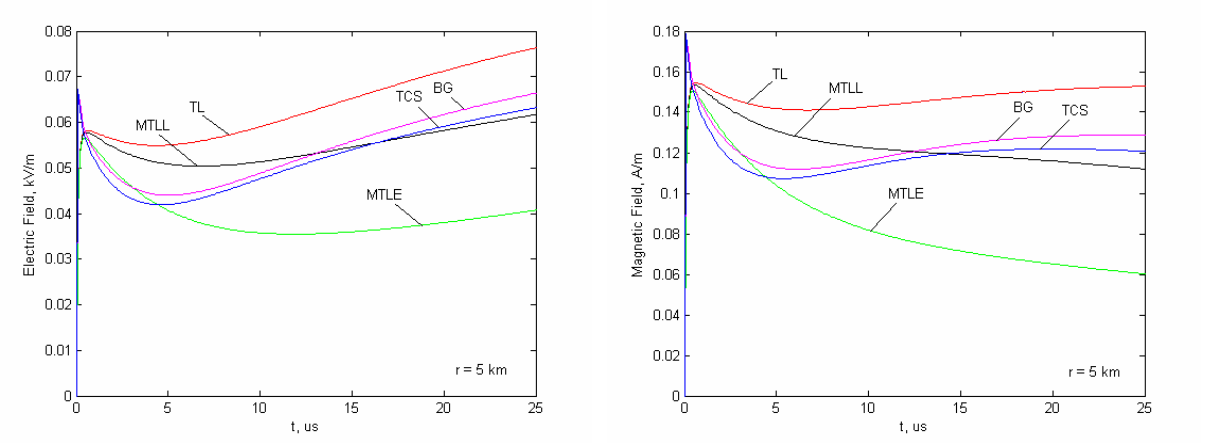


(a) (b)

Fig. 4.2 – Electric field (a) and magnetic field (b) radiated by a lightning strike to ground, calculated for five engineering models at a distance of 5 km.

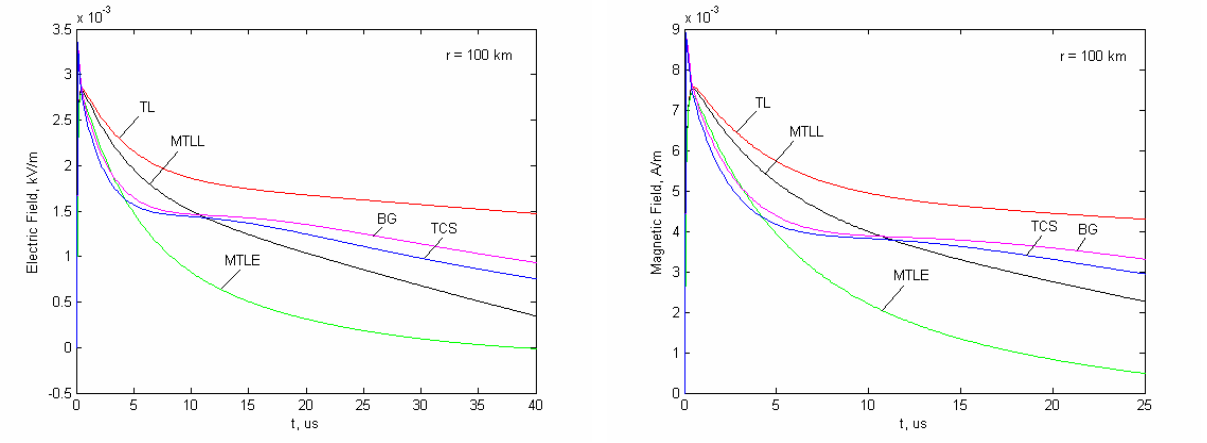


(a) (b)

Fig. 4.3 – Electric field (a) and magnetic field (b) radiated by a lightning strike to ground, calculated for five engineering models at a distance of 100 km.

## 4.3 Comparison among engineering models of lightning strikes to tall structures

The engineering models, initially proposed for ground-initiated lightning return strokes, have been recently extended to tower-initiated return strokes [*Rachidi, et al.*, 2002], in which, adopting a distributed-source representation of the channel, general equations for the spatial-temporal distribution of the current along the lightning channel and along the strike object have been derived [*Bermudez*, 2003; *Rachidi, et al.*, 2002]. Those equations, already introduced in Chapter 2 with labels (2.10) and (2.11), are just recalled here for sake of clarity:

$$i(z',t)=\left[P(z'-h)\,i_o\left(h,t-\frac{z'-h}{v^*}\right)-\rho_t\,i_o\left(h,t-\frac{z'-h}{c}\right)+\right.$$
$$\left.+(1-\rho_t)(1+\rho_t)\sum_{n=0}^{\infty}\rho_g^{n+1}\rho_t^{n}\,i_o\left(h,t-\frac{h+z'}{c}-\frac{2nh}{c}\right)\right]u\left(t-\frac{z'-h}{v}\right) \qquad \text{for } h<z'<H_0 \qquad (2.10)$$

$$i(z',t)=(1-\rho_t)\sum_{n=0}^{\infty}\left[\rho_t^{n}\,\rho_g^{n}\,i_o\left(h,t-\frac{h-z'}{c}-\frac{2nh}{c}\right)+\right.$$
$$\left.+\rho_t^{n}\,\rho_g^{n+1}\,i_o\left(h,t-\frac{h+z'}{c}-\frac{2nh}{c}\right)\right]u\left(t-\frac{h+z'}{c}-\frac{2nh}{c}\right) \qquad \text{for } 0\le z'\le h \qquad (2.11)$$

Equations (2.10) and (2.11) are based on the concept of 'undisturbed current' $i_0(t)$, which represents the idealized current that would be measured at the tower top if the current reflection coefficients at its both extremities were equal to zero.

In (2.10) and (2.11), $h$ is the height of the tower, $\rho_t$ and $\rho_g$ are the top and bottom current reflection coefficients for upward and downward propagating waves, respectively, $H_0$ is the height of the extending return-stroke channel, $c$ is the speed of light, $P(z')$ is a model-dependent attenuation function, $u(t)$ is the Heaviside unit-step function, $v$ is the return-stroke front speed, and $v^*$ is the current-wave speed.

The model-dependency of Eq. (2.10) is expressed by the two parameters $P(z')$ and $v^*$, whose values are summarized in table 2.1 (again, recalled from Chapter 2), in which $\lambda$ is the attenuation height for the MTLE model and $H_{tot}$ is the total height of the lightning channel.

Throughout this study, we will assume $\lambda$ = 2 km and $H_{tot}$ = 8 km. The value adopted for the return-stroke front speed is $v$ = 150 m/μs.

Recall of Table 2.1 - *P(z')* and *v** in Eq. (2.6) for five simple engineering models (adapted from [*Rakov*, 1997]).

| Model | *P(z')* | *v** |
|---|---|---|
| BG | 1 | ∞ |
| TCS | 1 | *-c* |
| TL | 1 | *v* |
| MTLL | $1-z'/H_{tot}$ | *v* |
| MTLE | $exp(-z'/\lambda)$ | *v* |

It is assumed that the current reflection coefficients $\rho_t$ and $\rho_g$ are constant. In addition, any upward connecting leader and any reflections at the return-stroke wavefront [*Shostak, et al.*, 2000] are disregarded.

### 4.3.1 Undisturbed current and representation of the tall tower

The five models are compared employing the same undisturbed current $i_o(t)$, assumed to have the same expression as the channel-base current described in Eq. (2.9) for ground-initiated strikes, which exhibits a peak value of 11 kA and a maximum time derivative of 105 kA/μs and whose waveform is presented in Fig. 2.3.

The spatial-temporal distribution of the current along the channel and along the strike object is calculated for each model, as well as the resulting electric and magnetic fields at three different distances, namely, 50 m, 5 km and 100 km (same distances as in [*Nucci, et al.*, 1990]). The elevated strike object is assumed to have a height $h = 168$ m (corresponding to the Peissenberg tower in Germany), with top and bottom reflection coefficients set, respectively, to $\rho_t = -0.53$ and $\rho_g = 0.7$ [*Heidler, et al.*, 2001].

### 4.3.2 Current distribution along the channel and the tower

Figure 4.4 [*Pavanello, et al.*, Submitted in 2005] shows the current distribution along the tower and along the channel, at different time instants ($t$ = 1, 2,.., 10 μs), predicted by each model. It can be seen that:

- in accordance with Eq. (2.11), the current distribution along the tower is independent of the return-stroke model.
- The BG and TCS models exhibit a strong discontinuity at the return-stroke wavefront, inherent in these models [*Nucci, et al.*, 1990; *Rakov and Uman*, 1998].

- Although the vertical scale of Fig. 4.4 does not allow resolution of current variation at the return-stroke wavefront for TL, MTLL and MTLE models, these models have also a discontinuity at the front. This discontinuity arises from the fact that the current injected into the tower at its top is reflected back and forth at its top and bottom ends, and portions of this current are transmitted into the channel; these transmitted pulses, which are assumed to travel at the speed of light, catch up with the return-stroke wavefront traveling at a lower speed, but are not allowed to propagate in the leader channel above the return-stroke front [*Pavanello, et al.*, 2004b; *Pavanello, et al.*, 2004d].

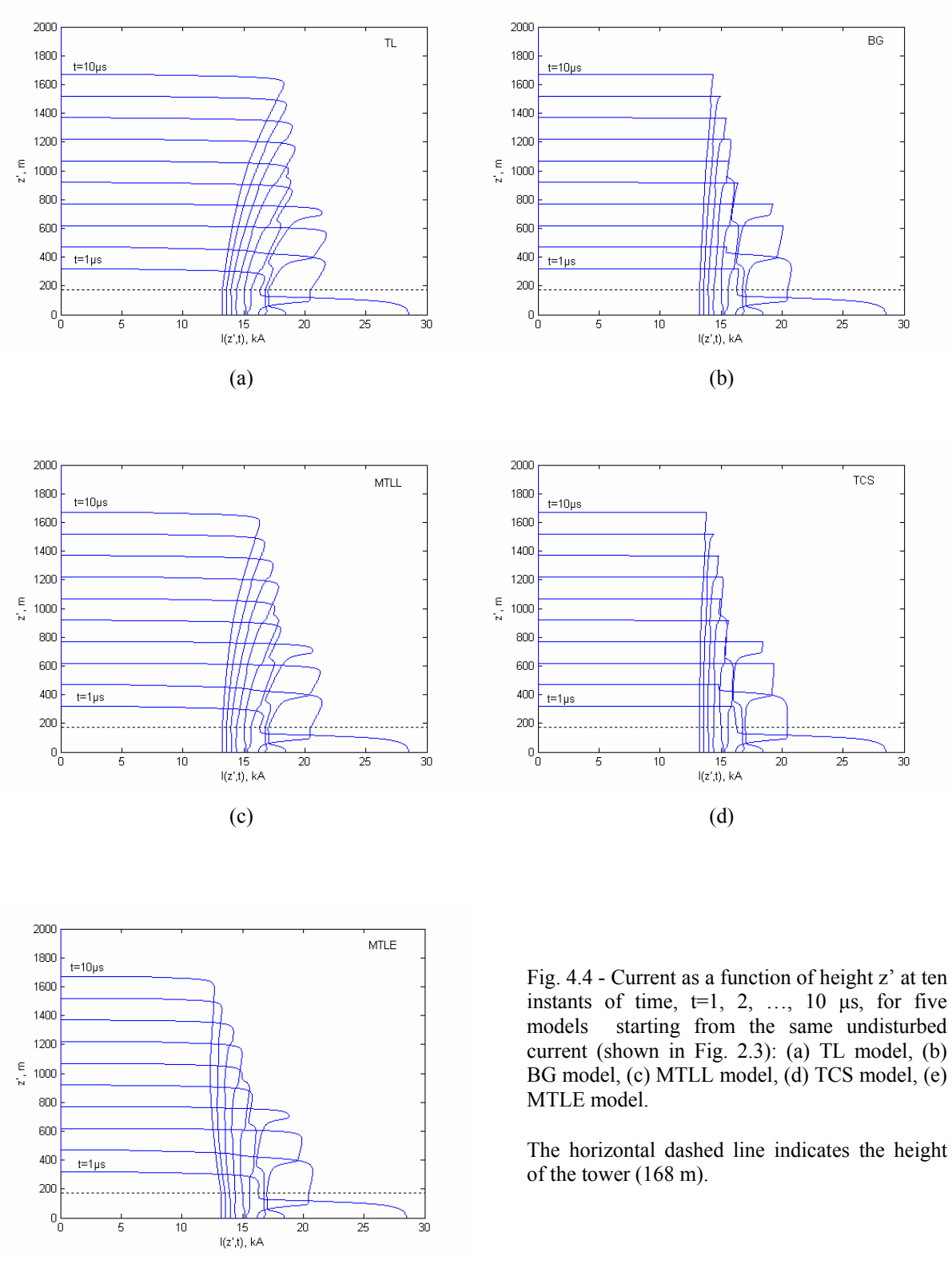


Fig. 4.4 - Current as a function of height z' at ten instants of time, t=1, 2, …, 10 μs, for five models starting from the same undisturbed current (shown in Fig. 2.3): (a) TL model, (b) BG model, (c) MTLL model, (d) TCS model, (e) MTLE model.

The horizontal dashed line indicates the height of the tower (168 m).

Figure 4.5 shows the waveforms of the current evaluated at the top (168 m) and the base (0 m) of the tower. The effects of the multiple reflections at the tower extremities are clearly

visible in the waveforms. It can also be seen that the current at the tower base has a higher peak value due to the contribution from the reflected wave at the ground level.

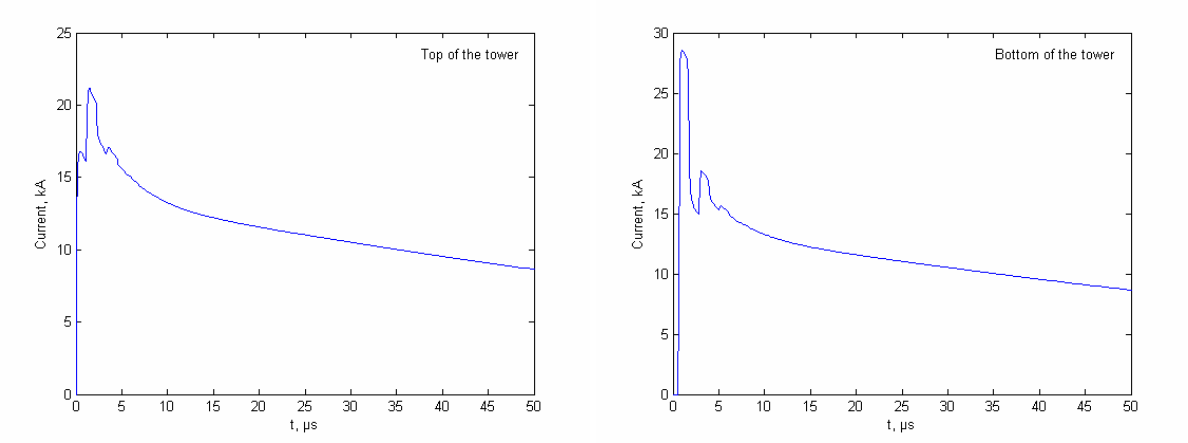


(a) (b)

Fig. 4.5 - Current at the top (a) and at the bottom (b) of a 168-m tower.

### 4.3.3 Electromagnetic fields

The electromagnetic fields will be calculated in this study assuming a perfectly conducting ground.

*Case 1: r = 50 m*

Figure 4.6 presents electric and magnetic fields calculated at a distance of 50 m from the tower base. At this distance, the electric field is dominated (at later times) by its electrostatic term. The model-predicted electric fields are very similar for the first 5 μs, beyond which the BG, TCS and MTLL models predict the flattening of the field, typically observed at close distances, while the TL model predicts field decay. The late-time E-field predicted by the MTLE model exhibits a ramp, as in the case of a ground-initiated return stroke. The usual value of 2 km proposed in [*Nucci, et al.*, 1988] is adopted here for the decay height constant λ for the MTLE model. Note, however, that, as proposed by Cooray et al. in [*Cooray, et al.*, 2004], choosing for λ a value equal to the product of the return-stroke velocity and the decay rate of the channel base current would produce instead a flattening of the E-field calculated with the MTLE model at close-range distances.

With the undisturbed current adopted in the present calculations (see Eq. (2.9)) the proposed choice leads to $\lambda = v$ and $\tau_3 = 15$ km, whose corresponding flattened electric field is shown in Subfig. 4.6(b).

Subfig. 4.6(c) shows that the predicted magnetic field is nearly model-independent. At this distance, the magnetic field is dominated by its induction term, and its waveshape is similar to the current at the base of the tower shown in Subfig. 4.5(b).

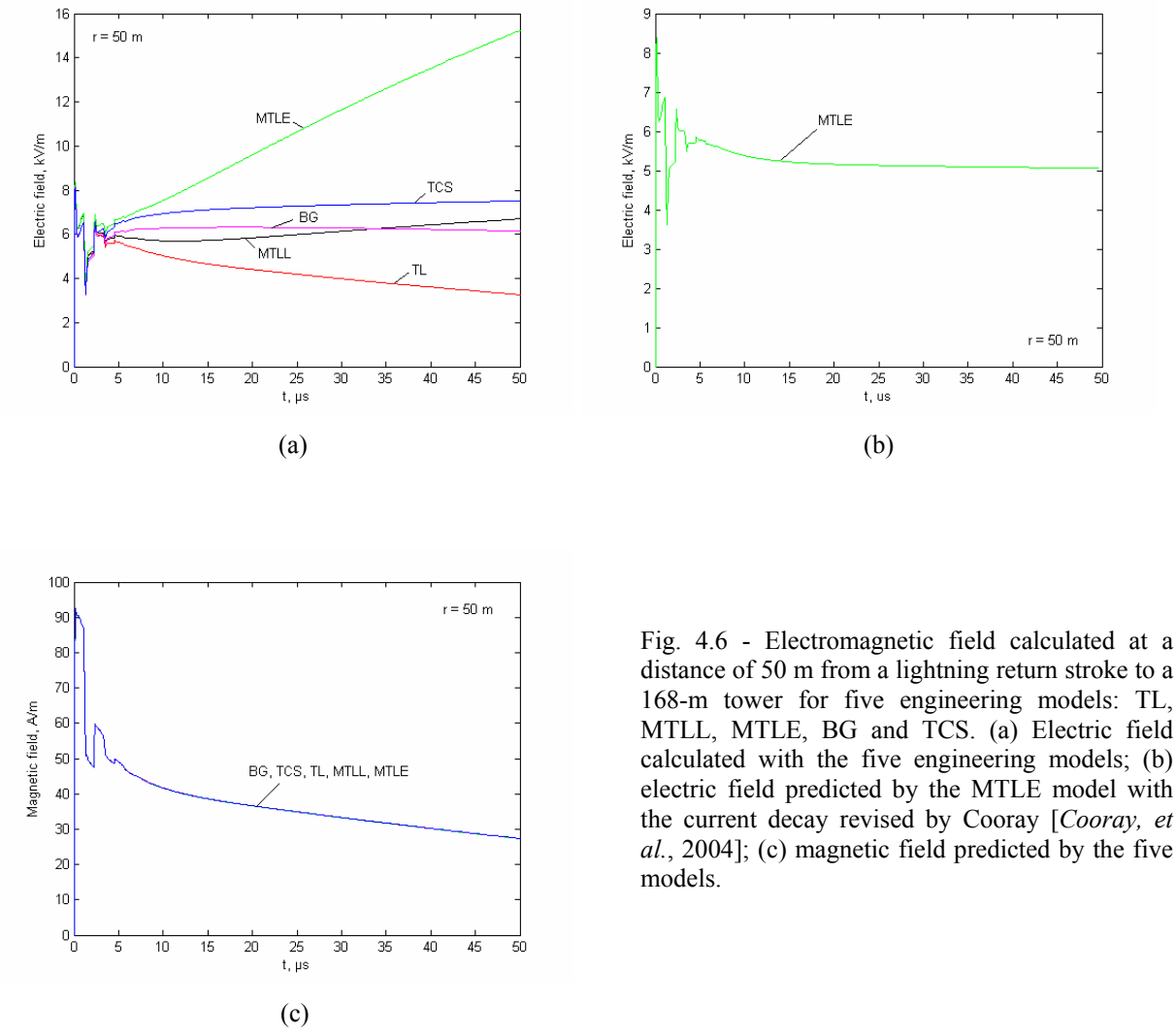


Fig. 4.6 - Electromagnetic field calculated at a distance of 50 m from a lightning return stroke to a 168-m tower for five engineering models: TL, MTLL, MTLE, BG and TCS. (a) Electric field calculated with the five engineering models; (b) electric field predicted by the MTLE model with the current decay revised by Cooray [*Cooray, et al.*, 2004]; (c) magnetic field predicted by the five models.

*Case 2: r = 5 km*

Figure 4.7 presents calculated electric and magnetic fields at a distance of 5 km. The electric and magnetic field waveshapes for the first 5 μs are dominated by the radiation term and hence they are very similar. No significant differences are found between the various models in this early-time region. The differences between the model predictions become more pronounced at late times, $t > 5$ μs or so, although they are unremarkable. Note that all the models predict flattening of the electric field at later times at a value that is significantly

smaller than the initial peak, behavior sensibly different than the one exhibited by the calculated electric fields for ground-initiated return strokes shown in Subfig. 4.2(a).

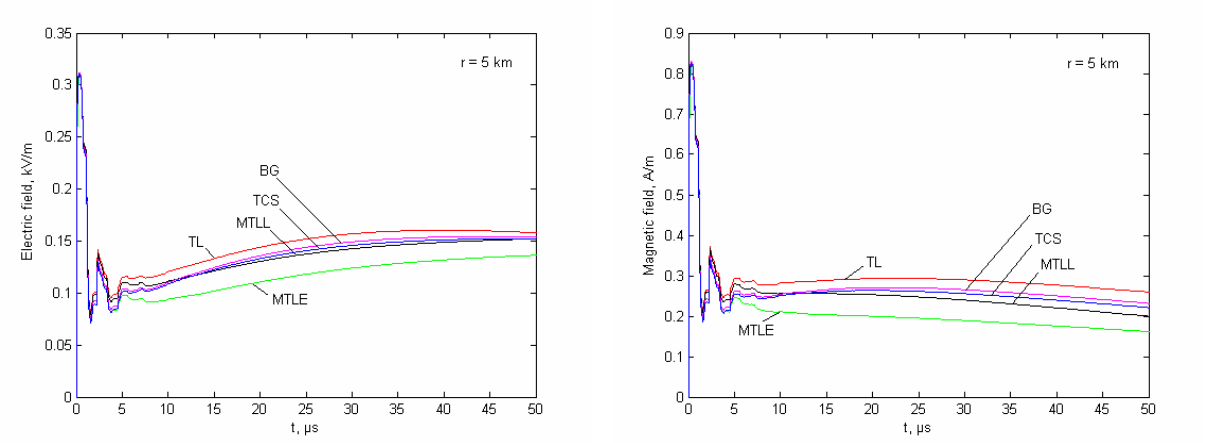


(a) (b)

Fig. 4.7 - Electric (a) and magnetic (b) fields calculated at a distance of 5 km from a lightning return stroke to a 168-m tower.

*Case 3: r = 100 km*

The electric and magnetic fields at a distance of 100 km are plotted in Fig. 4.8. At this distance, the fields are essentially radiation fields, and electric and magnetic fields have the same waveshape. The fields associated with ground-initiated return strokes at such distances exhibit a zero-crossing which is only reproduced by the MTLE and MTLL models [*Nucci, et al.*, 1990; *Rakov and Uman*, 1998]. As seen in Fig. 4.8, for the considered case of a 168-m tower-initiated return stroke, none of the models predicts a zero-crossing within the first 50 μs. The absence of zero-crossing, in particular for the MTLE and MTLL models, can be explained by the contribution of the so-called 'turn-on' term, thoroughly discussed in Section 3.4, which takes into account the contribution of any current discontinuity present at the return-stroke wavefront, to the total field [*Pavanello, et al.*, 2004b; *Pavanello, et al.*, 2004d]. The contribution of this turn-on term to the total electric field at 100 km calculated using the MTLE model is shown in Fig. 4.9.

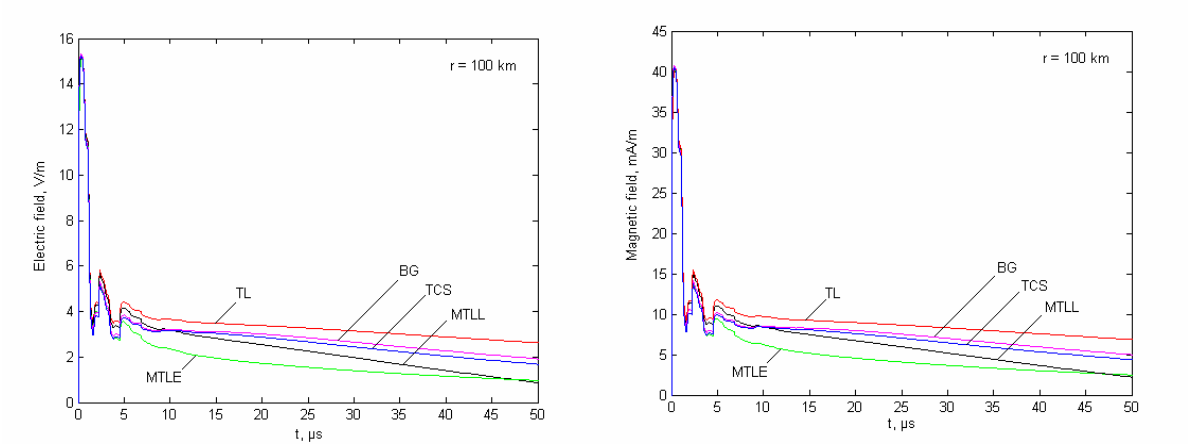


(a) (b)

Fig. 4.8 - Electric (a) and magnetic (b) fields calculated at a distance of 100 km from a lightning return stroke to a 168-m tower.

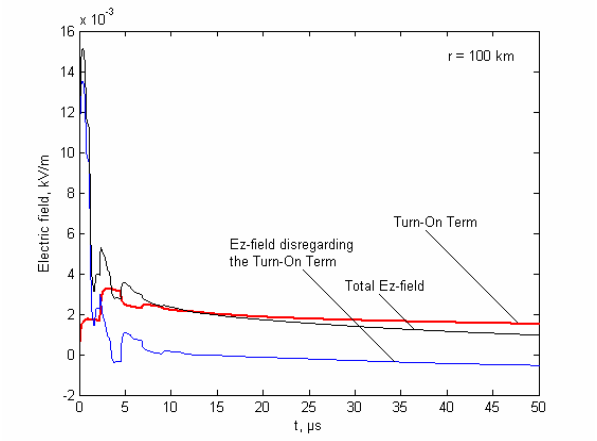


Fig. 4.9 - Contribution of the turn-on term to the electric field calculated at a distance of 100 km from a lightning return stroke to a 168-m tower, using MTLE model.

Figure 4.9 shows how the late-time electric field is dominated by the contribution from the turn-on term, which prevents the zero crossing to occur.

## 4.4 Far-field – Current relationship

Expressions relating radiated fields and return-stroke channel-base currents, initially derived for various 'engineering' return-stroke models for a ground-initiated lightning (e.g. [*Rachidi and Thottappillil*, 1993]), have been recently extended [*Bermudez, et al.*, 2005], for the sole TL model, to take into account the presence of an elevated strike object, whose presence is

included adopting the distributed-sources representation of the channel, mentioned in Section 2.6 [*Rachidi, et al.*, 2002].

In this section, the work of [*Bermudez, et al.*, 2005] for the TL-model representation of a tower-initiated strike is extended also to the other four engineering models, providing the analytical relationships between lightning return-stroke currents and far electromagnetic fields for all the five engineering models discussed in this thesis (BG, TL, TCS, MTLL and MTLE) [*Rakov and Uman*, 1998].

The general expressions for the vertical electric field and the azimuthal magnetic field from a vertical antenna above a perfectly conducting ground, for an observation point at ground level (see Fig. 4.10), are given by [*Uman*, 1985].

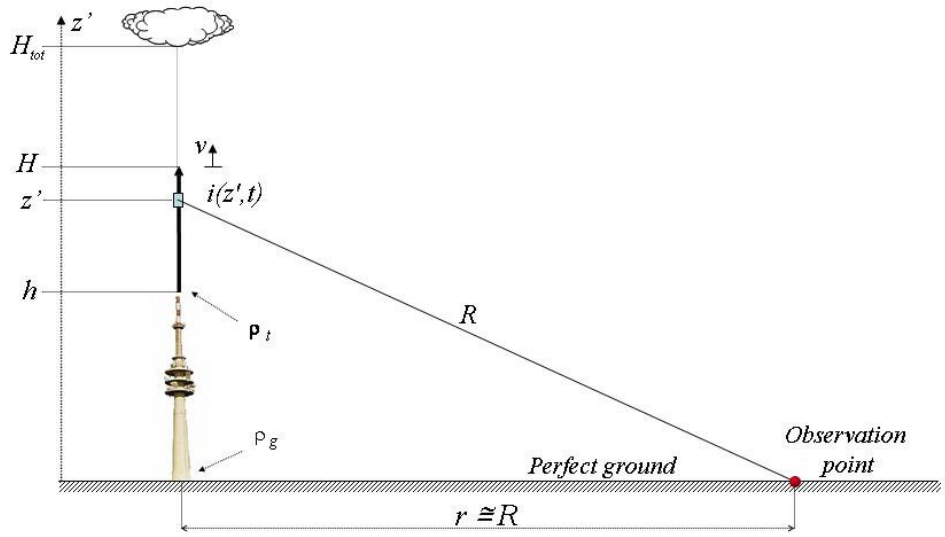


Fig. 4.10 - Geometry for the far-field calculation (*H* is the height of the return-stroke wavefront, as seen by the observer).

$$E_z(r,t)=\frac{1}{2\pi\varepsilon_o}\left[\int_0^H \frac{2z'^2-r^2}{R^5}\int_{R/c}^{t} i(z',\tau-R/c)\,d\tau\,dz' + \int_0^H \frac{2z'^2-r^2}{cR^4} i(z',t-R/c)\,dz' - \int_0^H \frac{r^2}{c^2R^3}\frac{\partial i(z',t-R/c)}{\partial t}\,dz'\right] \tag{4.1}$$

$$H_{\varphi}(r,t)=\frac{1}{2\pi}\left[\int_0^H \frac{r}{R^3} i(z',t-R/c)\,dz' + \int_0^H \frac{r}{cR^2}\frac{\partial i(z',t-R/c)}{\partial t}\,dz'\right] \tag{4.2}$$

where $H$ is the height of the return stroke wavefront as seen by the observer, $r$ is the horizontal distance between the channel and the observation point, and $R$ is the distance between a single dipole located at a height $z'$ above ground and the observation point ($R=\sqrt{r^2+z'^2}$).

Let us consider here only the radiated electromagnetic field. For distant observation points, neglecting the static and induction components of the electric field, and considering $R \cong r$ and $r >> H$, the general expression for the electric and magnetic field for an observation point located at ground level reduces to

$$E_z(r,t) \cong -\frac{1}{2\pi\varepsilon_o c^2 r}\int_0^H \frac{\partial i(z',t-r/c)}{\partial t}\,dz' \tag{4.3}$$

$$H_{\varphi}(r,t) \cong \frac{1}{2\pi c r}\int_0^H \frac{\partial i(z',t-r/c)}{\partial t}\,dz' \tag{4.4}$$

Introducing the general expressions for the spatial-temporal distribution of the current (2.10) and (2.11) into (4.3) and (4.4), and after appropriate mathematical manipulations, we obtain [*Pavanello, et al.*, 2004a]

$$E_z(r,t) \cong E_z^{\mathrm{rs}}(r,t)+E_z^{\mathrm{eso}}(r,t)+E_z^{\mathrm{to}}(r,t) \tag{4.5}$$

$$H_{\varphi}(r,t) \cong H_{\varphi}^{\mathrm{rs}}(r,t)+H_{\varphi}^{\mathrm{eso}}(r,t)+H_{\varphi}^{\mathrm{to}}(r,t) \tag{4.6}$$

in which:

- $E_z^{\mathrm{rs}}(r,t)$ and $H_{\varphi}^{\mathrm{rs}}(r,t)$ are the electric and magnetic fields due to the main return stroke pulse within the lightning channel (the first term on the right hand side of Equation (2.10)) and they are given by:

$$E_z^{\mathrm{rs}}(r,t) = -\frac{1}{2\pi\varepsilon_o c^2 r}\int_h^H P(z'-h)\cdot\frac{\partial}{\partial t}\left[i_o\left(h,t-\frac{z'-h}{v^*}\right)u\left(t-\frac{z'-h}{v}\right)\right]dz' \tag{4.7}$$

$$H_{\varphi}^{\mathrm{rs}}(r,t)=\frac{1}{2\pi cr}\int_{h}^{H}P(z'-h)\cdot\frac{\partial}{\partial t}\left[i_o\left(h,t-\frac{z'-h}{v*}\right)u\left(t-\frac{z'-h}{v}\right)\right]dz' \tag{4.8}$$

- $E_z^{\mathrm{eso}}(r,t)$ and $H_{\varphi}^{\mathrm{eso}}(r,t)$ are electric and magnetic fields resulting from the contribution of multiple-reflection process along the elevated strike object, including the contribution of pulses transmitted into the channel. They are given by [*Bermudez, et al.*, 2005]

$$E_z^{\mathrm{eso}}(r,t+r/c)=-\frac{1}{2\pi\varepsilon_o c^2 r}\left(1-2\rho_t\right)i_o(h,t)-\frac{1-\rho_t}{2\pi\varepsilon_o cr}\sum_{n=0}^{\infty}\left\{\begin{array}{l}\left(\rho_g-1\right)\rho_g^n\,\rho_t^n\,i_o\left(h,t-\dfrac{(2n+1)h}{c}\right)\\ +2\,\rho_g^{n+1}\rho_t^{n+1}\,i_o\left(h,t-\dfrac{2(n+1)h}{c}\right)\end{array}\right\} \tag{4.9}$$

$$H_{\varphi}^{\mathrm{eso}}(r,t+r/c)=\frac{1}{2\pi r}\left(1-2\rho_t\right)i_o(h,t)+\frac{1-\rho_t}{2\pi\varepsilon_o cr}\sum_{n=0}^{\infty}\left\{\begin{array}{l}\left(\rho_g-1\right)\rho_g^n\,\rho_t^n\,i_o\left(h,t-\dfrac{(2n+1)h}{c}\right)\\ +2\,\rho_g^{n+1}\rho_t^{n+1}\,i_o\left(h,t-\dfrac{2(n+1)h}{c}\right)\end{array}\right\} \tag{4.10}$$

- and, finally, $E_z^{\mathrm{to}}(r,t)$ and $H_{\varphi}^{\mathrm{to}}(r,t)$ are the so-called 'turn-on' electric and magnetic field terms [*Pavanello, et al.*, 2004b], associated with the current discontinuity at the return stroke wavefront. Indeed, the current distribution associated with the extended models[2] exhibits a discontinuity at the return stroke wavefront. This discontinuity arises from the fact that the current injected into the tower from its top is reflected back and forth at its ends, and portions of it are transmitted into the channel; these transmitted pulses, which are assumed to travel at the speed of light, catch up with the return stroke wave front traveling at a lower speed and no current is allowed to flow in the leader region above the front [*Pavanello, et al.*, 2004b]. This discontinuity needs to be carefully treated when calculating the radiated electromagnetic field through an additional 'turn-on' term in the electromagnetic field equations, given by:

$$E_z^{\mathrm{to}}=-\frac{I_{front}(H)}{2\pi\varepsilon_0 c^2 r}\cdot\frac{1}{\left(\dfrac{1}{v}+\dfrac{H}{cR}\right)} \tag{4.11}$$

[2] Models extended to take into account the presence of the elevated strike object.

$$H_{\varphi}^{\mathrm{to}} = \frac{I_{front}(H)}{2\pi cr} \cdot \frac{1}{\left(\frac{1}{v} + \frac{H}{cR}\right)} \tag{4.12}$$

where $I_{front}$ is the amplitude of the current discontinuity at the wavefront [*Pavanello, et al.*, 2004b].

It is interesting to note that the second and the third terms of the electromagnetic fields, namely, $E_z^{\mathrm{eso}}(r,t)$, $H_{\varphi}^{\mathrm{eso}}(r,t)$ and $E_z^{\mathrm{to}}(r,t)$, $H_{\varphi}^{\mathrm{to}}(r,t)$ are independent of the adopted model. The only model-dependent terms are $E_z^{rs}(r,t)$ for the electric field, and $H_{\varphi}^{rs}(r,t)$ for the magnetic field. Tables 4.1 and 4.2 summarize the specific expressions for $E_z^{rs}(r,t)$ and $H_{\varphi}^{rs}(r,t)$ developed for various models (e.g. [*Rachidi and Thottappillil*, 1993]).

Additionally, it is important to note that the BG and the TCS models exhibit an inherent discontinuity at the return stroke wavefront. This discontinuity gives rise to a turn-on term which is already included in the main pulse ( $E_z^{\mathrm{rs}}(r,t)$ and $H_{\varphi}^{\mathrm{rs}}(r,t)$ ) contributions.

Table 4.1 - Expressions to calculate $E_z^{rs}(r,t)$ for different return stroke models, far-field conditions. (Note: $k = 1 + v/c$ )

| Model | $E_z^{rs}(r,t)$ |
|---|---|
| BG | $-\frac{v}{2\pi\varepsilon_o c^2 r}\left[i_o(h,t) + t\frac{di_o(h,t)}{dt}\right]$ |
| TL | $-\frac{v}{2\pi\varepsilon_o c^2 r} i_o(h,t)$ |
| TCS | $-\frac{v}{2\pi\varepsilon_o c^2 r}\left[k i_o(h,kt) - i_o(h,t)\right]$ |
| MTLL | $-\frac{v}{2\pi\varepsilon_o c^2 r}\left[i_o(h,t-r/c) - \frac{v}{H_{tot}}\int_0^t i_o(h,\tau - r/c)\,d\tau\right]$ |
| MTLE | Solution of: $\left[\frac{E_z^{rs}(r,t+r/c)}{\lambda} + \frac{1}{v}\frac{dE_z^{rs}(r,t+r/c)}{dt}\right] = -\frac{1}{2\pi\varepsilon_o c^2 r}\frac{di_o(h,t)}{dt}$ |

Table 4.2 - Expressions to calculate $H_{\varphi}^{rs}(r,t)$ for different return stroke models, far-field conditions. (Note: $k = 1 + v/c$ )

| Model | $H_{\varphi}^{rs}(r,t)$ |
|---|---|
| BG | $\frac{v}{2\pi cr}\left[i_o(h,t) + t\frac{di_o(h,t)}{dt}\right]$ |
| TL | $\frac{v}{2\pi cr} i_o(h,t)$ |
| TCS | $\frac{v}{2\pi cr}\left[k i_o(h,kt) - i_o(h,t)\right]$ |
| MTLL | $-\frac{v}{2\pi cr}\left[i_o(h,t-r/c) - \frac{v}{H_{tot}}\int_0^t i_o(h,\tau - r/c)d\tau\right]$ |
| MTLE | Solution of: $\left[\frac{H_{\varphi}^{rs}(r,t+r/c)}{\lambda} + \frac{1}{v}\frac{dH_{\varphi}^{rs}(r,t+r/c)}{dt}\right] = -\frac{1}{2\pi cr}\frac{di_o(h,t)}{dt}$ |

### 4.4.1 Simulation results

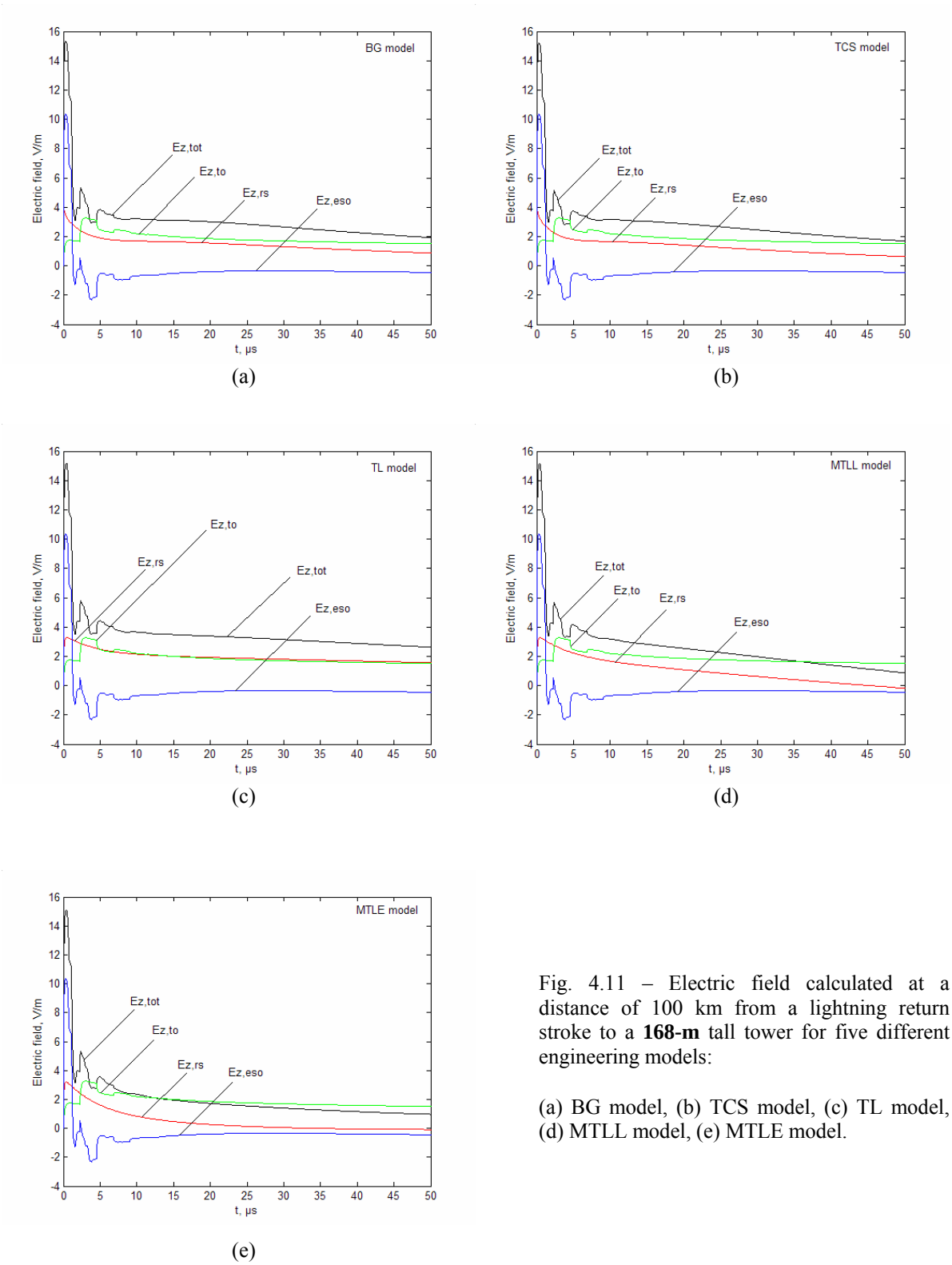


Fig. 4.11 – Electric field calculated at a distance of 100 km from a lightning return stroke to a **168-m** tall tower for five different engineering models:

(a) BG model, (b) TCS model, (c) TL model, (d) MTLL model, (e) MTLE model.

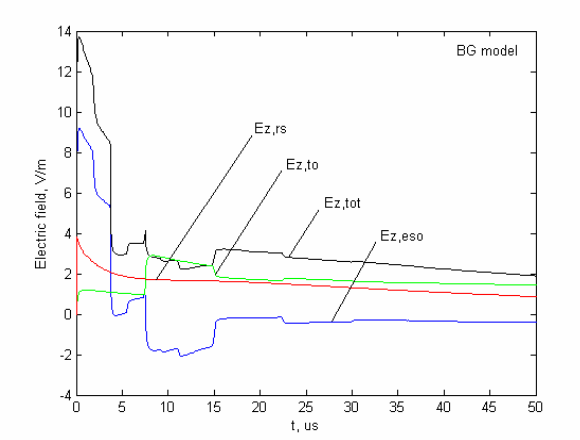


(a)

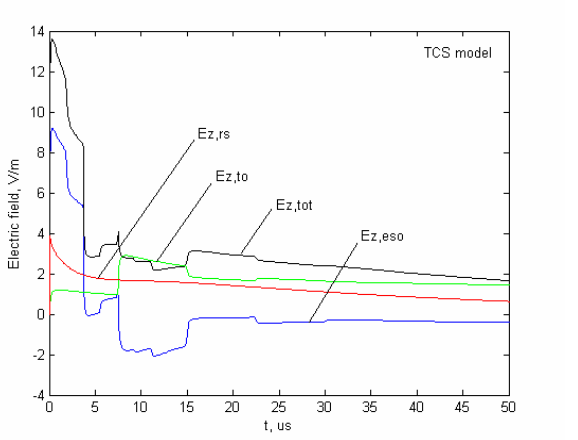


(b)

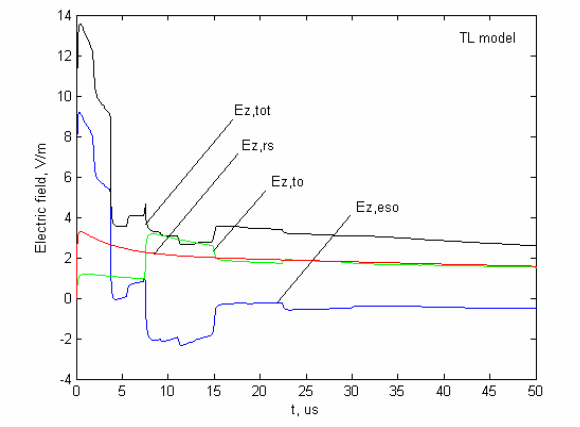


(c)

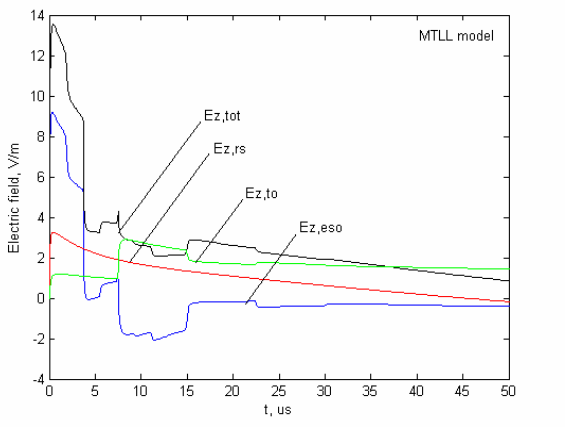


(d)

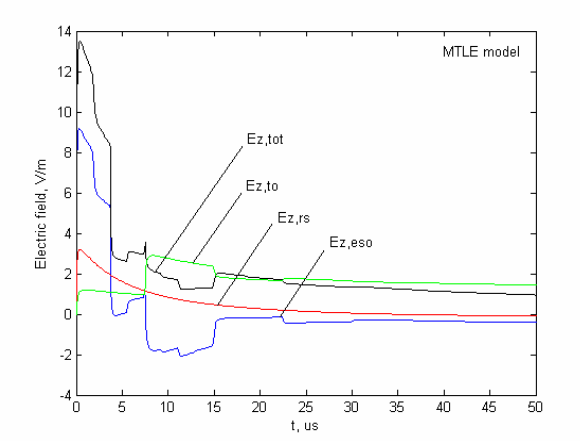


(e)

Fig. 4.12 – Electric field calculated at a distance of 100 km from a lightning return stroke to a **553-m** tall tower for five different engineering models:

(a) BG model, (b) TCS model, (c) TL model, (d) MTLL model, (e) MTLE model.

Figures 4.11 and 4.12 present simulation results for the electric field at a distance of 100 km, for the five considered models and considering two different elevated strike objects, 168-m

tall and 553-m tall, respectively. At this distance, the fields are essentially radiation fields, and electric and magnetic fields have the same waveshape. Only the electric field waveforms are reported in Figs. 4.11 and 4.12 because the curves relative to the magnetic field can be obtained by dividing the former ones by 377Ω. The computations are performed using the same undisturbed current $i_o(t)$ of Eq. (2.9) proposed by [*Nucci, et al.*, 1990].

Table 4.3 – Electric field peaks at 100 km as predicted by five engineering models.

| | 168-m tall tower | 553-m tall tower |
|---|---|---|
| Model | $E_{z\ peak}$ [V/m] | $E_{z\ peak}$ [V/m] |
| TL | 15.18 | 13.56 |
| MTLL | 15.16 | 13.54 |
| MTLE | 15.11 | 13.48 |
| BG | 15.32 | 13.69 |
| TCS | 15.23 | 13.59 |

Other considered parameters are λ = 2 km (for the MTLE model), $H_{tot}$ = 8 km (for the MTLL model) and the return stroke front speed $v$ = 150 m/μs.

The two considered elevated strike objects correspond to simplified models of the Peissenberg Tower in Germany and the CN Tower in Toronto. The Peissenberg-tower model is characterized by a height $h$ = 168 m and reflection coefficients of $\rho_t$ = -0.53 and $\rho_g$ = 0.7 [*Heidler, et al.*, 2001]. The adopted parameters of the CN-Tower model are given by: $h$ = 553 m, $\rho_t$ = -0.366 and $\rho_g$ = 0.8 [*Janischewskyj, et al.*, 1996].

In the same figures, the contributions of the three terms in Eq. (4.5) are also reproduced. The following conclusions can be drawn from the results presented in Figs. 4.11 and 4.12:

- No significant differences are found among the various models, especially in the early-time region where the peak field occurs (see also Table 4.3). This conclusion confirms the findings of [*Pavanello, et al.*, 2004c].
- As predicted by the theory, the contributions $E_z^{\mathrm{eso}}(r,t)$ and $E_z^{\mathrm{to}}(r,t)$ are independent of the considered models.

- The main contribution (about 70 %) to the field peak is given by the elevated strike object $E_z^{\mathrm{eso}}(r,t)$. Then comes the contribution of the main return stroke pulse $E_z^{rs}(r,t)$ (about 20-25 %), and finally, the contribution due to the turn-on-term is only about 15 % or less.
- The fast decay of the field right after the first peak occurs, respectively, at 1.1 μs for the 168-m tall tower and 3.7 μs for the 553-m tall one (namely, twice the travel time along the respective towers) and such a decay is produced by the reflection of the current wave at ground level.

### 4.4.2 Far-field Peak vs. current Peak relationship

As can be seen from the expressions in Tables 4.1 and 4.2, among the considered models, the TL is the only model for which it is possible to derive a simple, closed-form expression relating the distant electric and magnetic field peaks and the associated return-stroke current peaks. This has recently been done by Bermudez et al. [*Bermudez, et al.*, 2005] who derived specific expressions for tall and short (electrically speaking) strike objects.

For the case when the round-trip propagation time of the tall structure is greater than the zero-to-peak risetime $t_f$, the relation between far electric and magnetic field peaks and the associated undisturbed current peak at the top of the elevated object is given by [*Bermudez, et al.*, 2005][3]

$$E_{z\,peak}^{far} = -\frac{v}{2\pi\varepsilon_o c^2 r}\left[1+\frac{c}{v}\left(1-2\rho_t\right)\right] I_{\mathrm{o}\,peak} \tag{4.13}$$

$$H_{\varphi\,peak}^{far} = \frac{v}{2\pi c r}\left[1+\frac{c}{v}\left(1-2\rho_t\right)\right] I_{\mathrm{o}\,peak} \tag{4.14}$$

where $I_{o\,peak}$ is the first peak of the undisturbed current $i_o(h,t)$.

Note that, because of the condition $t_f < 2h/c$ imposed on the current, the above are independent of the structure's height $h$ and of the ground reflection coefficient $\rho_g$ [*Bermudez, et al.*, 2005].

For the case of a strike to ground when the reflections at ground level are taken into account, the relationships between far field peaks and the associated undisturbed current peak become [*Bermudez, et al.*, 2005]

[3] Note that Bermudez et al. [*Bermudez, et al*, 2005] disregarded in their derivation the effect of the discontinuity at the return stroke wavefront.

$$E_{z\,peak}^{far} = -\frac{v}{2\pi\varepsilon_o c^2 r}\left[1+\frac{c}{v}\rho_{ch-g}\right] I_{o\,peak} \tag{4.15}$$

$$H_{\varphi\,peak}^{far} = \frac{v}{2\pi c r}\left[1+\frac{c}{v}\rho_{ch-g}\right] I_{o\,peak} \tag{4.16}$$

in which $\rho_{ch-g} = (Z_{ch} - Z_g)/(Z_{ch} + Z_g)$ is the current reflection coefficient at ground level .

Comparing (4.13)-(4.14) with (4.15)-(4.16), it can defined the far-field enhancement factor due to the presence of a tall strike object as follows

$$k_{tall} = \frac{1+\frac{c}{v}(1-2\rho_t)}{1+\frac{c}{v}\rho_{ch-g}} \tag{4.17}$$

Baba and Rakov [*Baba and Rakov*, 2005] have derived a similar expression for the far field enhancement factor using their model[4] and they have presented a thorough analysis of the distance dependences of electric and magnetic fields due to a lightning strike to a tall object and due to the same lightning strike to flat ground.

In what follows, it is expressed the relationship between the far electromagnetic field peak and the peak current that would be measured at the top of a tall strike object [*[Bermudez, et al., 2005]*

$$E_{z\,\mathrm{peak}}^{far} = -\frac{v}{2\pi\varepsilon_o c^2 r} k'_{tall}\, I_{\mathrm{peak}} \tag{4.18}$$

$$H_{\varphi\,peak}^{far} = \frac{v}{2\pi c r} k'_{tall}\, I_{peak} \tag{4.19}$$

where $k'_{tall}$ is defined as

$$k'_{tall} = \frac{1+(1-2\rho_t)c/v}{1-\rho_t} \tag{4.20}$$

and $I_{\mathrm{peak}}$ is the peak amplitude of the current that would be measured at the top of the elevated strike object.

[4] The expression for the far field enhancement factor in the model of Baba and Rakov is slightly different from (4.17). As shown in [*Baba and Rakov*, 2005], the difference is due to the fact the speed of current waves propagating along the lightning channel is assumed to be the speed of light in the present study (which is based on the Rachidi et al. model [*Rachidi et al.*, 2002]), whereas in the model by Baba and Rakov, the current waves along the channel are assumed to travel at the return stroke speed *v*.

A short discussion on the terminology is in order. Bermudez et al. [*Bermudez, et al.*, 2005] used the notation $k_{tall}$ instead of $k'_{tall}$ and called this factor the 'tower enhancement factor'. In the present study, the notation and definition of Baba and Rakov [*Baba and Rakov, 2005*] are followed, in which the term 'tower enhancement factor' is attributed to the ratio of the far field associated with a strike to a tall tower to the far field associated with a similar strike to ground, expressed by $k_{tall}$ , and given by (4.17) within the model adopted in this study.

Results obtained using (4.19) will be compared in Chapter 5 with experimental data consisting of simultaneous measurements of magnetic fields and of the return-stroke current associated with lightning strikes to the Toronto CN Tower (553 m) obtained during the Summer of 2005.

Figure 4.13 presents the variation of the factor $k'_{tall}$ as a function of the reflection coefficient at the tower top. The adopted value for the return-stroke speed is $v$ = 150 m/μs. It can be seen that a variation of $\rho_t$ from 0 to -1 results in a variation of $k'_{tall}$ in the range 3 to 3.5.

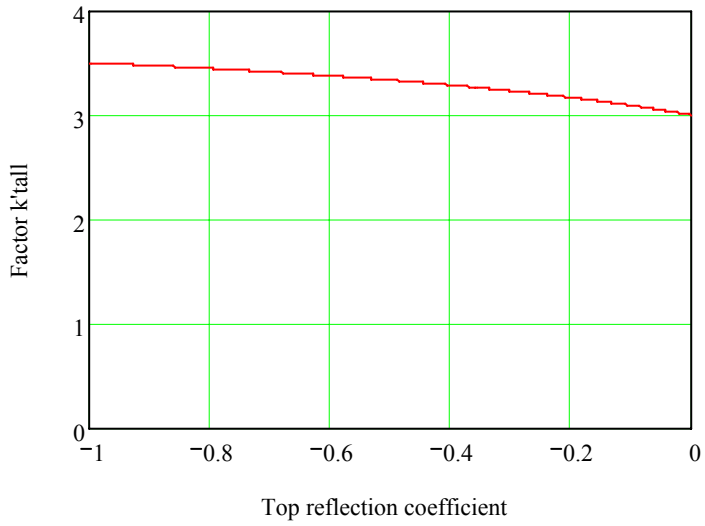


Fig. 4.13 - Variation of $k'_{tall}$ for a tall tower as a function of the top reflection coefficient $\rho_t$. The return-stroke speed is assumed to be $v = 1.5 \cdot 10^8$ m/s.

Figure 4.14 presents the variation of the factor $k'_{tall}$ as a function of the return-stroke speed. This time, the value of $\rho_t$ has been chosen to be equal to -0.4. Note that, in Figure 4.14, the factor $k'_{tall}$ is somewhat more sensitive to the return-stroke speed. However, it is important to realize that, in the expression relating the far electric field peak and the current peak (see (4.19)), the return-stroke speed $v$ appears not only within $k'_{tall}$ but also as a separate

proportionality factor. The overall effect of the return-stroke speed on the far-field – current relation is presented in Fig. 4.15. In this figure, two typical values for the return-stroke speed have been considered, namely, 100 m/μs and 200 m/μs. It can be seen that the peak E-field and H-field radiated by a lightning return stroke to a tall structure is little sensitive to the return-stroke speed.

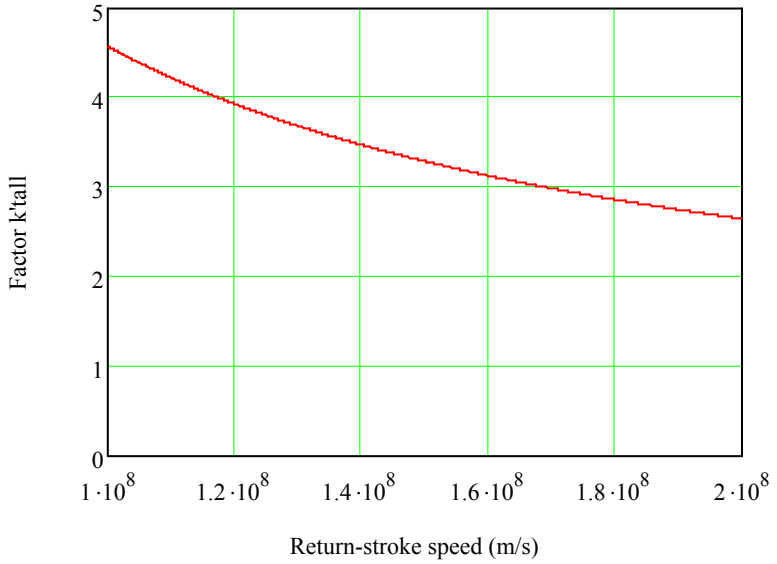


Fig. 4.14 - Variation of $k'_{tall}$ for a tall tower as a function of the return-stroke speed.
The top reflection coefficient $\rho_t$ is assumed to be equal to -0.4.

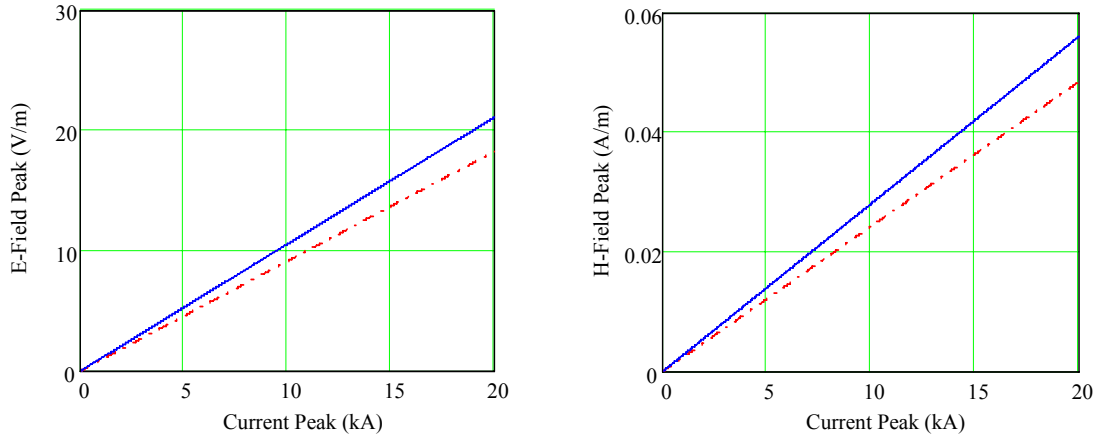


(a) (b)

Fig. 4.15 – Electric field peak (a) and Magnetic field peak (b) as a function of return-stroke current peak.
The observation point is located at a distance of 100 km from the strike location.
The top reflection coefficient $\rho_t$ is assumed to be equal to -0.4
(Solid line: return stroke speed: $v = 2 \cdot 10^8$ m/s. Dashed line: $v = 10^8$ m/s).

## 4.5 Conclusions

The importance of modeling is crucial for the determination of electromagnetic fields generated by a lightning channel, and, for the indirect estimation of return-stroke current from measurements of remote electromagnetic fields, as it is done, for example, by Lightning Location Systems.

This chapter presented the comparison among five engineering return stroke models, extended to include the presence of an elevated strike object, namely the Bruce-Golde (BG) model, the transmission line (TL) model, the traveling current source (TCS) model, and the two modified transmission line models (MTLL and MTLE). The current profile along the channel and along the strike object, as well as radiated electric and magnetic fields at different distances, predicted by these models, are presented and discussed.

Except for the case of very close (50 m) electric field, it was found that the computed electromagnetic fields associated with a strike to a 168-m tall tower are less model-dependent than those corresponding to a strike to ground. In addition, it was found that none of the models predicts the zero crossing of the field at far distances within a time window of 50 μs, a typically-observed feature for ground-initiated lightning return strokes.

Some experimental data at these distances were gathered in the framework of this thesis. As it will be shown in Sections 5.3.2 and 5.3.3, the collected data do exhibit a zero-crossing, although further measurements are needed to confirm this far field behaviour for tower-initiated return strokes.

In Section 4.4, analytical expressions relating far-fields and currents associated with lightning strikes to tall towers were derived. The derived equations are general and can be used with any of the five engineering models presented, expressed in terms of $P(z')$ (height-dependent current attenuation factor) and $v^*$ (current-wave propagation speed).

It was shown that the far field can be decomposed into three terms, namely, (1) contribution of the main return stroke pulse along the lightning channel, (2) contribution of the multiple-reflection process along the elevated strike object, including the contribution of pulses transmitted into the channel, and (3) contribution of the so-called ‘turn-on’ terms, associated with the current discontinuity at the return stroke wavefront, which have been thoroughly discussed in Chapter 3.

Only the first term is model-dependent.

It was found that the computed electromagnetic fields associated with a strike to a tall tower are not very sensitive to the adopted model for the return stroke. This is especially true

for the early time response of the field and, in particular, the peak field value.

It was demonstrated, in addition, that the TL is the only model for which it is possible to derive simple analytical formulas relating current peak and far field peak values. Such derivation has been recently presented by Bermudez et al. [*Bermudez, et al.*, 2005]. The electromagnetic field peak value being nearly independent of the adopted model, the TL expression becomes a general expression that can be applied for any engineering return-stroke model in case of tower-initiated lightning.

It is shown that the relationship between far electromagnetic fields and the current that would be measured at the top of an elevated strike object is relatively insensitive both to the value of the return-stroke speed and the top reflection coefficient. The factor $k'_{tall}$ could find a useful application in correcting current peak estimates obtained from remote field measurements for strikes to tall structures, particularly when these are used to calibrate the performance of lightning location systems.

Results and findings of this study emphasize the differences between return strokes initiated at ground level (or from short strike objects) and those striking tall towers:

- Electromagnetic fields associated with tall strike objects are less model-sensitive than those corresponding to a strike to ground. In particular, the early-time response of the field is nearly model-insensitive.
- Unlike ground-initiated strikes, for which the far-field peak is strongly dependent on the return stroke speed (proportional according to for the TL model), far field peaks associated with strikes to tall strike objects are little sensitive to the return stroke speed. This is an interesting result when lightning currents are measured directly on instrumented towers to calibrate the performance of lightning location systems, since in most practical cases the value of the return stroke speed is unknown.

# References

Baba, Y., and V. A. Rakov (2005), Lightning electromagnetic environment in the presence of a tall grounded strike object, *Journal of Geophysical Research*, *110*.

Bermudez, J. L. (2003), Lightning currents and electromagnetic fields associated with return strokes to elevated strike objects, 178 pp, Ph.D. Thesis, EPFL, Lausanne, Switzerland.

Bermudez, J. L., F. Rachidi, W. Janischewskyj, V. Shostak, M. Rubinstein, D. Pavanello, A. M. Hussein, J. S. Chang, C. A. Nucci, and M. Paolone (2005), Far-field - current relationship based on the TL model for lightning return strokes to elevated strike objects, *IEEE Transactions on Electromagnetic Compatibility*, *47*, 146-159.

Bruce, C. E. R., and R. H. Golde (1941), The lightning discharge, *The journal of the institution of electrical engineers*, *88*, 487-520.

Cooray, V., V. A. Rakov, F. Rachidi, C. A. Nucci, and R. Montaño (2004), On the constraints imposed by the close electric field signature on the equivalent corona current in lightning return stroke models, paper presented at International Conference on Lightning Protection, ICLP 2004, Avignon, France.

Cummins, K. L., E. P. Krider, and M. D. Malone (1998), The US National Lightning Detection Network (TM) and applications of cloud-to-ground lightning data by electric power utilities, *IEEE Transactions on Electromagnetic Compatibility*, *40*, 465-480.

Heidler, F. (1985), Traveling current source model for LEMP calculation, *Electromagnetic Compatibility*, *626*.

Heidler, F., J. Wiesinger, and W. Zischank (2001), Lightning Currents Measured at a Telecommunication Tower from 1992 to 1998, paper presented at 14th International Zurich Symposium on Electromagnetic Compatibility, Zurich, Switzerland, February 20 - 22, 2001.

Herodotou, N., W. A. Chisholm, and W. Janischewskyj (1993), Distribution of lightning peak stroke currents in Ontario using an LLP system, *IEEE Transactions on Power Delivery*, *8*, 1331-1339.

Janischewskyj, W., V. Shostak, J. Barratt, A. M. Hussein, I. Rusan, and J. S. Chang (1996), Collection and use of lightning return stroke parameters taking into account characteristics of the struck object, paper presented at 23rd ICLP (International Conference on Lightning Protection), Florence, Italy.

Nucci, C. A., G. Diendorfer, M. Uman, F. Rachidi, M. Ianoz, and C. Mazzetti (1990), Lightning return stroke current models with specified channel-base current: a review and comparison, *Journal of Geophysical Research*, *95*, 20395-20408.

Nucci, C. A., C. Mazzetti, F. Rachidi, and M. Ianoz (1988), On lightning return stroke models for LEMP calculations, paper presented at 19th international conference on lightning protection, Graz, may 1988.

Pavanello, D., F. Rachidi, J. L. Bermudez, and M. Rubinstein (2004a), Engineering lightning return stroke models including an elevated strike object: far field-current relationship, paper presented at International Symposium on Electromagnetic Compatibility, EMC EUROPE 2004, Eindhoven, September 2004.

Pavanello, D., F. Rachidi, J. L. Bermudez, M. Rubinstein, and C. A. Nucci (2004b), Electromagnetic Field Radiated by Lightning to Tall Towers: Treatment of the Discontinuity at the Return Stroke Wavefront, *Journal of Geophysical Research*, *109*.

Pavanello, D., F. Rachidi, V. A. Rakov, C. A. Nucci, and J. L. Bermudez (2004c), Return Stroke Current Profiles and Electromagnetic Fields Associated with Lightning Strikes to Tall Towers: Comparison of Engineering Models, paper presented at International Conference on Lightning Protection, ICLP 2004, Avignon, France, September 2004.

Pavanello, D., F. Rachidi, V. A. Rakov, C. A. Nucci, and J. L. Bermudez (Submitted in 2005), Return Stroke Current Profiles and Electromagnetic Fields Associated with Lightning Strikes to Tall Towers: Comparison of Engineering Models, *Journal of Electrostatics*.

Pavanello, D., F. Rachidi, M. Rubinstein, J. L. Bermudez, W. Janischewskyj, V. Shostak, C. A. Nucci, A. M. Hussein, and J. S. Chang (Submitted in 2006), On Return-Stroke Currents and Remote Electromagnetic Fields Associated with Lightning Strikes to Tall Structures - Part I: Computational Models, *Journal of Geophysical Research*.

Pavanello, D., F. Rachidi, M. Rubinstein, J. L. Bermudez, and C. A. Nucci (2004d), On the calculation of electromagnetic fields radiated by lightning to tall structures, paper presented at International Conference on Lightning Protection, ICLP 2004, Avignon, France, September 2004.

Rachidi, F., and C. A. Nucci (1990), On the Master, Uman, Lin, Standler and the Modified Transmission Line lightning return stroke current models, *Journal of Geophysical Research*, *95*, 20389-20394.

Rachidi, F., V. A. Rakov, C. A. Nucci, and J. L. Bermudez (2002), The Effect of Vertically-Extended Strike Object on the Distribution of Current Along the Lightning Channel, *Journal of Geophysical Research*, *107*, 4699.

Rachidi, F., and R. Thottappillil (1993), Determination of lightning currents from far electromagnetic fields, *Journal of Geophysical Research*, *98*, 18315-18320.

Rakov, V. A. (1997), Lightning electromagnetic fields: modeling and measurments, paper presented at 12th International Zurich symposium and Technical Exhibition on electromagnetic compatibility, Zurich.

Rakov, V. A., and A. A. Dulzon (1987), Calculated electromagnetic fields of lightning return strokes, *Tekhnicheskaya Elektrodinamika*, *no. 1*, 87-89.

Rakov, V. A., and M. A. Uman (1998), Review and evaluation of lightning return stroke models including some aspects of their application, *IEEE Transactions on Electromagnetic Compatibility*, *40*, 403-426.

Shostak, V., W. Janischewskyj, A. Hussein, and B. Kordi (2000), Electromagnetic fields of lightning strikes to a tall tower: a model that accounts for upward-connecting discharges, paper presented at 25th ICLP (International Conference on Lightning Protection), Rhodes, Greece, 2000.

Uman, M. A. (1985), Lightning return stroke electric and magnetic fields, *Journal of Geophysical Research*, *90*, 6121-6130.

Uman, M. A., and D. K. McLain (1969), Magnetic field of the lightning return stroke, *Journal of Geophysical Research*, *74*, 6899-6910.

# Chapter 5

# Simultaneous measurements of return-stroke current, electric and magnetic fields at three distance ranges associated with lightning strikes to the CN Tower

## 5.1 Introduction

Studies on lightning striking the Toronto Canadian National (CN) Tower have been performed and reported by the "CN Tower Lightning Studies Group (CNT-LSG)" since 1978 (e.g. [*Hussein, et al.*, 2004; *Janischewskyj, et al.*, 1997; *McComb, et al.*, 1980; *Rachidi, et al.*, 2001]). An active collaboration exists since 1997 between the CNT-LSG and the Swiss Federal Institute of Technology in Lausanne and researchers from Switzerland regularly participate to tower-initiated-lightning measurement campaigns in Toronto during the summertime. Recently, Bermudez et al. [*Bermudez, et al.*, 2005] presented a theoretical analysis corroborated by experimental data relating lightning return-stroke currents and far radiated electric and magnetic fields taking into account the presence of an elevated strike object. The theoretical predictions presented in that work were sustained by the simultaneous records, gathered during the summers of 2000 and 2001, of the return-stroke current and its associated electric and magnetic fields measured at two distances, namely, 2 km and 16.8 km, related with lightning strikes to the CN Tower.

During the Summer of 2005, a third measuring station was added to the historical sites adopted in the past. The location of the new station was chosen on the opposite shore of Lake Ontario, 50.9 km away from the CN Tower, providing important information about the propagation effects experienced by the field radiated along the surface of the lake.

The aim of the present chapter, which is, with the exception of Section 5.5, based on [*Pavanello, et al.*, Submitted in 2006a], is to report on the simultaneous measurements performed during the Summer of 2005 of the return-stroke currents from lightning striking the CN Tower, the corresponding electric and magnetic fields measured at *three* distances and the video images of the trajectory of the flashes. To our knowledge, this is the first time where simultaneous measurements of lightning return stroke currents and corresponding electric and magnetic fields at three distances have been ever performed. The GPS-time stamping of the data, another feature not available in the previous lightning measurement campaigns performed by the CNT-LSG, allowed matching the recorded flashes with data obtained by the US NLDN (United States National Lightning Detection Network), drawing, therefore, important conclusions about the accuracy of the current estimation provided by lightning location systems in case of lightning impacts to tall structures.

The obtained data are used to test and validate the return-stroke models and the theoretical expressions, presented in [*Pavanello, et al.*, Submitted in 2006b], relating far-field peaks to current peaks for lightning strikes to tall structures and, also, to validate the theory of wave propagation along a finitely conducting ground discussed in Section 3.5.

## 5.2 Experimental set-up and measuring stations

During the Summer of 2005, the first simultaneous measurements of return-stroke current from lightning striking the CN Tower and the corresponding electric and magnetic fields measured at three distances, as well as images using a video recording system (DVD format) and a high-speed camera system were obtained [*Pavanello, et al.*, 2006]. All mentioned measuring systems (except the high speed camera) had a GPS time stamping for unique identification of each single lightning return stroke. Fig 5.1 shows a top view of the location of the field measurement systems relative to the CN Tower. The nearest system to the CN Tower is installed on the roof of the Pratt building of the University of Toronto. Located 2.0 km away from the CN Tower, the Pratt Building is the seat of a permanent installation belonging to the CNT-LSG, which features, in addition to the electric and magnetic field measurement system, also a DVD-format video recording camera and a 2-ms-resolution hi-speed camera. The second location chosen for the measurement of the electric and magnetic fields was the roof of the main building of the Environment Canada offices in Toronto, 16.8 km away from the CN Tower. The third field measurement system was installed on the roof of a private building in Grimsby, on the shore of Lake Ontario facing the CN Tower from a

distance of 50.9 km.

It is worth noting that the propagation paths from the CN Tower to the Pratt building (2.0 km) and Environment Canada (16.8 km) stations were along the soil and through the city of Toronto, whereas, for the third location in Grimsby (50.9 km), the propagation path was nearly entirely across Lake Ontario.


Fig. 5.1 - Satellite view of the locations of the CN Tower and the three electromagnetic field measuring stations: the Pratt building of the University of Toronto, the Environment Canada building and the site in Grimsby (image obtained using Google Earth ©).

### 5.2.1 Instrumentation

The complete measuring systems operational during the Summer of 2005 can be summarized as follows: (1) the current derivative recording system, located at the CN Tower (reference point), (2) the electromagnetic field, DVD and high speed camera recording systems at 2.0 km (Pratt building), (3) the electromagnetic field recording system at 16.8 km (Environment

Canada building), and (4) the electromagnetic field recording system at 50.9 km (Grimsby, ON). The electromagnetic field measurement systems at 16.8 km and at 50.9 km were installed by the Swiss Federal Institute of Technology to enhance the permanent measurement system of the CN Tower Lightning Studies Group.

Details about the characteristics of each instrument and their relative settings are reported in [*Pavanello and Rachidi*, 2006], as well as the plots of all recorded quantities.

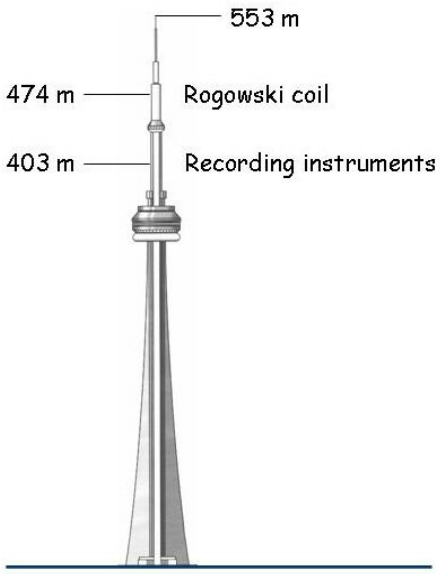


Fig. 5.2 - Location of the CN Tower lightning return-stroke current measuring system components.

### 5.2.2 Current derivative measuring system

The lightning current derivative on the CN Tower has been measured since 1990 using a 3-m, 40-MHz Rogowski coil [*Ward and Exon*, 1993] installed at a height of 474 m, as shown in Fig 5.2 [*Hussein, et al.*, 2004]. The coil is characterized by a risetime of 8.7 ns, a sensitivity of 0.359 V/(kA/μs), and an accuracy of ± 6 %. It is connected via a 102-m 50-Ω triaxial cable to the recording system located at 403 m. The whole chain composed by the coil, the transmission cable and the digitizer is characterized by 50-Ω connections, which provide a non-reflective configuration.

A second Rogowski coil with fiber-optic link is also installed at a height of 509 m since 1997. However, this system was not operational during the Summer 2005.

The recording system consists of a 250-MS/s, 8-bit digitizer with 1 MB memory per channel and a computer controller fitted with a GPS receiver for time stamping. The time scale of the

digitizer has a 4-ns resolution and is segmented for recording up to twenty 200-μs long strokes per lightning flash.

### 5.2.3 Vertical electric field and azimuthal magnetic fields measurement system at 2 km

The vertical component of the electric field ($E_z$) and the azimuthal component of the magnetic field ($H_\varphi$) were measured 2.0 km North of the CN Tower. Two active sensors are permanently installed on the roof of the four-floor Pratt building of the University of Toronto (see Fig. 5.3): a hemispheric electric field sensor (47 Hz – 100 MHz) for $E_z$ and a small loop magnetic field sensor (635 Hz – 134 MHz) for $H_\varphi$. They are both connected to the digitizer via 50-Ω triaxial cables. The recording system, identical to the one installed at the CN Tower, consists of an 8-bit digitizer with 1 MB memory per channel and a computer controller provided with GPS receiver for time stamping. The same time scale setup as used for the measurement of the current derivative is adopted here (4-ns resolution, up to 20 segments, 200 μs per segment).

(a) (b)

Fig. 5.3 - Electric (a) and Magnetic (b) field sensors permanently installed at the University of Toronto.

### 5.2.4 Vertical electric and azimuthal magnetic fields measurement system at 16.8 km

The vertical component of the electric field ($E_z$) and the azimuthal component of the magnetic field ($H_\varphi$) were measured 16.8 km North of the CN Tower. Two active sensors were located on the roof of the four-floor Environment Canada building: a spherical E-field sensor (TSN 245-E32, Thomson CSF, 1 kHz – 130 MHz) for $E_z$ and an H-field loop antenna sensor (TSN

245-H30, Thomson CSF, 4 kHz – 130 MHz) for $H_\varphi$ (see Fig. 5.4). The measured signals from the two sensors were relayed via fiber optic links to the recording system, consisting of a 100-MS/s, 8-bit digitizer with 1 MB memory per channel and a computer controller provided with GPS receiver for time stamping. The time scale of the digitizer has a 10-ns resolution and it is segmented for recording up to twenty 100-μs long strokes per lightning flash.

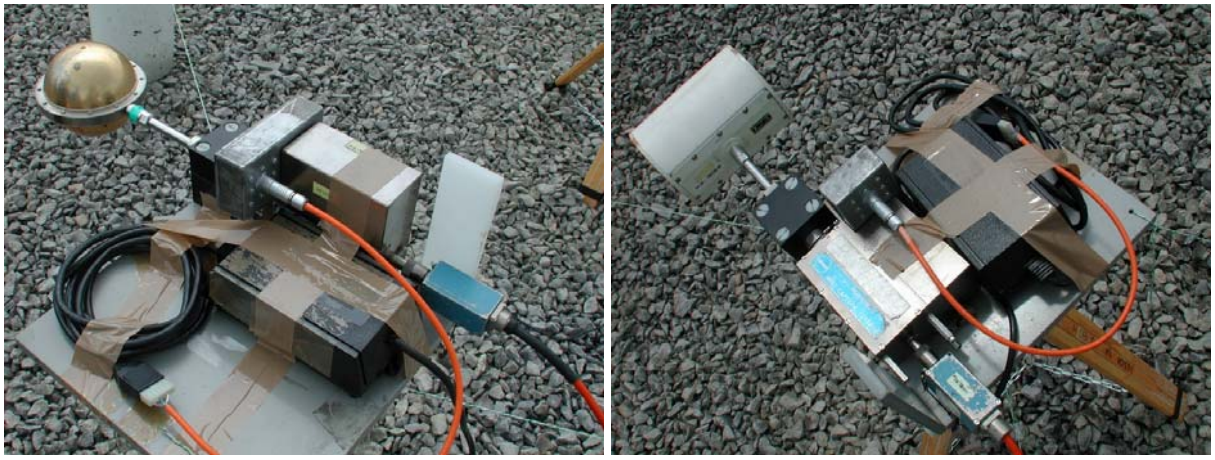

(a) (b)

Fig. 5.4 - Electric (a) and Magnetic (b) field sensors installed by the Swiss Federal Institute of Technology.

### 5.2.5 Vertical electric and azimuthal magnetic fields measurement system at 50.9 km

A system identical to the one used at 16.8 km was installed to measure the vertical component of the electric field ($E_z$) and the azimuthal component of the magnetic field ($H_\varphi$) at 50.9 km South-West of the CN Tower. The sensors were located on the roof of a private two-floor building in Grimsby (see Fig. 5.1). The propagation path from the CN Tower to this location, except for the first 2.3 km of mixed soil-water path to cross the Toronto Island and the last 50 m over grass, was across Lake Ontario.

## 5.3 Experimental data

### 5.3.1 General observations

The whole set of simultaneous data recorded during the Summer of 2005 was gathered during one day, August 19$^{th}$. A total of eight flashes striking the CN Tower were recorded on that day and were confirmed by DVD video recording. Two of them, which occurred in the

morning, were rather weak and none of the three field measuring systems was able to detect them. Six other flashes, for which simultaneous data were recorded, occurred in the afternoon of that same day and contained more than 30 strokes. An interesting study, complementary to the one presented in this chapter, which presents a detailed analysis of return-stroke multiplicity relative to the same data of CN Tower lightning of August 19th 2005 can be found in [*Janischewskyj, et al.*, 2006].

A representative set of simultaneously measured return-stroke current and associated electric and magnetic fields at 2.0 km, 16.8 km, and 50.9 km, respectively, related to the second stroke of a CNT flash on Aug. 19th (14:13:13, Toronto time), whose trajectory is shown in Fig 5.5 from DVD-format video recording, is reported in Fig 5.6. It is worth noting that some periodic noise, characterized by a frequency of about 760 kHz, affects the field recorded at the distance of 50.9 km. This noise, clearly discernible in Subfigs 5.6(g) and 5.6(h), is due to a broadcasting radio station located a few hundred meters West from the field measuring site and, therefore, should not be related with propagation effects.

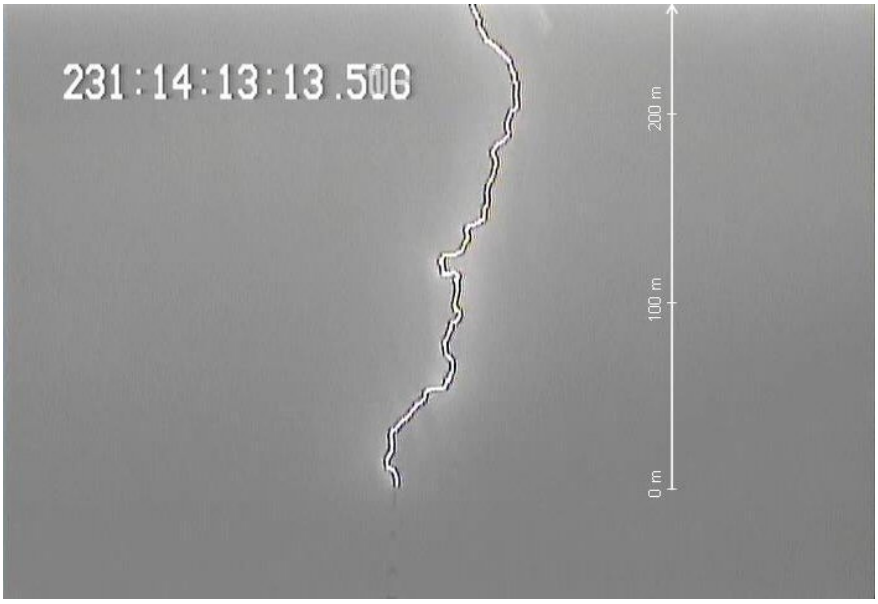


Fig. 5.5 - Flash striking the CN Tower tip at 14:13:13 on August 19th, 2005 (frame captured by the DVD recording system at Pratt building).

Table 5.1 summarizes, for the analyzed set of data obtained in 2005, the peak values of the return-stroke currents, as well as their associated electric and magnetic field peaks. In the table are also included the electric-to-magnetic field peak ratios (wave impedance). It is well-known that at the considered distances (2 km and beyond), the initial peak of the field is

essentially due to the radiation component (e.g. [*Rachidi, et al.*, 2001]). As a result, the E-field peak to H-field peak ratio should be about the free space wave impedance, namely, 377 Ω. However, it can be seen from Table 5.1 that this ratio (noted as *Z*) is 450-500 Ω at Pratt Building (2 km), 500-560 Ω in Grimsby (50.9 km) and about 1800 at Environment Canada Building (16.8 km). One possible reason explaining the relatively large values for wave impedance could be ascribed to the enhancement effect introduced by the buildings on which the electromagnetic fields were measured [*Bermudez, et al.*, 2004; *Bermudez, et al.*, 2002; *Bonyadi Ram, et al.*, 2001]. Metallic beams and other conducting parts in those structures cause an enhancement effect on the measured fields. It has been shown [*Bermudez, et al.*, 2004] that, although an enhancement is seen both on the electric and the magnetic fields, the degree of enhancement is actually greater for the electric field than for the magnetic field.

Therefore, the value of the wave impedance could give an estimate of the enhancement effect of the building on the electric field. Indeed, as can be seen from Table 5.1, at each specific measuring site, this value does not vary significantly. Assuming that the enhancement of the magnetic field can be neglected relative to the enhancement of the electric field, the building enhancement on the electric field is about 20-30 % for Pratt Building, 30-50 % for the station in Grimsby, and, more than 400 % for the Environment Canada building. This large value could be due to the particular location and configuration of the Environment Canada building and the presence of several monitoring and measuring pieces of equipment with metallic parts, which are permanently installed on the roof of the building, near the installed sensors.

### 5.3.2 Observations on the current waveforms

All the current pulses recorded at the CN Tower during the thunderstorm of August 19, 2005 were associated with negative strokes. This information has not been included in the presented data because the attention here is focused on the absolute value of the return-stroke current peaks, which has been conventionally assumed as positive.

All the recorded current waveforms present the usual shape observed in lightning data recorded using instrumented towers: they are characterized by an initial peak, considered as the actual value of the return-stroke current injected by lightning on the tower top, followed by a second, higher, peak, due to reflection from ground of the current wave. The recorded currents exhibit (first) peak values distributed in the range of 3 kA to 12 kA, risetime (defined

as 10 % to 90 % of the first peak) varying between 0.2 μs and 2.8 μs (see Table 5.1) and a typical duration (to 50 % of the first peak) of about 80 μs.

It is worth mentioning that none of the current-derivative waveforms recorded on August 19, 2005 is corrupted by the 110-kHz signal of the Loran-C radionavigation system, previously observed affecting CNT data by [*Liatos and Hussein*, 2005].

Table 5.1 – Summary of the parameters associated with strokes recorded during the Summer 2005 ($Iz_{rs}$ is the 10% - 90% current risetime and *Z* represents the wave impedance, defined as the $Ez_{peak}$ to $H\varphi_{peak}$ ratio).

| Flash time | Return stroke # | $Iz_{peak}$ [kA] | $Iz_{rs}$ [μs] | D = 2 km | | | D = 16.8 km | | | D = 50.9 km | | |
|---|---|---|---|---|---|---|---|---|---|---|---|---|
| | | | | $Ez_{peak}$ [V/m] | $H\varphi_{peak}$ [A/m] | Z [Ω] | $Ez_{peak}$ [V/m] | $H\varphi_{peak}$ [A/m] | Z [Ω] | $Ez_{peak}$ [V/m] | $H\varphi_{peak}$ [A/m] | Z [Ω] |
| 13:55:56 | 1 | 3.7 | 1.2 | 328.2 | 0.674 | 486.9 | 130.3 | 0.0692 | 1882.9 | 13.2 | 0.0259 | 509.65 |
| | 3 | 6.9 | 0.2 | 589.4 | 1.274 | 462.6 | | | | 25.1 | 0.0463 | 542.12 |
| | 4 | 6.3 | 0.4 | 555.1 | 1.190 | 466.5 | | | | 23.2 | 0.0409 | 567.24 |
| | 5 | 3.2 | 0.4 | 294.4 | 0.629 | 468.0 | | | | | | |
| | 6 | 4.0 | 0.4 | 353.5 | 0.783 | 451.5 | | | | 14.7 | 0.0263 | 558.94 |
| | 7 | 3.0 | 0.4 | 278.5 | 0.600 | 464.2 | | | | | | |
| | 8 | 3.0 | 0.4 | 273.8 | 0.581 | 471.3 | | | | | | |
| | 9 | 4.5 | 0.4 | 401.8 | 0.871 | 461.3 | | | | 15.4 | 0.0293 | 525.60 |
| | 10 | 5.0 | 1.2 | 470.0 | 0.930 | 505.4 | | | | 18.2 | 0.0320 | 568.75 |
| 14:11:41 | 1 | 7.9 | 0.8 | 684.6 | 1.398 | 489.7 | 267.3 | 0.1603 | 1667.5 | 28.9 | 0.0537 | 538.18 |
| | 2 | 5.4 | 0.6 | 473.5 | 1.020 | 464.2 | 191.7 | 0.1006 | 1905.6 | 20.2 | 0.0340 | 594.12 |
| | 5 | 4.0 | 2.8 | 337.0 | 0.706 | 477.3 | 121.4 | 0.0658 | 1845.0 | 12.2 | 0.0235 | 519.15 |
| | 6 | 7.6 | 0.6 | 650.0 | 1.392 | 467.0 | 259.8 | 0.1413 | 1838.6 | 25.8 | 0.0479 | 538.62 |
| | 9 | 5.8 | 1.6 | 527.8 | 1.044 | 505.6 | | | | 19.7 | 0.0369 | 533.88 |
| 14:13:13 | 1 | 8.6 | 0.8 | 827.5 | 1.675 | 494.0 | 349.1 | 0.1917 | 1821.1 | 32.4 | 0.0602 | 538.21 |
| | 2 | 5.5 | 0.4 | 492.0 | 1.006 | 489.1 | 202.4 | 0.1063 | 1904.0 | 21.4 | 0.0374 | 572.19 |
| | 3 | 11.7 | 1.0 | 1124 | 2.293 | 490.2 | 433.1 | 0.2378 | 1821.3 | 42.9 | 0.0789 | 543.73 |
| | 4 | 5.0 | 0.4 | 452.8 | 1.011 | 447.9 | 181.1 | 0.0950 | 1906.3 | 19.2 | 0.0352 | 545.45 |
| | 5 | 4.4 | 0.2 | 398.7 | 0.869 | 458.8 | 156.2 | 0.0820 | 1904.9 | 15.8 | 0.0296 | 533.78 |
| | 7 | 4.5 | 1.2 | 444.2 | 0.881 | 504.2 | 161.3 | 0.0867 | 1860.4 | 17.5 | 0.0322 | 543.48 |
| 14:37:08 | 1 | 7.1 | 0.6 | 560.4 | 1.205 | 465.1 | 224.2 | 0.1193 | 1879.3 | 23.4 | 0.0435 | 537.93 |
| 14:37:52 | 1 | 5.4 | 0.8 | 504.5 | 1.000 | 504.5 | 195.9 | 0.1072 | 1827.4 | 21.0 | 0.0382 | 549.74 |
| | 2 | 6.8 | 1.4 | 611.0 | 1.238 | 493.5 | 234.6 | 0.1283 | 1828.5 | 24.9 | 0.0459 | 542.48 |
| | 3 | 12.0 | 1.6 | 1082 | 2.222 | 486.9 | | | | 44.8 | 0.0793 | 564.94 |
| | 4 | 7.4 | 0.4 | 639.0 | 1.350 | 473.3 | | | | 27.4 | 0.0490 | 559.18 |
| 15:26:00 | 1 | 6.9 | 0.8 | 620.1 | 1.224 | 506.6 | | | | | | |
| | 2 | 5.3 | 2.0 | 455.0 | 0.905 | 502.8 | | | | | | |
| | 3 | 5.9 | 0.4 | 500.5 | 0.979 | 511.2 | | | | | | |
| | 4 | 6.1 | 1.6 | 542.3 | 1.050 | 516.5 | | | | | | |
| | 5 | 3.0 | 0.4 | 241.1 | 0.523 | 461.0 | | | | | | |
| | 6 | 5.3 | 0.4 | 434.7 | 0.930 | 467.4 | | | | | | |

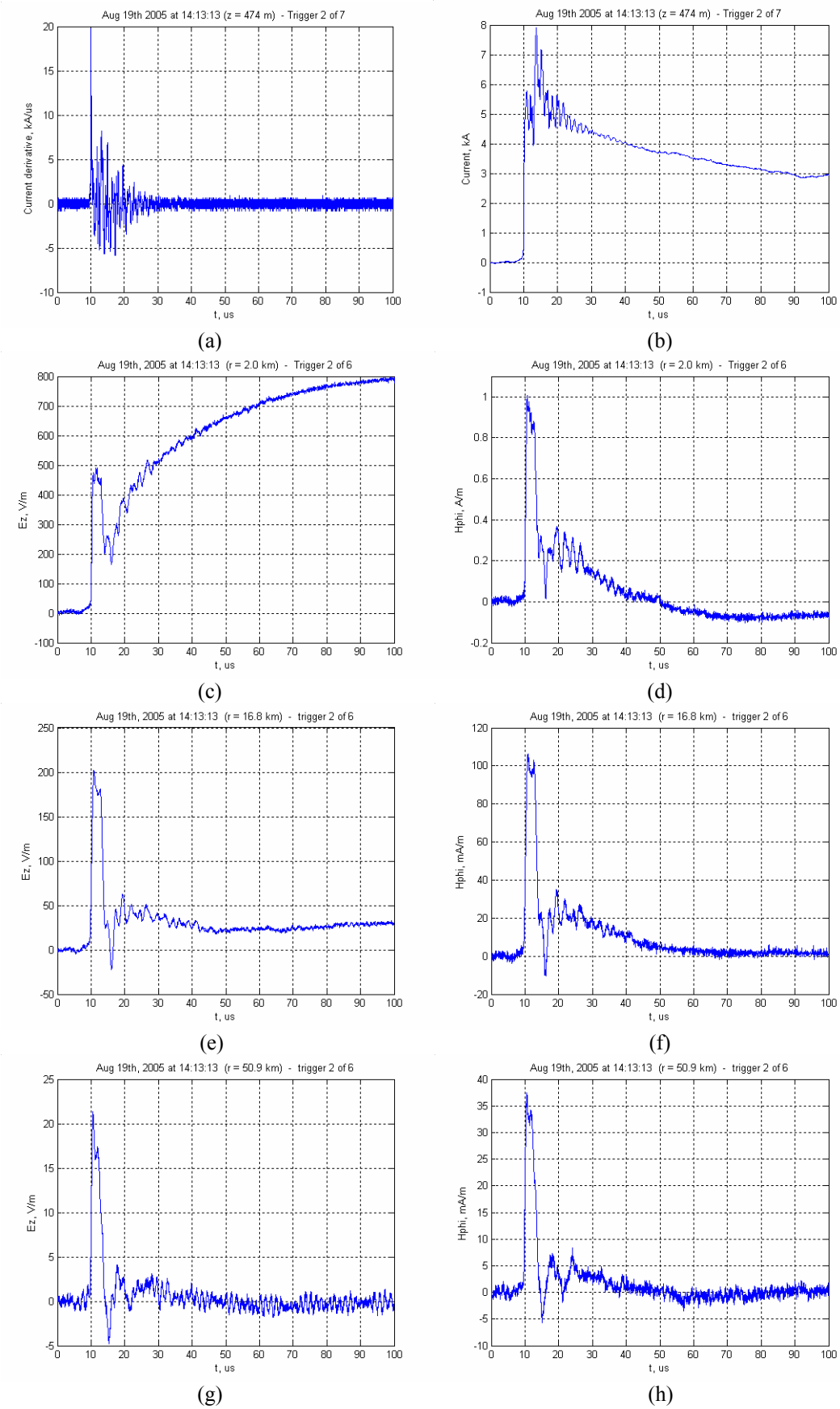


Fig. 5.6 - Simultaneous records of (a) return-stroke current derivative, (b) current (numerically integrated), (c) electric and (d) magnetic fields at 2 km, (e) electric and (f) magnetic fields at 16.8 km, and (g) electric and (h) magnetic fields at 50.9 km. 2nd stroke of the flash striking the CN Tower tip at 14:13:13 on August 19th, 2005.

### 5.3.3 Observations on the field waveforms

The atmospheric-electricity sign convention is adopted in this thesis for the electric field (positive field for a downward vertical E-field).

Observation of Fig 5.6 shows that, at 2 km, the electric field is characterized by its initial peak followed by an increasing ramp, and that the magnetic field is characterized by an initial peak followed by a hump. These features are in agreement with characteristics of fields at this distance range for direct strikes to ground as reported in [*Lin, et al.*, 1979], although fields associated with strikes to tall structures have a more pronounced initial peak [*Bermudez, et al.*, 2005; *Rachidi, et al.*, 2001]. It has to be noted, however, that the magnetic field at 2 km exhibits a pronounced zero-crossing after about 50 μs. This feature, typically observed for larger distances, should not be present at 2 km from the lightning channel and can be explained by a poor response of the University of Toronto magnetic field sensor for low frequencies (short time constant of the integrator). At 16.8 km and 50.9 km, the electric and magnetic fields are characterized by similar waveforms, typical of distant fields.

The waveforms of the electric and magnetic fields at 16.8 km and 50.9 km exhibit a first zero-crossing about 5 microseconds after the onset of the return-stroke. This early zero-crossing is part of a narrow undershoot. The fact that the observed undershoot is clearly discernible in both the electric and the magnetic fields suggests that the feature is not an artifact of the measurement system. Such an early undershoot, also rarely observed on the field waveforms at 2 km [*Janischewskyj, et al.*, 1998], can be attributed to the transient processes along the tower (see e.g. [*Pavanello, et al.*, 2005; *Rachidi, et al.*, 2001; *Shostak, et al.*, 2000]). Simulation results in [*Pavanello, et al.*, 2005; *Rachidi, et al.*, 2001; *Shostak, et al.*, 2000] indicate that the undershoot occurs at a time given approximately by twice the propagation time along the tower.

For fields at 50.9 km, the expected zero-crossing at about 40 microseconds [*Lin, et al.*, 1979] is also observed. Interestingly, this zero-crossing is not reproduced by the models once the ‘turn-on’ term is taken into account. The zero-crossing is also absent in the field predicted using AT-type models. Further work is needed to understand this point.

### 5.3.4 Discussion on the propagation effects

It is well-known [*Bermudez, et al.*, 2002; *Cooray*, 1987; *Cooray, et al.*, 2006; *Cooray and Lundquist*, 1983; *Lin, et al.*, 1979; *Pavanello, et al.*, 2005; *Uman, et al.*, 1976] that the propagation of lightning electromagnetic fields over a finitely conducting ground results in

the attenuation of high frequency components of the field spectrum. This causes the amplitude of the field to decrease faster than the expected theoretical behavior over a perfectly conducting ground, and its risetime to increase with increasing propagation distance and/or decreasing ground conductivity.

Fig 5.7 presents the magnetic field peaks as a function of the corresponding return-stroke current (first) peaks. The values of the field peaks at 16.8 km and 50.9 km were normalized to those at 2 km assuming 1/*r* dependence. It can be seen that there is a nearly linear correlation between current peaks and corresponding field peaks. It can also be seen that the values of the normalized peak fields at 16.8 and 50.9 km are, on average, lower than those measured at 2 km.

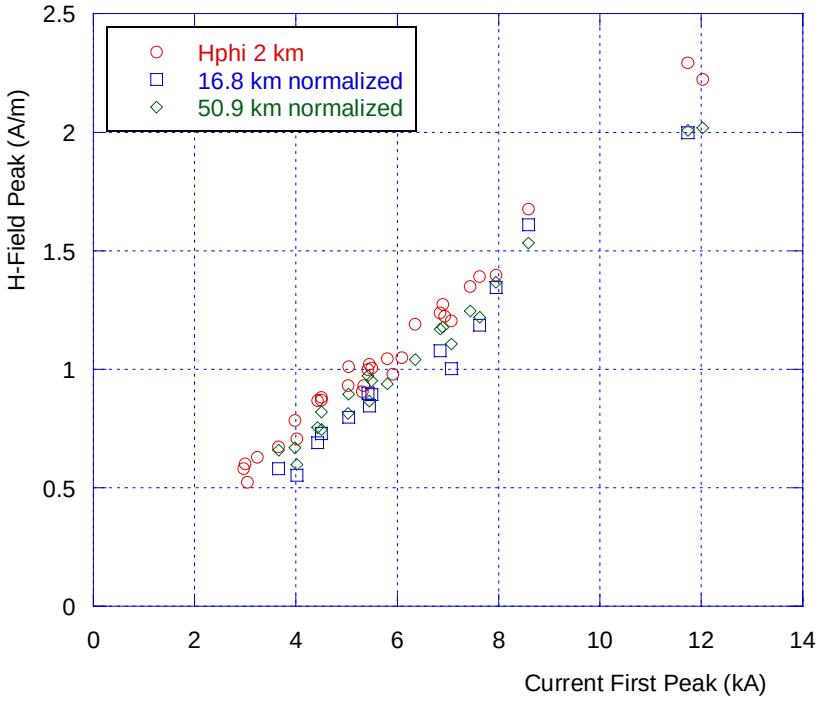


Fig. 5.7 - Measured magnetic field peaks as a function of measured current first peak. The values for the measured field peaks at 16.8 km and 50.9 km have been normalized to those at 2 km assuming 1/*r* dependence.

In order to better illustrate this effect, Fig 5.8 presents the ratio of the magnetic field peak to the current peak, for the three observation locations, namely, at 2, 16.8 and 50.9 km. Again, the H-field peak values at 16.8 and 50.9 km are normalized to those at 2 km assuming a 1/r dependence. The median values of the normalized magnetic field at 2, 16.8 and 50.9 km are, respectively, 1 A/m, 0.89 A/m and 0.96 A/m  Note that, at 2 km, the static and induction terms of the electric field may have a contribution to the total field [*Rachidi, et al.*, 2001].

However, this contribution appears to be insignificant for the observed risetimes (0.2-2.8 μs).

The results indicate the effect of the propagation on the attenuation of the field peak. It is interesting to note that the fields at 50.9 km are less affected by such attenuation than those at 16.8 km, presumably because the path of propagation is mostly across Lake Ontario. Estimates of the electrical parameters of the Ontario Lake are as follows: conductivity $\sigma = 8 \cdot 10^{-3}$ S/m, relative permittivity $\varepsilon_r = 81$ [*Chisholm*, 2006]. The area from the CN Tower up to the University of Toronto and Environment Canada buildings is formed by a high fraction of industrialized / developed area with most construction being of clay brick, steel or reinforced concrete, underlaid by a water system with grid spacing of about 15 m (minor lines) and 200 m (major lines, one along each street). It is therefore very difficult to estimate the value of the equivalent ground conductivity, but this equivalent value could be expected to be somewhat lower than that associated with Lake Ontario [*Chisholm*, 2006].

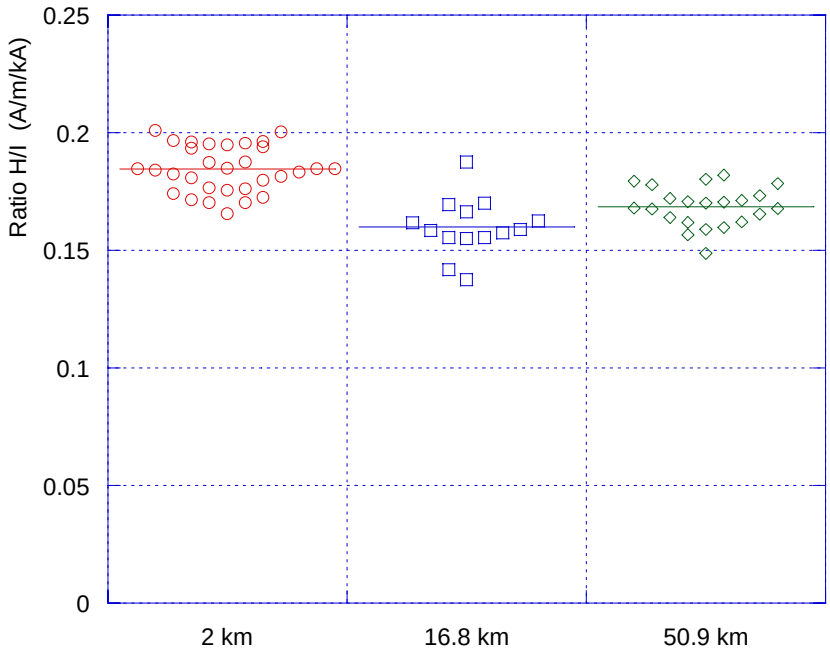


Fig.5.8 - Ratio of the magnetic field peak to the return-stroke current peak for the 31 recorded strokes and for the three considered distances. The values for the field peaks at 16.8 km and 50.9 km have been normalized to those at 2 km assuming 1/*r* dependence.

Fig 5.9 shows the magnetic field maximum steepness as a function of current maximum steepness. The values for the steepness at 16.8 km and 50.9 km have been normalized to those at 2 km assuming a 1/r dependence. It can be seen, as expected [*Cooray*, 2003], that the

propagation effects are more pronounced for the field derivatives. The propagation along a finitely-conducting ground results essentially in the attenuation of high frequency components of the field spectrum [*Cooray*, 2003]. Indeed, observations presented in Fig 5.9 show larger attenuations for higher current steepness. Cooray [*Cooray and Ye*, 1994] predicted on the basis of theoretical calculations that, in the case of sea to land propagation, the rise time increases monotonically as the length of the land section increases.

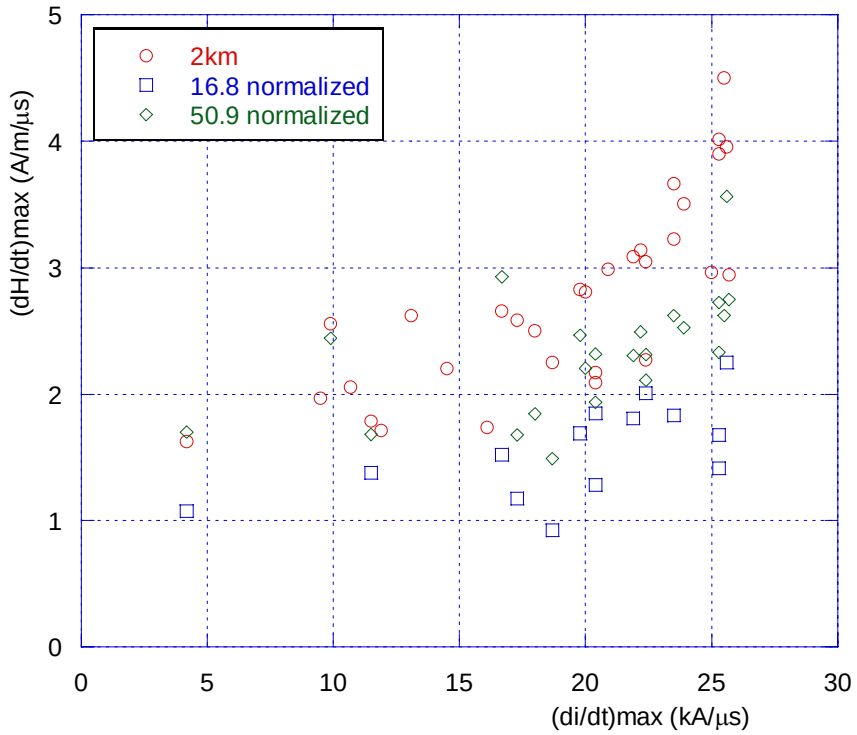


Fig. 5.9 - Magnetic field maximum steepness as a function of current maximum steepness. The values for the steepnesses at 16.8 km and 50.9 km have been normalized to those at 2 km assuming 1/*r* dependence.

## 5.4 Comparison with theoretical results

### 5.4.1 Comparison with predictions of engineering models

Engineering models for lightning strikes to tall towers use as input the so-called undisturbed current, as well as the values for the reflection coefficients at the top and at the bottom of the strike objects [*Rachidi, et al.*, 2002]. The extraction of the undisturbed current and reflection coefficients associated with the strike object is a complex problem and was the subject of several studies (e.g. [*Beierl*, 1992; *Bermudez, et al.*, 2003; *Guerrieri, et al.*, 1998; *Janischewskyj, et al.*, 1996]). In the present section, the engineering models' approach,

described in Chapters 2 and 3, is adopted to reproduce the measurements of return-stroke current and radiated electric and magnetic fields at three distances exposed in Fig. 5.6, which correspond to the 2nd stroke of the flash striking the CN Tower at 14:13:13 of Aug 19, 2005. The values adopted in the simulations for the reflection coefficients of the CN-Tower model, namely, $\rho_t$ = -0.366 and $\rho_g$ = 0.8 for the top and the bottom coefficients, respectively, have been inferred from experimental data [*Janischewskyj, et al.*, 1996].

The undisturbed current was represented analytically using the sum of two Heidler functions [*Heidler*, 1985] according with the following expression:

$$i_o(h,t) = \frac{I_{o1}}{\eta_1} \frac{(t/\tau_{11})^2}{1+(t/\tau_{11})^2} e^{(-t/\tau_{21})} + \frac{I_{o2}}{\eta_2} \frac{(t/\tau_{12})^2}{1+(t/\tau_{12})^2} e^{(-t/\tau_{22})} \tag{5.1}$$

where the values of the parameters have been chosen using an iterative trial-and-error approach to match the recorded waveform at 474 m with the current predicted at the same height by Eq. (2.11):

$I_{o1}$ = 1.8 kA, $\eta_1$ = 0.578, $\tau_{11}$ = 0.3 μs, $\tau_{21}$ = 2 μs,
$I_{o2}$ = 2.5 kA, $\eta_2$ = 0.939, $\tau_{12}$ = 0.3 μs, $\tau_{22}$ = 150 μs.

Based on the described choice of undisturbed current $i_o(h,t)$ and reflection coefficients at the tower extremities, $\rho_t$ and $\rho_g$ , the current calculated at 474 m using the theory of the engineering models is shown in Fig 5.10, compared with the actual current measured at the same height on the CN Tower.

It is worth noting that, according to the engineering models and neglecting any reflection at the return-stroke wavefront, the distribution of the current along the elevated strike object is model-independent [*Rachidi, et al.*, 2002]. It can be seen that the measured current can be represented reasonably well, even though some oscillation and fine structure, presumably due to CN Tower's structural discontinuities, are not reproduced in the model.

The value assumed for the return-stroke speed in the field calculations is assumed $v$ = 120 m/μs, as reported by [*Wang, et al.*, 1995] from previous observations of CN-Tower flashes. For the simulation with the MTLL model, the total height of the channel, $H_{tot}$, has been chosen equal to 8 km, while the value of 2 km has been adopted for the current decay constant, λ, appearing in the MTLE model formulation.

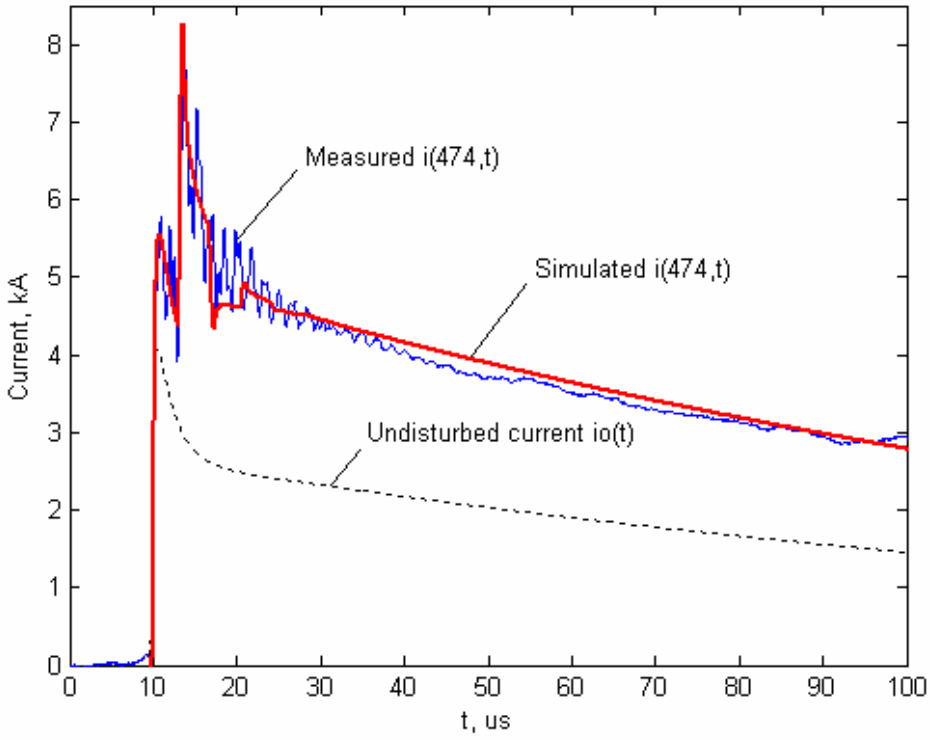


Fig. 5.10 - Comparison between measured current on the CN Tower (474 m) and predicted current using engineering models. The undisturbed current (also represented) and the values for the reflection coefficients ($\rho_t$ = -0.366 and $\rho_g$ = 0.8) are inferred from the experimental data.

Fig 5.11 presents comparisons between the electric and magnetic field waveforms measured at three distances from the tower and the theoretical predictions obtained using the five engineering return-stroke models (extended to include the presence of the strike object [*Rachidi, et al.*, 2002]) presented in Chapters 3 and 4, namely, TL, MTLL, MTLE, BG and TCS.

From the results presented in Fig. 5.11, the following observations can be made:

(1) The model-predicted magnetic fields are in reasonable agreement with the experimental waveforms for the three considered distances. However, the peak values of the computed fields are systematically about 25 % lower than measured values.

(2) The measured electric field peaks are significantly larger than the theoretical predictions. The differences are most significant at 16.8 km. This effect can be ascribed to the building enhancement effect and has already been discussed in Section 4.1.

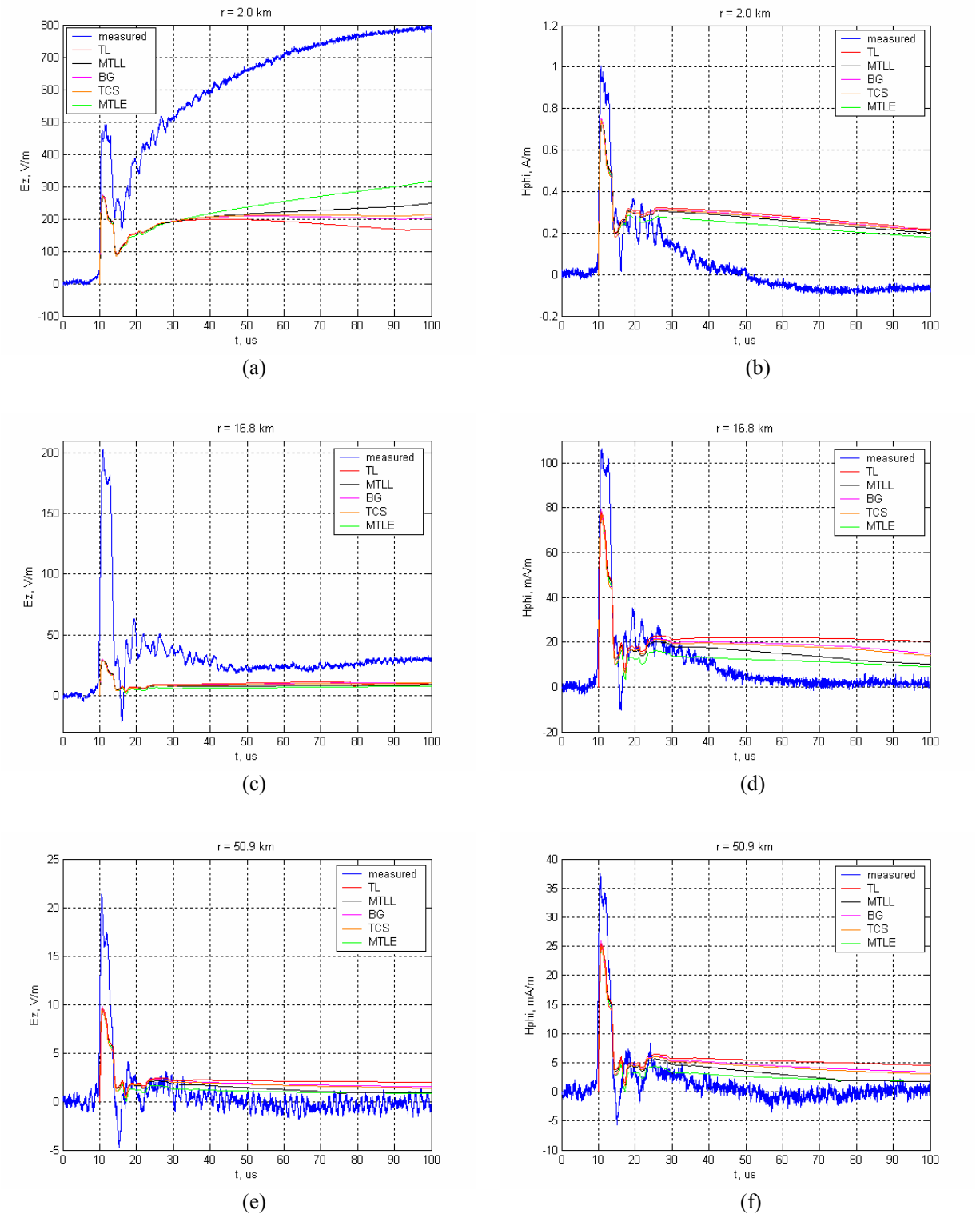


Fig. 5.11 - Comparison between measured electric and magnetic fields and theoretical predictions of five engineering models for the 2nd stroke of the event of August 19th, 2005, at 14:13:13. (a) electric and (b) magnetic fields at 2 km, (c) electric and (d) magnetic fields at 16.8 km, and (e) electric and (f) magnetic fields at 50.9 km.

(3) The early zero-crossing and the narrow undershoot are not reproduced by the models.

(4) Oscillations visible in the experimental waveforms are not reproduced by the models.

These oscillations are presumably due to the transient processes occurring at the discontinuities along the CN Tower. Indeed, similar oscillations are also discernible in the current waveform (see Fig. 5.10).

The differences between theoretical predictions and experimental data can be explained by assumptions in the theoretical model, experimental errors, the uncertainty in the adopted values for $\rho_t$ and $v$, the effect of reflections at structural discontinuities of the CN Tower and, finally, the field enhancement effect of the buildings on which the electromagnetic field sensors were installed. Note that the term "enhancement factor" is generally used for the effect of the structure on the electric fields and the term "site error" is used for the distortion of the magnetic field due to the structure and surrounding metallic environment.

### 5.4.2 Comparison with analytical formulas relating far-field peaks to current peaks

In this section, the peak values of the electric and magnetic fields obtained using model-based theoretical equations, which include the effect of the elevated strike object [*Pavanello, et al.*, Submitted in 2006b], are compared with the experimental data described in Section 5.3. For the comparison, the adopted values for the reflection coefficients and the return-stroke speed are the ones described in the previous section, namely, $\rho_t$ = -0.366, $\rho_g$ = 0.8 and $v$ = 120 m/μs.

As discussed in Section 4.4.2, when the round-trip propagation time along a tall structure is greater than the zero-to-peak risetime $t_f$ of the lightning current injected at the tower tip, the relation between far magnetic field peak and the associated current peak measured on the top of the elevated object is given by Eq. (4.19). This equation has been reproduced here for convenience and labelled as (5.2):

$$H_{\varphi\,\mathrm{peak}}^{far} = \frac{v}{2\pi c r} k'_{tall}\, I_{\mathrm{peak}} \tag{5.2}$$

where $k'_{tall}$ is given by

$$k'_{tall} = \frac{1+(1-2\rho_t)c/v}{1-\rho_t} \tag{5.3}$$

Note that the discontinuity at the return stroke wavefront, discussed in Chapter 3, was disregarded in the derivation of (5.2) and (5.3). Note also that, as mentioned in Section 4.4.2, Bermudez et al. [*Bermudez, et al.*, 2005] used unprimed notation ($k_{tall}$) to denote (5.3). In this study, the notation of Baba and Rakov [*Baba and Rakov*, 2005] is used.

Figure 5.12 presents a scatter plot of the experimentally-measured peak magnetic field

versus the peak current as well as the predictions of Equation (5.2), the latter including the presence of the elevated strike object.

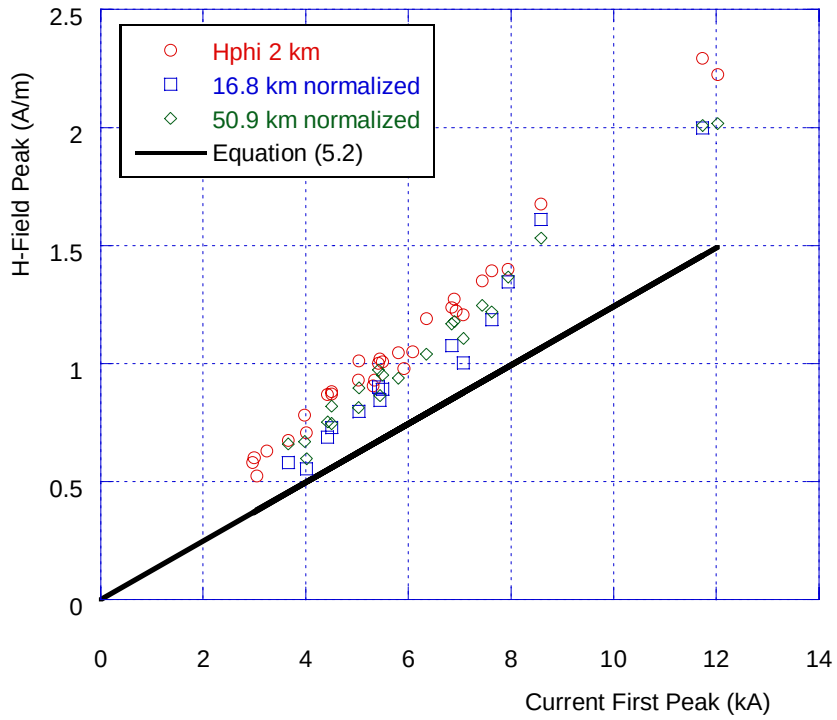


Fig. 5.12 - Magnetic field peak as a function of return-stroke current peak. Comparison between experimental data (31 strokes out of 6 flashes) and computed results using the Equation (5.2). The values for the field peaks at 16.8 km and 50.9 km have been normalized to those at 2 km assuming 1/*r* dependence.

It can be seen that the theoretical field peak estimates are in reasonably good agreement with experimental data, although they tend to underestimate the measured values. As discussed earlier, this underestimation can be attributed to factors such as the field enhancement effect of the buildings on which electromagnetic fields were measured, uncertainties in the values of the return-stroke speed and the top reflection coefficient, and reflections at structural discontinuities of the CN Tower.

## 5.5 Comparison with data recorded by the US NLDN

Recently, lightning research groups were interested in evaluating the performance characteristics of lightning location systems, namely, their detection efficiency, their location accuracy and their current peak estimate by means of 'ground-truth' measurements using either instrumented towers (e.g. [*Diendorfer, et al.*, 2002; *Schulz and Diendorfer*, 2004]) or rocket-triggered lightning [*Jerauld, et al.*, 2005].

Diendorfer et al. [*Diendorfer, et al.*, 2002] compared lightning peak currents measured at

the Gaisberg tower (100-m tall) with correlated lightning peak currents reported by the Austrian lightning location system ALDIS, finding a surprisingly good agreement, quantified in terms of a current peak estimate from ALDIS equal to 95 % the value recorded at the tower.

Jerauld et al [*Jerauld, et al.*, 2005] evaluated the performance characteristics of the US NLDN using rocket-triggered lightning data acquired during the summers 2001-2003 at Camp Blanding, Florida, reporting a tendency of NLDN to underestimate peak currents, with a median peak current estimation error of about 18 %.

Some of the return strokes recorded on August 19 2005 at the CN Tower were also detected by the United States National Lightning Detection Network (US NLDN). In this section, the peak value of the actual current recorded at the CN Tower will be compared with its estimation provided by the US NLDN from the measurement of the corresponding return-stroke field. Unlike the Gaisberg tower, whose height above ground is only 100 m and hence is an electrically-short tower for typical lightning return-stroke currents, the CN Tower with its 553 m tallness is tall enough so that the condition current risetime $t_r < h/c$ is often satisfied. Therefore, it is expected that a non-negligible enhancement effect takes place for strikes to the CN Tower. In fact, a lightning detection network, composed by a certain number of field measuring stations, is not able to distinguish between a strike to ground and a strike to a tall object. As a result, the inferred current peak for a tall tower-initiated event might be overestimated because of the tower factor (expressed in terms of the coefficient $k'_{tall}$ in Eq. (5.3)).

This discrepancy was also observed in the past by Montandon [*Montandon*, 1992] between the return-stroke current estimations provided by the Lightning Positioning And Tracking System (LPATS) installed in Switzerland in 1990 by Swiss PTT and the lightning currents actually recorded using two different instrumented towers: the 168-m-tall Peissenberg Tower in Germany and the 250-m-tall St. Chrischona Tower in Switzerland, reporting an overestimation of the current peaks by the LPATS system of 15 to 20 dB.

In Fig 5.13, the current peaks inferred for each return-stroke detected by US NLDN are shown as a function of the corresponding current peaks measured at the CN Tower. The best-fit straight line of the points shows that the current estimation provided by the lightning detection network for those tower strokes is about 3.5 times higher than the actual measurement.

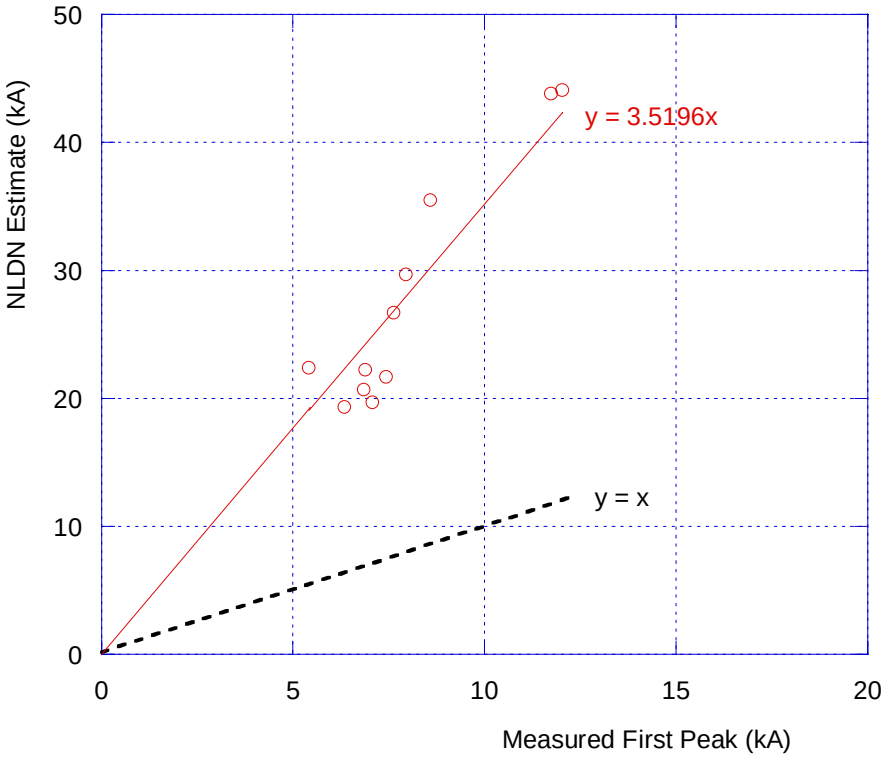


Fig. 5.13 - Comparison of peak current measurements at the CN Tower with peak currents of correlated events reported by NLDN. The solid line represents the linear curve fit. The dashed line represents the ideal relation between the directly measured currents and NLDN estimates (NLDN data courtesy of K. Cummins, Vaisala).

This result agrees very well with the value obtained for the factor $k'_{tall}$ discussed above. Indeed, assuming that NLDN uses a classical TL relation [*Cummins, et al.*, 1998] to infer the current peak, the presence of a tall strike object would result in an overestimation of the inferred value by a factor $k'_{tall}$ (see Section 4.4.2). For the adopted values ($\rho_t$ = -0.366 and $v$ = 120 m/μs), this factor is equal to 3.9. Consequently, the current-peak estimation of the detected CN Tower strikes has been corrected in Fig 5.14 plotting the current peaks inferred by the US NLDN divided by the factor $k'_{tall}$ = 3.9, as a function of the corresponding current peaks measured at the CN Tower. The best-fit straight line for the corrected points shows now a very satisfactory estimation of the current peaks from the lightning detection network.

Note, finally, that this excellent agreement is not due to a judicious choice of the parameters $\rho_t$ and $v$. Indeed, as it has been shown in Chapter 4, the far field peaks associated with strikes to tall strike objects are very little sensitive to $\rho_t$ and $v$.

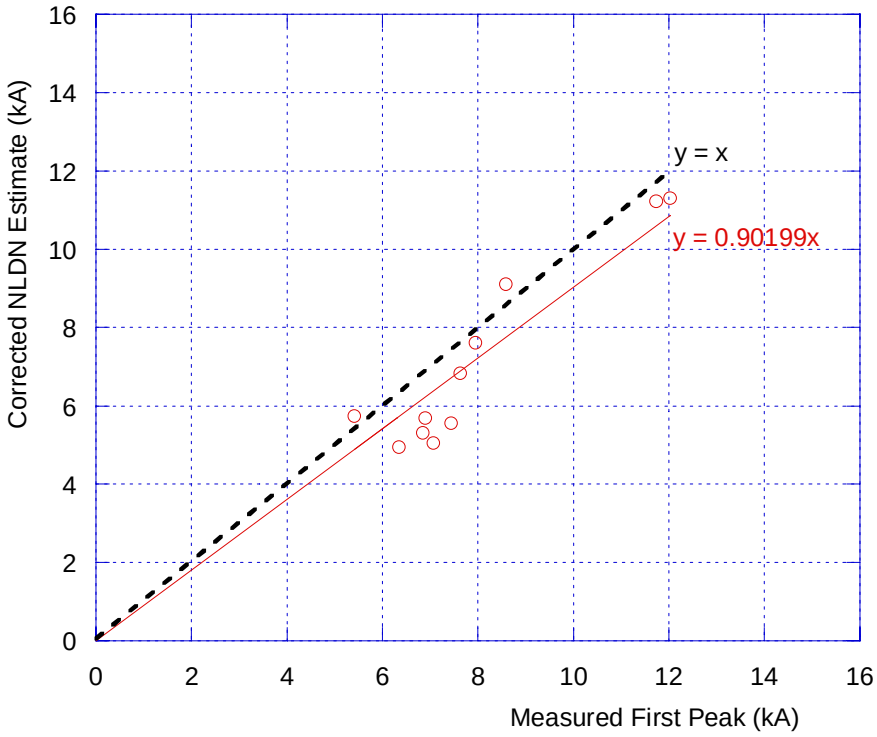


Fig. 5.14 - Comparison of peak current measurements at the CN Tower with peak currents of correlated events reported by NLDN, after correction using the tower factor $k'_{tall}$. The solid line represents the linear curve fit. The dashed line represents the ideal relation between the directly measured currents and corrected NLDN estimates (NLDN data courtesy of K. Cummins, Vaisala).

## 5.6 Conclusions

This chapter reported on the simultaneous GPS-time-stamped measurements of the return-stroke current and of the electric and magnetic fields at three distances associated with lightning strikes to the Toronto CN Tower (553 m) during the Summer of 2005. The lightning return-stroke current was measured using a Rogowski coil installed at a height of 474 m. The vertical component of the electric field and the azimuthal component of the magnetic field were measured simultaneously at distances of 2.0 km (Pratt building of the University of Toronto), 16.8 km (Environment Canada Building), and 50.9 km (Grimsby, ON) from the CN Tower. The propagation path from the CN Tower to Pratt (2.0 km) and Environment Canada (16.8 km) stations was along the soil and through the Toronto city, whereas for the third location in Grimsby (50.9 km), the propagation path was nearly entirely across Lake Ontario.

The waveforms of the electric and magnetic fields at 16.8 km and 50.9 km exhibit a first zero-crossing about 5 microseconds after the onset of the return-stroke. This early zero-crossing is part of a narrow undershoot. The fact that the observed early undershoot is clearly

discernible in both the electric and the magnetic fields suggests that the feature is not an artifact of the measurement system. On the basis of some simulation results, this early undershoot may be attributed to the transient processes along the tower.

For fields at 50.9 km, the expected zero-crossing at about 40 microseconds is also observed.

Metallic beams and other conducting parts in buildings on which electric and magnetic field sensors were located cause an enhancement effect on the measured fields. Although an enhancement can be identified both on the electric and the magnetic fields, the degree of enhancement is actually more important for the electric field than for the magnetic field. It is shown that the value of the wave impedance (E-field peak to H-field peak ratio) could give an estimate of the enhancement effect of the building on the electric field.

Propagation effects (decrease of field amplitude and increase of its risetime) could also be observed in experimental records. It has been shown that the fields at 50.9 km are less affected by such attenuation, compared to those at 16.8 km, presumably because the path of propagation is mostly across Lake Ontario. The measured waveforms have been compared with the theoretical predictions obtained using the five engineering return-stroke models, extended to include the presence of the strike object, namely, TL, MTLL, MTLE, BG and TCS. A reasonable agreement is found for the magnetic field waveforms for the three considered distances. However, the peak values of the computed magnetic fields are systematically about 25 % lower than measured values. None of the considered models was able to reproduce the early zero-crossing and the narrow undershoot.

The expression for tall strike objects relating current and field peaks, recently derived by Bermudez et al. was also tested versus the obtained sets of simultaneously-measured return-stroke currents and fields associated with lightning strikes to the CN Tower. The overall agreement between the theoretically predicted and the experimentally observed field-to-current ratio is reasonable, although the theoretical expression appears to underestimate the experimentally measured ratio (by about 25 %). This may be due, at least in part, to the enhancement effect of the buildings on which the field measurement antennae were installed.

Finally, the directly-measured lightning currents at the tower have been correlated and compared with US NLDN current peak estimates. It has been shown that the NLDN inferred values overestimate actual current peaks, because the presence of the tall struck object is not included in the algorithm used to infer lightning current peaks from remote field measurements. However, correcting the NLDN estimates using the tower factor $k'_{tall}$ results in

an excellent estimation of lightning current peaks. This is an important conclusion of this study which shows that the estimation of lightning peak currents for tall-tower strikes can be greatly improved by considering the tower factor $k'_{tall}$.

# References


Baba, Y., and V. A. Rakov (2005), Lightning electromagnetic environment in the presence of a tall grounded strike object, *Journal of Geophysical Research*, *110*.

Beierl, O. (1992), Front Shape Parameters of Negative Subsequent Strokes Measured at the Peissenberg Tower, paper presented at 21st ICLP (International Conference on Lightning Protection), Berlin, Germany, 21-25.09.1992.

Bermudez, J. L., T. Gazizov, A. Negodyaev, D. Pavanello, F. Rachidi, A. Rubinstein, and M. Rubinstein (2004), On the enhancement of electric and magnetic fields from lightning due to close-by metallic structures, paper presented at European Electromagnetics EUROEM'2004, Magdeburg, Germany.

Bermudez, J. L., F. Rachidi, W. Janischewskyj, A. M. Hussein, V. Shostak, M. Rubinstein, C. A. Nucci, J. S. Chang, P. Joe, and M. Nyffeler (2002), Simultaneous Measurements of Electromagnetic Fields at Two Distances and of Current Associated with Lightning Return Strokes to the CN Tower, paper presented at 26th ICLP (International Conference on Lightning Protection), Cracow, Poland, September 2002.

Bermudez, J. L., F. Rachidi, W. Janischewskyj, V. Shostak, M. Rubinstein, D. Pavanello, A. M. Hussein, J. S. Chang, C. A. Nucci, and M. Paolone (2005), Far-field - current relationship based on the TL model for lightning return strokes to elevated strike objects, *IEEE Transactions on Electromagnetic Compatibility*, *47*, 146-159.

Bermudez, J. L., M. Rubinstein, F. Rachidi, F. Heidler, and M. Paolone (2003), Determination of Reflection Coefficients at the Top and Bottom of Elevated Strike Objects Struck by Lightning, *Journal of Geophysical Research*, *108*, 4413, doi: 4410.1029/2002JD002973.

Bonyadi Ram, S., R. Moini, S. H. H. Sadeghi, and A. Mahanfar (2001), The effects of tall buildings on the measurement of electromagnetic fields due to lightning return strokes, paper presented at 2001 IEEE EMC International Symposium, IEEE EMC Society, Montreal, Canada, August, 2001.

Chisholm, W. A. (2006), Private Communication.

Cooray, V. (1987), Effects of propagation on the return stroke radiation fields, *Radio Science*, *22*, 757-768.

Cooray, V. (2003), *The Lightning Flash*, IEE, London, UK.

Cooray, V., G. Diendorfer, C. A. Nucci, D. Pavanello, F. Rachidi, M. Becerra, M. Rubinstein, and W. Schulz (2006), On the effect of finite ground conductivity on electromagnetic field radiated from lightning to tall towers, paper presented at International conference on Lightning Protection, ICLP 2006, Kanazawa, Japan.

Cooray, V., and S. Lundquist (1983), Effects of propagation on the rise times and the initial peaks of radiation fields from return strokes, *Radio Science*, *18*, 409-415.

Cooray, V., and M. Ye (1994), Propagation effects an the lightning-generated electromagnetic fields for homogeneous and mixed sea-land paths, *Journal of Geophysical Research*, *99*, 10641-10652.

Cummins, K. L., E. P. Krider, and M. D. Malone (1998), The US National Lightning Detection Network (TM) and applications of cloud-to-ground lightning data by electric power utilities, *IEEE Transactions on Electromagnetic Compatibility*, *40*, 465-480.

Diendorfer, G., W. Hadrian, F. Hofbauer, M. Mair, and W. Schulz (2002), Evaluation of lightning location data employing measurements of direct strikes to a radio tower, 6 pp, Session 2002 CIGRE, Paris, France.

Guerrieri, S., C. A. Nucci, F. Rachidi, and M. Rubinstein (1998), On the influence of elevated strike objects on directly measured and indirectly estimated lightning currents, *IEEE Transactions on Power Delivery*, *13*, 1543-1555.

Heidler, F. (1985), Traveling current source model for LEMP calculation, paper presented at 6th Symposium and Technical Exhibition on Electromagnetic Compatibility, Zurich, Switzerland.

Hussein, A., W. Janischewskyj, M. Milewski, V. Shostak, W. A. Chisholm, and J. S. Chang (2004), Current waveform parameters of CN Tower, *Journal of Electrostatics*, *60*, 149-162.

Janischewskyj, W., J. S. Chang, A. M. Hussein, V. Shostak, F. Rachidi, W. A. Chisholm, D. Pavanello, E. Petrache, I. Boev, and M. Milewski (2006), Lightning Multiplicity at the CN Tower in Toronto as recoded by six different instruments, paper presented at International Conference on Grounding and Earthing & 2nd International Conference on Lightning Physics and Effects - Ground 2006 and 2nd LPE Maceió, Brazil.

Janischewskyj, W., A. M. Hussein, V. Shostak, I. Rusan, J. X. Li, and J. S. Chang (1997), Statistics of lightning strikes to the Toronto Canadian National Tower (1978-1995), *IEEE Transactions on Power Delivery*, *12*, 1210-1221.

Janischewskyj, W., V. Shostak, J. Barratt, A. M. Hussein, I. Rusan, and J. S. Chang (1996), Collection and use of lightning return stroke parameters taking into account characteristics of the struck object, paper presented at 23rd ICLP (International Conference on Lightning Protection), Florence, Italy.

Janischewskyj, W., V. Shostak, and A. M. Hussein (1998), Comparison of lightning electromagnetic field characteristics of first and subsequent return strokes to a tall tower 1. Magnetic field, paper presented at 24th ICLP (international conference on lightning Protection), Birmingham, U.K., sept. 1998.

Jerauld, J., V. A. Rakov, M. A. Uman, K. J. Rambo, and D. M. Jordan (2005), An evaluation of the performance characteristics of the U.S. National Lightning Detection Network in Florida using rocket-triggered lightning, *Journal of Geophysical Research*, *110*.

Liatos, P., and A. M. Hussein (2005), Characterization of 100-kHz noise in the lightning current derivative signals measured at the CN tower, *IEEE Transactions on Electromagnetic Compatibility*, *47*, 986 - 997

Lin, Y. T., M. A. Uman, J. A. Tiller, R. D. Brantley, W. H. Beasley, E. P. Krider, and C. D. Weidman (1979), Characterization of lightning return stroke electric and magnetic fields from simultaneous two-station measurements, *Journal of Geophysical Research*, *84*, 6307-6314.

McComb, T. R., H. Linck, E. A. Cherney, and W. Janischewskyj (1980), Preliminary Measurements of Lightning Flashes to the CN Tower in Toronto, *Canadian Electrical Engineering Journal*, *5*, 3-9.

Montandon, E. (1992), Lightning Positioning and Lightning Parameter Determination: Experiences and Results of the Swiss PTT Research Project, paper presented at International Conference on Lightning Protection - ICLP, Berlin, Germany, September 21-25, 1992.

Pavanello, D., V. Cooray, F. Rachidi, M. Rubinstein, A. Negodyaev, M. Paolone, and C. A. Nucci (2005), Propagation effects on the electromagnetic field radiated by lightning to tall towers, paper presented at VIII International Symposium on Lightning Protection, SIPDA, São Paulo, Brazil, 21-25 November 2005.

Pavanello, D., and F. Rachidi (2006), Report on the 2005 Lightning Measurement Campaign, Toronto, Canada.

Pavanello, D., F. Rachidi, W. Janischewskyj, M. Rubinstein, A. M. Hussein, E. Petrache, V. Shostak, I. Boev, C. A. Nucci, W. A. Chisholm, M. Nyffeler, J. S. Chang, and A. Jaquier (Submitted in 2006a), On Return-Stroke Currents and Remote Electromagnetic Fields Associated with Lightning Strikes to Tall Structures - Part II: Experiment and Model Validation, *Journal of Geophysical Research*.

Pavanello, D., F. Rachidi, W. Janischewskyj, M. Rubinstein, A. M. Hussein, E. Petrache, V. Shostak, C. A. Nucci, J. S. Chang, I. Boev, W. A. Chisholm, and M. Nyffeler (2006), Simultaneous Measurements of Return Stroke Current, Electric and Magnetic Fields at Three Distance Ranges Associated with Lightning Strikes to the CN Tower, paper presented at International Conference on Lightning Protection, ICLP 2006, Kanazawa, Japan.

Pavanello, D., F. Rachidi, M. Rubinstein, J. L. Bermudez, W. Janischewskyj, V. Shostak, C. A. Nucci, A. M. Hussein, and J. S. Chang (Submitted in 2006b), On Return-Stroke Currents and Remote Electromagnetic Fields Associated with Lightning Strikes to Tall Structures - Part I: Computational Models, *Journal of Geophysical Research*.

Rachidi, F., W. Janischewskyj, A. M. Hussein, C. A. Nucci, S. Guerrieri, B. Kordi, and J. S. Chang (2001), Current and electromagnetic field associated with lightning return strokes to tall towers, *IEEE Trans. on Electromagnetic Compatibility*, *43*.

Rachidi, F., V. A. Rakov, C. A. Nucci, and J. L. Bermudez (2002), The Effect of Vertically-Extended Strike Object on the Distribution of Current Along the Lightning Channel, *Journal of Geophysical Research*, *107*, 4699.

Schulz, W., and G. Diendorfer (2004), Lightning peak currents measured on tall towers and measured with lightning location systems, paper presented at 18th International Lightning Detection Conference ILDC 2004, Helsinki, Finland.

Shostak, V., W. Janischewskyj, and A. M. Hussein (2000), Expanding the modified transmission line model to account for reflections within the continuously growing lightning return stroke channel, paper presented at IEEE Power Engineering Society Summer Meeting, Cat. IEEE, Piscataway, USA, 2000.

Uman, M. A., C. E. Swanberg, J. A. Tiller, Y. T. Lin, and E. P. Krider (1976), Effects of 200 km propagation on Florida lightning return stroke electric field, *Radio Science*, *11*, 985-900.

Wang, D., Z. I. Kawasaki, K. Yamamoto, K. Matsuura, J. S. Chang, and W. Janischewskyj (1995), Luminous propagation of lightning attachment to CN tower, *Journal of Geophysical Research*, *100*, 11661-11667.

Ward, D. A., and J. L. T. Exon (1993), Using rogowski coils for transient current measurements, *Engineering Science and Education Journal*, 105-113.

# Chapter 6

# Measuring System Specially Designed for Lightning Electromagnetic Fields

## 6.1 Introduction

The state-of-the-art measurement of lightning electromagnetic fields is challenging since, especially for nearby flashes, the required field, current, and optical sensors are necessarily immersed in the very rough electromagnetic environment they are designed to measure [*Rubinstein, et al.*, 2006].

One example of this is the contamination of measured electric fields due to the use of long cables to transmit the signals from the sensor to the recording equipment. Even if coaxial cables are used, their non-zero transfer impedance allows some of the lightning fields to couple onto them and, thus, to distort the physical quantity being measured. For this reason, and with the advantage of galvanic isolation, a number of lightning research groups around the world use systems that carry the measured signals over fiber optics.

In addition, to obtain meaningful statistical results, lightning measurement systems need to operate for long periods of time under harsh environmental conditions and at different distances from the lightning channel. Such a mode of operation requires high robustness and the possibility of remotely selecting the gain and performing a calibration is a strongly desirable feature. Portability of the measurement sensors and signal transmission systems is also required if the equipment is to be used at different sites.

The scarcity of commercial systems designed specifically for lightning measurements explains why most of the current pool of data has been obtained using either high-priced commercial sensors, whose high frequency response is well beyond that required for

lightning, or sensors that are designed and built by the individual research groups, each to its own specifications.

As a result, measurements from different groups are not, in general, directly and easily comparable, which limits the capacity to combine the data from different sources to increase the measurement base and restricts the ability to verify their accuracy. It would therefore be advisable to define the specifications for performance, endurance, reliability and test and calibration procedures for different lightning measurement systems for electric field, magnetic field and return-stroke current.

The first part of this chapter (Section 6.2) is intended opening a discussion on the need for guidelines for reporting lightning data obtained experimentally.

The second part of the chapter (Section 6.3) presents then the design and the construction of a lightning field measuring system for the simultaneous measurement of three components of the electromagnetic field radiated by lightning. The proposed system presents the advantage of using one single optical link for the transmission of the three signals, appropriately digitized and multiplexed, lowering considerably the overall cost of the system itself.

## 6.2 Need for guidelines for reporting lightning data

Experiments are used to (1) understand the physical mechanisms at play in lightning discharge processes, and, (2) to test theoretical models and numerical simulations. Lightning measurement campaigns need in general to last several months or years. As a result, they can be significantly expensive and could not always yield satisfactory results because of the random nature and scarcity of lightning occurrence.

In order to increase the size of the data pool used to validate one's theory (important to draw conclusions based on a statistical basis) or to be able to compare/include measurement results obtained somewhere else, it may be desirable having the possibility to use data collected by other research groups.

This can be accomplished only if the lightning data reported from other researchers are provided with all the information necessary to situate those data in the context in which they have been collected. In other words, some guidelines are needed to define what information should be included in a measurement report to 'decontaminate' the data from the influence of the local conditions and from the aim of that particular measurement campaign and make

them adaptable for any objective comparison involving data gathered under different conditions.

Every research team performs its own calibration to assure proper functioning of its measurement system. It is therefore essential to standardize the reporting of the calibration results [*Pavanello, et al.*, 2005].

Only wideband, linear systems will be consider here, designed to measure time-domain lightning waveforms such as the channel-base current or the electromagnetic fields generated by the return stroke. Let us discuss the typical information on measurement systems and measured data found in technical and scientific publications along with plotted data.

A parameter which is often presented as a constant is the peak amplitude calibration, which is the factor that relates the output of the used sensor to the local physical quantity being measured (for instance, electric field or current) [*Rubinstein, et al.*, 2006]. Since the local quantities are not necessarily the quantities which are actually of interest, other factors, such as the building enhancement factor, may also be required.

This enhancement factor, which takes into account the geometry of the building on which the sensors are mounted, depends on the geometry of the sensor's supporting structure and on sharp-corner proximity effects, proximity-to-lightning effects. It is worth noting that some of these effects may be directional.

The enhancement factor is a difficult parameter to determine. Ideally, for field measurements, a well calibrated, reference antenna would be placed at ground level, on flat terrain, at approximately the same distance to the lightning as the sensor under test. A synchronized measurement with the sensor under test would then be used to determine the enhancement factor. In practice, however, flat terrain with an unobstructed view to the lightning is not always available. In addition, the measurement may prove costly since the GPS time stamps or coordinated triggering may be needed.

Numerical methods are an attractive alternative to experimental measurement of the enhancement factor but tests need to be conducted to verify the validity of computer-generated results. The enhancement factor is rarely estimated and reported.

The rise and the decay times offer an indication of the frequency response of the measurement system. When these parameters are given, the implicit assumption is often made that the measurement system is linear and that the frequency response is dominated by single poles at low and high frequencies. Complementary information is needed since these assumptions are often poor approximations.

Several sources of non-linearities may exist, such as, for example, near saturation effects, magnetic cores in magnetic field and current sensors, and non-linear quantization in analog to digital converters. The introduction of controlled non-linearities may be useful to increase the dynamic range, but the end-to-end response of the system should remain linear.

Constant calibration factors do not suffice to allow the proper interpretation of data for the purpose of comparison with similar data from other sources. If the end-to-end measurement systems are linear, it is possible to introduce a frequency domain calibration function *C(f)* with its corresponding time-domain equivalent *c(t)*. The calibrated measurement are then obtained in the time domain by convolution of the measured quantity with the calibration function *c(t)* or, in the frequency domain, by multiplication of the corresponding frequency domain functions. Although *C(f)* or *c(t)* could, in principle, be obtained experimentally, it may be possible to obtain them theoretically and even analytically for many existing systems.

To analyze the calibration problem, Fig. 6.1 includes a model representing the transformations, in the frequency domain, that a measurement of the physical quantity to be measured $D_s(f)$ follows as it is processed and stored by the measurement system, including the preparation for publication.

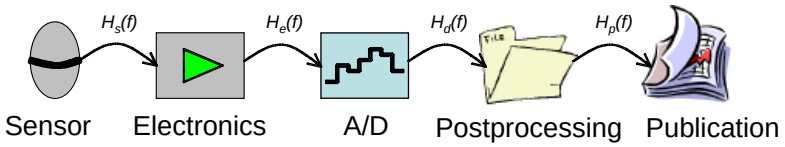


Fig. 6.1 - Model of a linear measurement system from the sensor all the way to the publication of the data (adapted from [*Rubinstein, et al.*, 2006])

The transfer functions $H_x(f)$ in the figure represent frequency dependent multiplicative factors relating the input and the output of each of the blocks in the chain. Note that, although some of the transformations suffered by the data can indeed be represented by way of multiplicative factors, others are better represented by transformations. All transformations, however, will be presented here as factors for illustration purposes. The different functions are:

- $H_s(f)$ is the sensor transfer function, which relates the physical quantity being measured to a current or voltage out of the sensor (excluding any electronics in it).
- $H_e(f)$ is the transfer function of the analog electronics that preprocesses the waveforms out of the sensor and before digitization.

- $H_d(f)$ is the transfer function of the digitizer. This includes sampling and quantization. This process is nonlinear but, for modeling purposes, in uniform quantization, a linear transfer function can be defined in conjunction with the concept of quantization noise.
- $H_p(f)$ represents the transfer function of any post-processing done on the waveforms before publication of the results.

The overall relation between the published waveform and the original physical quantity is determined in what follows, assuming the presence of additive noise components:

- $N_s(f)$ is the noise added to the wanted physical quantity by the sensor and by other external processes. An example would be the proximity of the sensor to power radio transmitters.
- $N_e(f)$ is the noise introduced by the electronics.
- $N_q(f)$ is the quantization noise which is due to the fact that the signal has to be approximated to the nearest quantization level.

With these definitions, the published field can be calculated as:

$$D_p(f) = (((D_s(f) + N_s(f))H_s(f) + N_e(f))H_e(f) + N_d(f))H_d(f)H_p(f) \tag{6.1}$$

The characterization of a measured waveform for the purpose of comparison with similar data requires a description of the measurement sensor, knowledge of the transfer function and characterization of the noise.

Information about particular settings of the measurement system, such as the value of adjustable gains, the trigger type and the trigger levels is also important for the statistical interpretation of the data.

It is also important that the sampling rate and the bandwidth of the system before digitization be explicitly given. This can be used to estimate the amount of aliasing, if any.

The sensor transfer function $H_s(f)$ is generally well known [*Baum, et al.*, 1982]. The noise $N_s(f)$ introduced by the sensor and the surrounding unwanted sources, however, needs to be measured.

The transfer function of the electronics, $H_e(f)$, and the electronics noise level, $N_e(f)$, are easily measurable in the laboratory but provisions for the measurement of this function in the field should be made if these do not demand unreasonable effort and resources.

The digitization transfer function and the corresponding quantization noise can be determined theoretically from a description of the amplitude and time resolutions and the characteristics of the A/D converters, which may include companding techniques. These characteristics, however, may be difficult to obtain and to interpret, especially if a digital oscilloscope is used.

Finally, any postprocessing done before publication, such as noise reduction and equalization, should be well documented and carefully reported.

## 6.3 Designed measuring system for lightning electromagnetic fields

### 6.3.1 General description of the system

The system is designed for the simultaneous measurement of the vertical component of the electric field and two perpendicular components of the magnetic field radiated by lightning. A flat-plate antenna is used for the vertical electric field measurement and two identical passive loop antennas, mounted orthogonally to each other, for the measurement of two linearly independent components of the horizontal magnetic field [*Pavanello, et al.*, 2005].

The signals provided by the antennas are integrated, amplified and filtered before being digitized and transmitted serially via a high speed optical fiber link to the recording station accessible to the user.

The particular design presented here has the advantage of using a single optic link for transmitting three signals, lowering the overall cost of the system considerably. A schematic diagram of the system is shown in Fig. 6.2. The system allows for a remote control of the sensors' gain, as well as for the calibration of the circuit. At the receiver side, both analog and digital outputs are available.

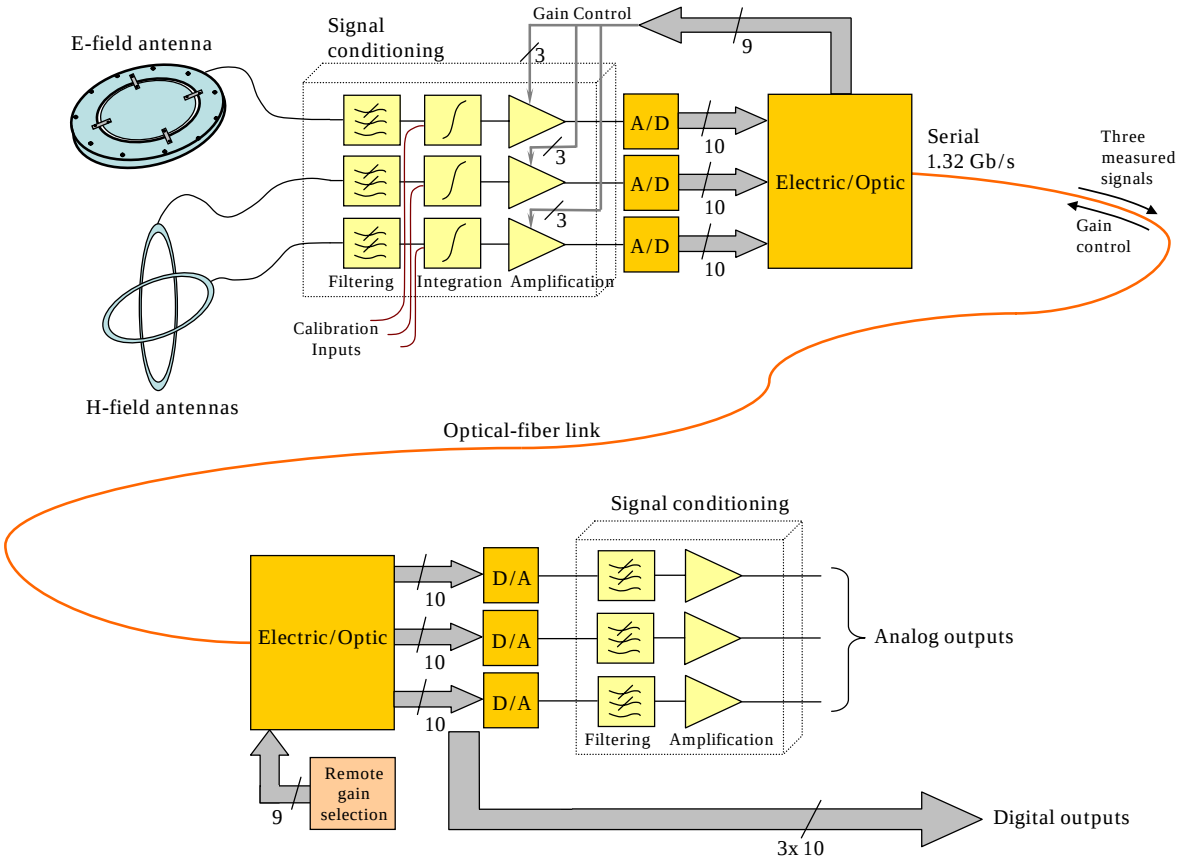


Fig. 6.2 - Schematic of the system

### 6.3.2 Electric and magnetic field sensors

Flat plate antennas are often used to measure electric field changes from lightning. One of the commonly used types of flat plate antenna consists of a metallic box (aluminum in our case) with a disk cut out of one of its sides [*Uman*, 1987].

The disk is put back in place but it does not make direct galvanic contact with the rest of the box. Assuming the vertical component $E_z$ of the electric field to be uniformly distributed over the plate, this will induce a total amount of charge on the surface $A$ of the disk equal to:

$$Q = A\varepsilon_o E_z \tag{6.2}$$

where $\varepsilon_o$ is the permittivity of vacuum.

Changes in the electric field translate into changes in the induced charges. Taking the derivative of Equation (6.2), it can be obtained:

$$i = \frac{dQ}{dt} = A\varepsilon_o \frac{dE_z}{dt} \tag{6.3}$$

According to Equation (6.3), the current produced by the electric field change is proportional to the time derivative of the electric field.

Both magnetic field antennas are single-turn shielded loops made using coaxial cable with a gap in the shield.

The voltage induced in the antenna loop is proportional to the time derivative of the magnetic flux density *dB/dt*, according to:

$$V = A\cos\theta \frac{dB}{dt} \tag{6.4}$$

where $A$ is the surface area of the loop and $\theta$ is the angle between the magnetic field and the vector perpendicular to the plane of the loop [*Krider and Noggle*, 1975].

The same circular area $A = 0.28$ m$^2$ has been chosen for the disk cut out from the electric field antenna and for the loops of the magnetic field antennas. The antennas are shown in Fig. 6.3.

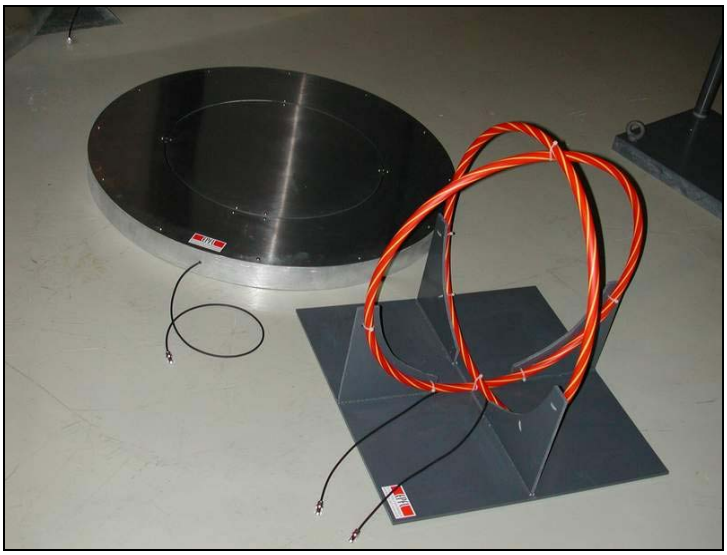

Fig. 6.3 – Passive antennas for Electric and Magnetic fields

### 6.3.3 Data acquisition unit

The three signals coming from the passive antennas are acquired simultaneously by three independent circuits on the data acquisition card [*Pavanello, et al.*, 2005].

With the exception of the input impedance of the circuits, namely, 50 Ω for the signal coming from the flat plate antenna and 1 MΩ for the ones coming from the loop antennas, the three circuits are identical (see Fig. 6.4).

Each circuit is provided with protecting diodes against excessively high voltages and with a voltage follower to guarantee the impedance transformation of the signal from the antenna to the integrator.

As discussed before, the signals provided by the passive flat plate antenna and by the two passive loop antennas are proportional to the time derivatives of, respectively, the vertical electric field and the two orthogonal components of the horizontal magnetic field.

The integrator circuit is designed to have a decay time constant of 1.5 ms, large enough for the measurement of return stroke fields without running into the risk of saturation of the operational amplifier due to the low frequency components of the $dE_z/dt$ signal [*Thomson, et al.*, 1988; *Uman*, 1987].

Although the case of the measurement of fields radiated by the whole flash will not be discussed here, the system can be adapted to this task by modifying the values of the resistive T network adopted in the integrator feedback to increase the decay time constant of the circuit.

The system is designed to detect the electromagnetic fields radiated by lightning strikes to ground (or to tall structures) at a range of distances varying from 1 km to 100 km. Hence, in order to adapt the integrated signals to the input voltage range of the A/D converter, they are first passed through two cascaded amplifiers whose gains can be controlled remotely. The use of two amplifiers instead of just one improves the overall gain-bandwidth product.

It is also possible to bypass the integration stage if the measured signal does not require integration. An example of this is the use of a shunt to measure the lightning current.

The signal level is then shifted up by 1.25 V to adapt it to the unipolar input range of the A/D converter.

A simple RC low-pass filter composed of R = 820 Ω and C = 8.2 pF protects the ADC against excessive input current and, at the same time, protect the analog circuit from perturbations introduced by the A/D conversion.

The 10-bit analog to digital converter chosen is the National ADC10040, which includes an on-chip sample-and-hold circuit and whose clock input is driven to provide a conversion rate of 33 MSPS.The three 10-bit digital words are processed by the commercially-available Inova GigaStar® ING_TRF full-duplex serial link-optical piggyback board, equipped with parallel Tx-Rx interfaces, each 36 bit @ 33 MHz, which translates into a serial bit stream of 1.188 Gb/s (payload data rate) over a duplex multimode fiber optic link.

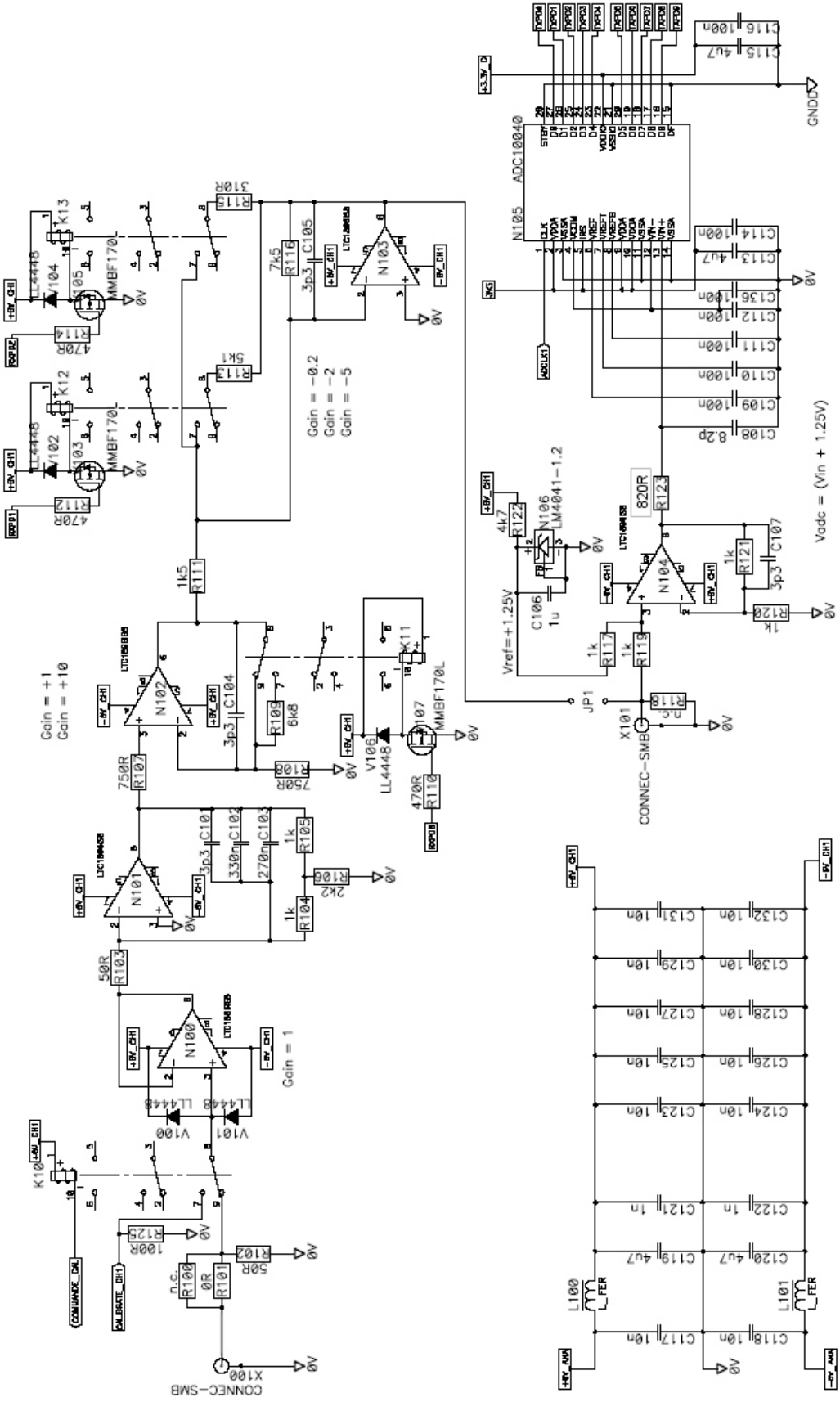


Fig. 6.4 - Schematic of one channel of the data acquisition unit

The data acquisition unit is expected to operate very close to the passive antennas in order to minimize possible signal contamination due to the coupling of the lightning electromagnetic field onto the coaxial cables carrying the signals measured by the antennas.

In order to protect then the electronics implementing the data acquisition unit (along with its power supply) against a potentially harsh electromagnetic environment and hostile weather conditions typical of a thunderstorm, a special EMC-shielded, waterproof metallic enclosure has been realized, which is shown in Fig. 6.5.

In that figure, it is possible to see the three coaxial cables carrying the signals from the passive antennas to the printed circuit board of the data acquisition unit and the fiber optic link carrying then the bit flow to the receiver unit.

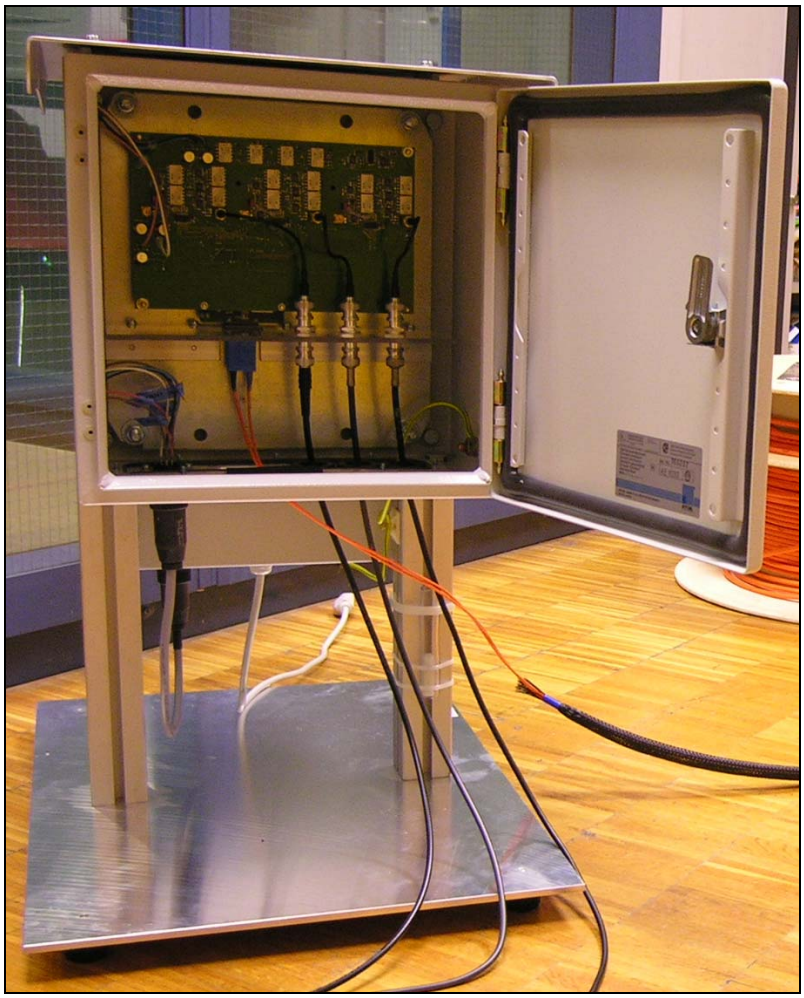

Fig. 6.5 – Shielded enclosure for the data acquisition unit.

### 6.3.4 Receiver unit

An optical piggyback board identical to the one mounted on the acquisition data card converts the received serial bit stream into three parallel 10-bit words.

If the corresponding analog signals are desired, the receiver provides the D/A conversion of the signals (see Fig. 6.6).

For each channel, the 10-bit digital-to-analog converter chosen is the Analog Devices AD9760, which provides differential current outputs and 100-kΩ output impedance for a conversion rate fixed at 33 MSPS.

A differential amplifier is then employed to recover the information contained in the output current of the D/A converter and drive it into the analog voltage BNC outputs of the system.

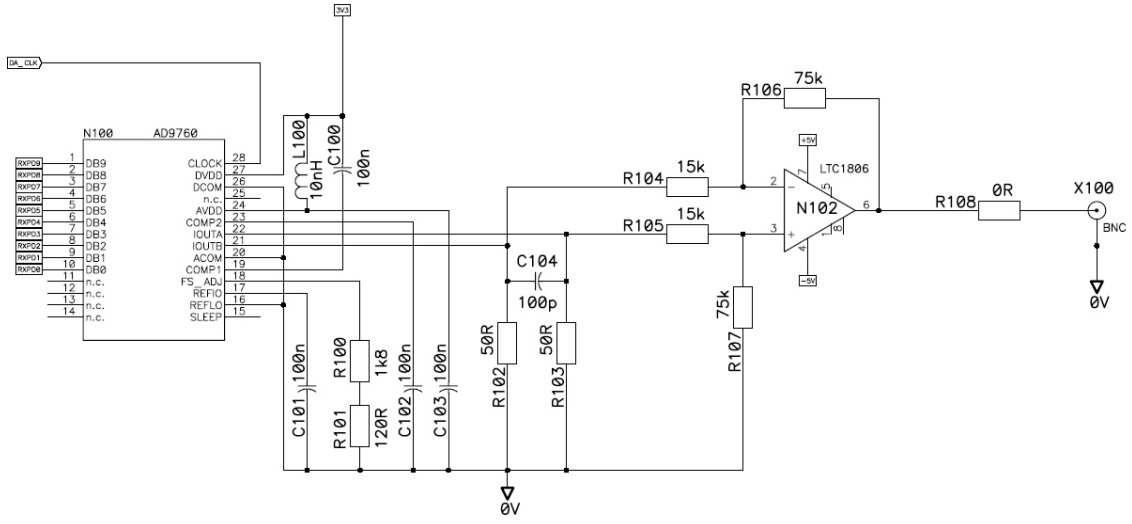


Fig. 6.6 - Schematic of one channel of the receiver unit

The operational amplifier used on both, the data acquisition card and on the receiver card, is the Linear Technology LT1806, which provides a 325-MHz gain-bandwidth product, 140-V/μs slew-rate and 550-μV max input offset voltage.

The bi-directional optical transmission allows the user to start the calibration test of the three channels and select the gain of each channel from the receiver unit.

The calibration circuit on the data acquisition card generates a sequence of alternating, 100-μs-wide pulses with 100-Hz frequency. The calibration procedure is controlled remotely.

Three relays switch the inputs of the $E_z$- and $H$-field circuits on the calibration signal which flows trough the whole chain up to the receiver for each channel.

The various dc power supply levels needed by the system are obtained from the ac line via a custom-built linear transformer-rectifier-filter chain, a solution that has been preferred over a circuit based on switching power supplies because of the need of adjustable levels and because of the better noise performance of a linear chain.

Particular attention has been devoted to the EMC performance of the PCBs, namely, the use of separate ground planes for analog and digital circuits and distances of the tracks from the power supplies.

### 6.3.5 Preliminary tests on the performance of the system

The analog circuit of the data acquisition card from its input to the digital conversion stage has been tested and the noise level was always within 4mV.

The digital transmission has been tested applying first a low-noise dc level to the input of the A/D converter, and comparing each one of the 10 bits with the corresponding bits of the received word after electro-optical conversion. The obtained result, with eight bits stable and the two LSBs noisy, was considered satisfactory. The linearity of the digital transmission in dynamic conditions has then been evaluated observing the signal obtained taking the difference between a triangular signal injected at the input of the A/D converter and the analog signal produced by the D/A converter on the receiver card after scaling. Taking into account the limitations of the measurement performed with an oscilloscope with only 8 bits for the vertical resolution, the obtained result can be considered satisfactory.

The time-domain integral of the response of the passive antennas has been compared with the response of high performance, commercially available active antennas, assumed as the reference, for the simultaneous measurement of the electric and magnetic fields generated with an impulse generator in a high voltage laboratory.

The result of this preliminary calibration is shown for one of the loop antennas in Fig. 6.7.

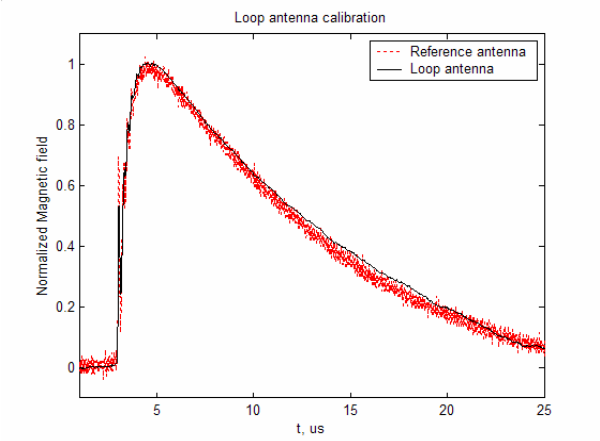


Fig. 6.7 - Calibration of one of the loop antennas

## 6.4 Conclusions

In order to increase the size of the data pool used to validate one's theory or to be able to compare/include measurement results obtained somewhere else, it may be desirable having the possibility to use data collected by other research groups.

This can be accomplished only if the lightning data reported from other researchers are provided with all the information necessary to situate those data in the contest in which they have been collected.

The first part of this chapter (Section 6.2) aimed at opening a discussion on the need for guidelines for reporting lightning data obtained experimentally.

The second part of the chapter (Section 6.3) presented the design and the construction of a low-cost, multi-channel lightning field measuring system for the simultaneous measurement of three components (two magnetic and one electric) of the electromagnetic field radiated by lightning. The proposed system uses one single optical link for the transmission of the three signals, appropriately digitized and multiplexed, lowering considerably the overall cost of the system itself. The system allows, in addition, controlling remotely the gain of the field antennas.

Preliminary evaluation tests have been performed showing a very good performance of the system.

# References

Baum, C. E., E. L. Breen, F. L. Pitts, G. D. Sower, and M. E. Thomas (1982), The measurement of lightning environmental parameters related to interaction with electronic systems, *IEEE Trans. On Electromagnetic Compatibility*, *EMC-24*.

Krider, E. P., and R. C. Noggle (1975), Broadband antenna systems for lightning magnetic fields, *Journal of Applied Meteorology*, 252-258.

Pavanello, D., M. Rubinstein, F. Rachidi, J. L. Bermudez, D. Bommottet, P. Favre, and F. Baumgartner (2005), On the need for unified criteria describing the quality of lightning data and the design of a lightning field measurement system, paper presented at VIII International Symposium on Lightning Protection, SIPDA, São Paulo, Brazil.

Rubinstein, M., D. Pavanello, V. Muelhauser, F. Rachidi, J. L. Bermudez, D. Bommottet, P. Favre, F. Baumgartner, and E. Montandon (2006), Measuring System Specially Designed for Lightning Electromagnetic Fields, paper presented at International Conference on Lightning Protection, ICLP 2006, Kanazawa, Japan.

Thomson, E. M., P. J. Medelius, and M. A. Uman (1988), A remote sensor for the three components of transient electric fields, *IEEE Transactions on Industrial Electronics*, *35*, 426-433.

Uman, M. A. (1987), *The lightning discharge*, 377 pp., Academic Press, London, UK.

# Chapter 7

# Summary, Conclusions and Perspectives

## 7.1 Summary and Conclusions

The work presented in this thesis lies within the efforts of the scientific community to improve the understanding of the electromagnetic consequences of the impact of lightning strikes to tall structures.

Chapter 2 introduced to the phenomenology of cloud-to-ground lightning and the importance of lightning return-stroke modeling.

Among the different classes of return-stroke models existing in the literature, the attention was focused in this thesis on the so-called engineering models, which allow describing the current distribution along the channel as a function of the current at the channel base and the return-stroke speed, two quantities for which data can be obtained experimentally.

After presenting a review of five engineering return-stroke models describing lightning strikes to ground (namely, the Bruce-Golde (BG) model, the Transmission Line (TL) model, the Traveling Current Source (TCS) model, and the two Modified Transmission Line models (MTLL and MTLE)), the extension of the engineering models which takes into account the presence of an elevated strike object based on a distributed source representation of the lightning channel [*Rachidi, et al.*, 2002] was presented in Section 2.7. Section 2.8 presented then a discussion sustaining the adequacy of an idealized representation for the elevated strike object.

Chapter 3 was devoted to the computation of the electromagnetic field produced by lightning return strokes to elevated strike objects, based on the extension of the engineering models to include an elevated strike object presented in Chapter 2.

It was shown for the first time that the current distribution associated with these extended models exhibits a discontinuity at the return stroke wavefront which needs to be taken into account by an additional term in the equations for the electromagnetic field, the so-called 'turn-on' term. This discontinuity appears equally in the case of a ground-initiated lightning when the reflection at the channel base resulting from the grounding conditions is taken into account.

A general analytical formula describing the 'turn-on' term associated with this discontinuity for various engineering models was derived and simulation results illustrating the effect of the 'turn-on' term on the radiated electric and magnetic fields were also presented. This discontinuity (which, although not physically conceivable, is predicted by the model) has been disregarded in most studies dealing with the calculation of electromagnetic fields radiated by lightning to tall towers and, until a new model providing a non-discontinuous current at the return-stroke front is developed, needs to be carefully treated when calculating the radiated electromagnetic field.

In the second part of Chapter 3 (Section 3.5), dedicated to the investigation of the propagation effects on lightning electromagnetic field traveling along a finitely-conducting ground, the commonly used assumption of an idealized perfectly-conducting ground was relaxed in order to analyze how the electromagnetic field is affected while propagating along a soil characterized by a finite conductivity.

It was shown that the propagation along an imperfectly conducting ground causes the amplitude of the field to decrease and its risetime to increase with decreasing ground conductivity.

The results showed that the attenuation of the initial peak of the radiation field resulting from the propagation over finitely conducting ground depends strongly on the risetime of the current, the tower height and the ground conductivity.

It was also shown that, in general, the attenuation of the radiation field of lightning flashes striking towers is larger than that striking flat ground. In particular, this attenuation is generally more pronounced for higher current risetimes and reaches its maximum for risetime values which are close to the travel time of the current waves along the tower.

Chapter 4 presented a comparison among the five engineering models introduced in Chapter 2, extended to include the presence of an elevated strike object. The current profile along the channel and along the strike object, as well as radiated electric and magnetic fields at different distances, predicted by these models, were presented and discussed.

It was found that the computed electromagnetic fields associated with a strike to a tall tower are generally less model-dependent than those corresponding to a strike to ground, especially as far as the first-peak value is concerned, which is nearly model-insensitive in case of tall-tower strikes.

In addition, it was found that none of the models predicts the zero-crossing of the field at far distances within a time window of 50 μs, a typically-observed feature for ground-initiated lightning return strokes.

Analytical expressions relating far-fields and currents associated with lightning strikes to tall towers were derived in Section 4.4, which are general and can be used within any of the five engineering models considered in this thesis. It was shown that the far field can be decomposed into three terms, among which only the first one is model-dependent.

It was demonstrated, in addition, that the TL is the only model among the five presented for which it is possible to derive simple analytical formulas relating current peak and far field peak values. The electromagnetic field peak value being nearly independent of the adopted model, the TL expression becomes a general expression that can be applied for any engineering return-stroke model in case of tower-initiated lightning.

It was also shown that the peak amplitude of the electromagnetic field radiated by a lightning strike to a tall structure is relatively insensitive to both the values of the top reflection coefficient and the return stroke speed. This latter result is important, in particular, because, unlike ground-initiated strikes, for which the far-field peak is strongly dependent on the return-stroke speed (proportional, according to the TL model), far field peaks associated with strikes to tall structures are little sensitive to the return stroke speed. This is an interesting result when lightning currents are measured directly on instrumented towers to calibrate the performance of lightning location systems, since in most practical cases the value of the return stroke speed is unknown.

Chapter 5 reported on the simultaneous GPS-time stamped measurements of the return-stroke current and, for the first time, of the electric and magnetic fields at three distances associated with lightning strikes to the Toronto CN Tower (553 m) during the summer of 2005.

Two propagation paths for the electromagnetic field to the first and to the second field

measurement stations (located, respectively, 2.0 km and 16.8 km away from the CN Tower) were along the soil and through the Toronto city, whereas for the third location (50.9 km away) the propagation path was nearly entirely across the fresh water of Lake Ontario.

It was shown that the waveforms of the electric and magnetic fields at 16.8 km and 50.9 km exhibit a first zero-crossing about 5 microseconds after the onset of the return-stroke, which is part of a narrow undershoot and which may be attributed to the transient processes along the tower. For fields at 50.9 km, the expected zero-crossing at about 40 microseconds is also observed.

Effects of propagation (decrease of field amplitude and increase of its risetime) could also be observed in experimental records. It was shown that the fields at 50.9 km were less affected by such attenuation, compared to those at 16.8 km, presumably because the path of propagation was mostly across Lake Ontario.

The measured waveforms were compared with the theoretical predictions obtained using five engineering return-stroke models, extended to include the presence of the strike object, namely, TL, MTLL, MTLE, BG and TCS. A reasonable agreement was found for the magnetic field waveforms for the three considered distances. However, the peak values of the computed magnetic fields were systematically about 25 % lower than measured values. None of the considered models was able to reproduce the early zero-crossing and the narrow undershoot.

The expression for tall strike objects relating current and field peaks, recently derived in *[Bermudez, et al., 2005]* was also tested versus the obtained sets of simultaneously-measured return-stroke currents and fields associated with lightning strikes to the CN Tower. The overall agreement between the theoretically predicted and the experimentally observed field-to-current ratio is reasonable, although the theoretical expression appears to underestimate the experimentally measured ratio (by about 25 %). This may be due, at least in part, to the enhancement effect of the buildings on which the field measurement antennas were installed.

Finally, the directly-measured lightning currents at the tower were correlated and compared with US NLDN current peak estimates. It was shown that the NLDN-inferred values overestimate actual current peaks, because the presence of the tall struck object is not included in the algorithm used to infer lightning current peaks from remote field measurements. However, correcting the NLDN estimates using the tower factor $k'_{tall}$ results in an excellent estimation of lightning current peaks. This is an important conclusion of this study, showing that the estimation of lightning peak currents for tall-tower strikes can be

greatly improved by considering the tower factor $k'_{tall}$.

Chapter 6 presented in its first part (Section 6.2) useful elements of discussion about the need for guidelines for reporting lightning data obtained experimentally.

The second part of the chapter (Section 6.3) presented the design and the construction of a low-cost, multi-channel lightning field measuring system for the simultaneous measurement of three components of the electromagnetic field radiated by lightning. The proposed system uses one single optical link for the transmission of the three signals, appropriately digitized and multiplexed, lowering considerably the overall cost of the system itself. The system allows, in addition, controlling remotely the gain of the field antennas.

Preliminary evaluation tests have been performed showing a very good performance of the system.

## 7.2 Perspectives

With respect to the issue of return-stroke modeling treated in Chapter 2, although not explicitly discussed in this thesis, some works have been published on the application of Antenna-Theory (AT) models to the computation of currents and radiated electromagnetic fields from lightning strikes to the CN Tower [*Petrache, et al.*, 2005a; *Petrache, et al.*, 2005b]. The use of the NEC-4 simulation tool [*Burke*, 1992] employed in those studies allowed reproducing fine details of the actual tower geometry, including, for the first time, both its buried structure and the finite ground conductivity. The results showed a very good agreement with experimental data and encourage further investigations in this direction, starting from the analysis of the effect produced by the presence of vertically stratified ground.

A second suggestion for further investigation related to return-stroke modeling is the use of AT models to confirm the results presented in [*Baba and Rakov*, 2005], where FDTD simulations suggested that the waveguide properties of a biconical antenna (representing a tower) depend on the direction of propagation. Precisely, while the current pulses suffer no attenuation while traveling from the tower apex to its base, the attenuation is significant when pulses propagate from the base to the apex. This finding might render questionable the validity of reflection coefficients at ground level inferred from the measurements of current at the top of the tower.

An interesting and constructive discussion was recently initiated within the lightning research community questioning about the most appropriate way to model the lightning attachment to the tip of an elevated strike object. The discussion, in particular, is intended to find an adequate electrical equivalent source for the current distribution predicted by the engineering models. The question is still open and further work is needed to clarify this point.

The current discontinuity predicted by all engineering models at the return-stroke wavefront, although not physically plausible, required special care when computing the electromagnetic field predicted by such models, as discussed in Chapter 3 of this work. Further efforts are needed to review the formulation of the engineering models to eliminate any sources of discontinuity in the current distribution.

Work is in progress also to study the effect of the propagation of electromagnetic fields radiated by tall structures along inhomogeneous (stratified, mixed sea-land) paths.

With respect to the calculation presented in Chapter 4 of this thesis, a suggestion for further investigation refers to the question of what should be the proper criterion to compare the predictions obtained with the engineering models for a return stroke to flat ground and the same stroke to a tall structure. At least two criteria appear to be possibly adopted: the one fixing the ‘same total charge transferred to ground’ for the comparison, and, the one which imposes the use of the ‘same undisturbed current’. This important point needs to be clarified in the future works.

The far-field enhancement factor introduced by the tower has been discussed and confirmed by experimental validations. What has also been observed in numerical simulations is that, at very close distances to the tower (within the tower height), the presence of a tall strike object results in an attenuation of the electric field. This ‘shadowing effect’ becomes more and more effective while moving closer to the tower, until the electric field exhibits an inversion of polarity at distances within few meters from the tower itself, according to the engineering models’ prediction. These unpublished results need to be confirmed by further investigation and could lead to important conclusions about the electromagnetic environment in the immediate vicinity of tall structures.

The electromagnetic fields predicted at 100 km by the engineering models for tower-initiated lightning did not show after some tens of microseconds the well-known zero-crossing typical of the field radiated by ground-initiated lightning at the same distances. Nevertheless, the

fields recorded at a comparable distance (50.9 km) from the CN Tower in Toronto presented in Chapter 5 seem to exhibit the inversion of polarity systematically observed for strikes to flat ground. Indeed, further experimental observations are needed to confirm the presence of such zero-crossing after some tens of microseconds in the field radiated by lightning to tall structures.

As usual practice in lightning experimental campaigns performed in urban areas, all the field measurements presented in this work were obtained using sensors installed on the roof of buildings. If such a sensor location allows keeping undesired people out from the measurement site, it is known that the recorded field can be affected by an enhancement effect produced by the building itself. Work is in progress to provide estimations of the effect of the building on electric and magnetic fields recorded on its roof exploring both numerical modeling and experimental records.

Several research groups in the world are active in lightning measurement campaigns, each of them adopting its own specifications for data acquisition and reporting. The need for guidelines for reporting lightning data obtained experimentally, expressed in Chapter 6, has been recently accepted within the workplans of the Working Group 2 of the COST[1] Action P18 on 'the Physics of Lightning Flash and its Effects'. It is envisaged that such guidelines will become available and published in the near future.

# References

Baba, Y., and V. A. Rakov (2005), On the interpretation of ground reflections observed in small-scale experiments simulating lightning strikes to towers, *IEEE Transactions on Electromagnetic Compatibility*, *47*.

Bermudez, J. L., F. Rachidi, W. Janischewskyj, V. Shostak, M. Rubinstein, D. Pavanello, A. M. Hussein, J. S. Chang, C. A. Nucci, and M. Paolone (2005), Far-field - current relationship based on the TL model for lightning return strokes to elevated strike objects, *IEEE Transactions on Electromagnetic Compatibility*, *47*, 146-159.

Burke, G. J. (1992), Numerical Electromagnetics Code NEC-4 Method of Moments, Lawrence Livermore National Laboratory.

Petrache, E., F. Rachidi, D. Pavanello, W. Janischewskyj, A. M. Hussein, M. Rubinstein, V. Shostak, W. A. Chisholm, and J. S. Chang (2005a), Lightning Strikes to Elevated Structures: Influence of Grounding Conditions on Currents and Electromagnetic Fields, paper presented at IEEE International Symposium on Electromagnetic Compatibility, Chicago, August 2005.

[1] COST is an intergovernmental European framework for international co-operation between nationally funded research activities.

Petrache, E., F. Rachidi, D. Pavanello, W. Janischewskyj, M. Rubinstein, W. A. Chisholm, A. M. Hussein, V. Shostak, and J. S. Chang (2005b), Influence of the finite ground conductivity on the transient response to lightning of a tower and its grounding, paper presented at 28th General Assembly of International Union of Radio Science (URSI), New Delhi, India., October 23-29, 2005.

Rachidi, F., V. A. Rakov, C. A. Nucci, and J. L. Bermudez (2002), The Effect of Vertically-Extended Strike Object on the Distribution of Current Along the Lightning Channel, *Journal of Geophysical Research*, *107*, 4699.

# Curriculum Vitae

Davide Pavanello
Born on June 15, 1974 in Rivoli (Italy)
Italian
Married

## Education

2002 M.S. degree in Electronics Engineering from the 'Politecnico di Torino', Italy

## Professional experience

2003-present Research and teaching assistant at the Power Systems Laboratory (LRE) of the Swiss Federal Institute of Technology in Lausanne (EPFL), Switzerland

## Distinctions

Sept. 2006 Diploma for high quality presentation of the paper *"Simultaneous Measurements of Return Stroke Current, Electric and Magnetic Fields at Three Distance Ranges Associated with Lightning Strikes to the CN Tower"* at the 28th International Conference on Lightning Protection - ICLP 2006, Kanazawa, Japan

## Publications

### Journal papers

Submitted 2006 Pavanello, D., Rachidi, F., Rubinstein, M., Bermudez, J. L., Janischewskyj, W., Shostak, V., Nucci, C. A., Hussein, A. M., and Chang, J. S. (Submitted in 2006). *"On Return-Stroke Currents and Remote Electromagnetic Fields Associated with Lightning Strikes to Tall Structures - Part I: Computational Models"*, submitted to Journal of Geophysical Research.

Pavanello, D., Rachidi, F., Janischewskyj, W., Rubinstein, M., Hussein, A. M., Petrache, E., Shostak, V., Boev, I., Nucci, C. A., Chisholm, W. A., Nyffeler, M., Chang, J. S., and Jaquier, A., *"On Return-Stroke Currents and Remote Electromagnetic Fields Associated with Lightning Strikes to Tall Structures - Part II: Experiment and Model Validation"*, submitted to Journal of Geophysical Research.

Accepted 2006 D. Pavanello, F. Rachidi, V.A. Rakov, C.A. Nucci, J.L. Bermudez, *"Return Stroke Current Profiles and Electromagnetic Fields Associated with Lightning Strikes to Tall Towers: Comparison of Engineering Models"*, to be published in Journal of Electrostatics.

J. L. Bermudez, F. Rachidi, W. Janischewskyj, V. Shostak, M. Rubinstein, A.M. Hussein, D. Pavanello, J.S. Chang, C.A. Nucci, M. Paolone, *"Determination of Lightning Currents from Far Electromagnetic Fields: Effect of a Strike Object"*, to be published in Journal of Electrostatics.

2005 J.L. Bermudez, F. Rachidi, M. Rubinstein, W. Janischewskyj, V. Shostak, D. Pavanello, J.S. Chang, A.M. Hussein, C.A. Nucci, M. Paolone, *"Far-field - current relationship based on the TL model for lightning return strokes to elevated strike objects"*, IEEE Trans. on Electromagnetic Compatibility, Vol. 47, No. 1, pp. 146-159, February 2005.

2004 D. Pavanello, F. Rachidi, J.L. Bermudez, M. Rubinstein and C.A. Nucci, *"Electromagnetic Field Radiated by Lightning to Tall Towers: Treatment of the Discontinuity at the Return Stroke Wavefront"*, Journal of Geophysical Research, Vol. 109, D06114, 2004.

2003 J.L. Bermudez, F. Rachidi, D. Pavanello, *"Currents and radiated electromagnetic fields in lightning strikes to tall structures"*, GAIA, Vol. 12, No. 4, pp. 291-294, December 2003.

## Conference proceedings

2006 V. Cooray, G. Diendorfer, C.A. Nucci, D. Pavanello, F. Rachidi, M. Rubinstein, W. Schulz, *"On the Effect of the Finite Ground Conductivity on Electromagnetic Field Radiated by Lightning to Tall Towers"*, presented at the International Conference on Lightning Protection ICLP, Kanazawa, September 2006.

M. Rubinstein, D. Pavanello, V. Muehauser, F. Rachidi, J.L. Bermudez, D. Bommottet, P. Favre, F. Baumgartner, *"Measuring System Specially Designed for Lightning Electromagnetic Fields"*, presented at the International Conference on Lightning Protection ICLP, Kanazawa, September 2006.

D. Pavanello, F. Rachidi, W. Janischewskyj, M. Rubinstein, A.M. Hussein, E. Petrache, V. Shostak, C.A. Nucci, J.S. Chang, *"Simultaneous Measurements of Return Stroke Current, Electric and Magnetic Fields at Three Distance Ranges Associated with Lightning Strikes to the CN Tower"*, presented at the International Conference on Lightning Protection ICLP, Kanazawa, September 2006.

V. Shostak, W. Janischewskyj, F. Rachidi, A.M. Hussein, J.S. Chang, D. Pavanello and E. Petrache, "*Estimation of lightning-caused stresses in a MV distribution line using a three-wire approach"*, presented at the International Conference on Lightning Protection ICLP, Kanazawa, September 2006.

2005 D. Pavanello, M. Rubinstein, F. Rachidi, J.L. Bermudez, D. Bommottet, P. Favre, F. Baumgartner, *"On the need for unified criteria describing the quality of lightning data and the design of a lightning field measurement system"*, VIII International Symposium on Lightning Protection SIPDA, 21-25 November 2005, São Paulo, Brazil.

D. Pavanello, V. Cooray, F. Rachidi, M.Rubinstein, A. Negodyaev, M. Paolone, C.A. Nucci, *"Propagation effects on the electromagnetic field radiated by lightning to tall towers"*, VIII International Symposium on Lightning Protection SIPDA, 21-25 November 2005, São Paulo, Brazil.

J.S. Chang, A. Asakawa, S. Wada, W. Janischewskyj, K. Yamamoto, Z. Kawasaki, T. Shindo, A.M. Hussein, Y. Uchida, S. Iwasaki, D. Pavanello, K. Matsuura, J.L. Bermudez, F. Rachidi, and V. Shostak, *"Tall structure lightning return stroke velocity measurements for 553 m AGL CN telecommunication tower"*, VIII International Symposium on Lightning Protection SIPDA, 21-25 November 2005, São Paulo, Brazil.

E. Petrache, F. Rachidi, D. Pavanello, W. Janischewskyj, M. Rubinstein, W.A. Chisholm, A.M. Hussein, V. Shostak and J.S. Chang, *"Influence of the finite ground conductivity on the transient response to lightning of a tower and its grounding"*, 28th General Assembly of International Union of Radio Science (URSI), October 23-29, 2005, New Delhi, India.

E. Petrache, F. Rachidi, D. Pavanello, W. Janischewskyj, A.M. Hussein, M. Rubinstein, V. Shostak, W.A. Chisholm, J.S. Chang, *"Lightning Strikes to Elevated Structures: Influence of Grounding Conditions on Currents and Electromagnetic Fields"*, IEEE International Symposium on Electromagnetic Compatibility, Chicago, August 2005.

2004

D. Pavanello, F. Rachidi, J.L. Bermudez, M. Rubinstein, *"Engineering lightning return stroke models including an elevated strike object: far field-current relationship"*, International Symposium on Electromagnetic Compatibility, EMC EUROPE 2004, Eindhoven, The Netherlands, September 2004.

J. L. Bermudez, F. Rachidi, W. Janischewskyj, V. Shostak, M. Rubinstein, A.M. Hussein, D. Pavanello, J.S. Chang, C.A. Nucci, M. Paolone, *"Determination of Lightning Currents from Far Electromagnetic Fields: Effect of a Strike Object"*, International Conference on Lightning Protection, ICLP 2004, Avignon, France, September 2004.

J.L. Bermudez, C. A. Peña, F. Rachidi, F. Heidler, V. Rakov, *"Analytical Representation of Lightning Current Waveforms using Genetic Algorithms"*, International Conference on Lightning Protection, ICLP 2004, Avignon, France, September 2004.

D. Pavanello, F. Rachidi, V.A. Rakov, C.A. Nucci, J.L. Bermudez, *"Return Stroke Current Profiles and Electromagnetic Fields Associated with Lightning Strikes to Tall Towers: Comparison of Engineering Models"*, International Conference on Lightning Protection, ICLP 2004, Avignon, France, September 2004.

D. Pavanello, F. Rachidi, M. Rubinstein, J.L. Bermudez, C.A. Nucci, *"On the calculation of Electromagnetic Fields Radiated by Lightning to Tall Structures "*, International Conference on Lightning Protection, ICLP 2004, Avignon, France, September 2004.

D. Pavanello, F. Rachidi, M. Rubinstein, N. Theethayi, R. Thottappillil, *"Electromagnetic environment in the immediate vicinity of a tower struck by lightning"*, EUROEM 2004, Magdeburg, Germany, July 2004.

J.L. Bermudez, T. Gazizov, A. Negodyaev, D. Pavanello, F. Rachidi, A. Rubinstein, M. Rubinstein, *"On the enhancement of electric and magnetic fields from lightning due to close-by metallic structures"*, EUROEM 2004, Magdeburg, Germany, July 2004.

M. Rubinstein, D. Pavanello, J.L. Bermúdez, F. Rachidi, W. Janischewskyj, A.M. Hussein, V. Shostak, *"The Effect of the Measurement Time Constant of Analog Integrators on the Resulting Modeling and Simulation of Lightning"*, EUROEM 2004, Magdeburg, Germany, July 2004.

2003

J. L. Bermudez, F. Rachidi, W. Janischewskyj, A.M. Hussein, M. Rubinstein, D. Pavanello, V. Shostak, M. Paolone, and J.S. Chang, *"Influence of the Height of an Elevated Strike Object on the Enhancement of Lightning Radiated Fields"*, IEEE Power Tech 2003, Bologna, June 2003.

### Measurement reports

2006 D. Pavanello and F. Rachidi, *"Report on the 2005 lightning measurement campaign in Toronto, Canada"*, Lausanne, Switzerland, 2006.

2005 D. Pavanello and F. Rachidi, *"Report on the 2004 lightning measurement campaign in Toronto, Canada"*, Lausanne, Switzerland, 2005.

## Supervised student projects

### Master's projects

2006 V. Rey, *"Analyse des phénomènes transitoires sur une tour foudroyée: application à la CN Tower de Toronto"*, EPFL, February 2006.

2004 D. Ravaglia, *"Oggetti verticali colpiti da scariche atmosferiche: estensione dei modelli ingegneristici per il colpo di ritorno"*, University of Bologna, Italy, Februrary 2004.

2003 Alexey Negodyaev, *"Investigation of Scattering of Electromagnetic Field by a Cuboidal Building and by a conducting sphere"*, Tomsk University, Russia, July, 2003.

### Semester project

2004 S. Décoppet, *"Rayonnement électromagnétique associé à une décharge orageuse"*, EPFL, May 2004.

### Technical training

2006 A. Pagnetti, *"Test and calibration of a measurement system specifically designed for lightning signals"*, University of Bologna, Italy, March - July 2006.